ENHANCING IMMUNE RESPONSE IN THE ORAL CAVITY BY ANTIGEN-TARGETING

by

Yunnuo Shi

Submitted in partial fulfilment of the requirements
for the degree of Master of Science

at

Dalhousie University
Halifax, Nova Scotia
December 2016

Table of Content

List of Figures

List of Tables

Abstract

Mucosal vaccines that induce both local mucosal and systemic immune responses are ideal for preventing infections at the site of pathogen entry. Delivering antigen via molecules targeted specifically for receptors on the surface of antigen-presenting cells is potentially an excellent strategy to improve the immune response against the antigens delivered to mucosal sites. Many studies have reported that targeting antigen to CD40 via CD40 ligand or anti-CD40 antibody was able to strongly enhance antigen specific immune response; however, this approach has not been tested with protein-based mucosal immunization in the oral cavity. In this study, an antigen-targeting fusion protein OVA-CD40LS consisting of the C-terminal fragment of ovalbumin fused to the extracellular domain of mouse CD40 ligand and C-terminal fragment of ovalbumin alone (rOVA) as control protein were constructed and cloned into *Escherichia coli*. The two recombinant proteins were successfully purified from the insoluble fraction of *E. coli* cell lysate by nickel affinity chromatography coupled with different protein-refolding approaches. Biologically active OVA-CD40LS was generated via a 'two-round' protein-refolding strategy that was developed in the present study. The rOVA was successfully refolded via dialysis. Buccal intramucosal injection of 1 μg of OVA-CD40LS in the absence of adjuvant induced a rapid and strong Th1-skewed systemic antibody response while rOVA did not. Buccal topical immunization of 1 μg OVA-CD40LS did not induce a systemic or mucosal immune response. The most possible reasons for this lack immune response is the amount of fusion protein used was inadequate. This study has demonstrated that antigen targeting to CD40 via CD40LS could induce a strong systemic antibody response in the mouse oral cavity when the protein antigen was delivered into the mucosal layer.

List of Abbreviations Used

APC - Antigen-presenting cells

BCIP - 5-bromo-4-chloro-3-indoyl phosphate

BMDCs - Bone marrow-derived dendritic cells

Carbachol - Carbamylcholine chloride

CD40L - CD40 ligand

CD40LS - Extracellular domain of mouse CD40 ligand

CMC - Carboxymethylcellulose

CT - Cholera toxin

CTL - Cytotoxic T lymphocyte

DBP - Dibutyl phthalate

DCs - Dendritic cellsDibutyl phthalate

dNTP - Deoxynucleotide triphosphate

dTMP - Deoxythymidylic acid

dUMP - Deoxyuridine monophosphate

EDTA - Ethylenediaminetetraacetic acid

ELISA - Enzyme-linked immunosorbent assay

Ep-CAM - Epithelial cell adhesion molecule

FBS - Fetal bovine serum

Fc - Constant domain of antibody

FHA - Filamentous hemagglutinin

GM-CSF - Granulocyte-macrophage colony-stimulating factor

GTE - Glucose-Tris-EDTA

iDCs - Interstitial dendritic cells

IFN-γ - Interferon gamma

IPTG - Isopropyl-β-D-thiogalactoside

KAc - Potassium acetate

LB - Luria-Bertani

LCs - Langerhans cells

LP - Lamina propria

LPS - Lipopolysaccharide

MALT - Mucosal-associated lymphoid tissue

MHC - Major histocompatibility complex

NBT - Nitroblue tetrazolium

PBS - Phosphate-buffered saline

PBST - Phosphate-buffered saline with Tween-20

PCR - Polymerase chain reaction

pNPP - *p*-nitrophenyl phosphate

PRRs - Pattern recognition receptors

RLNs - Regional lymph nodes

rOVA - Recombinant C-terminal fragment of ovalbumin

S1S3 - S1 and S3 subunits of pertussis toxin

scFv - Single chain variable fragment antibody

SDS - Sodium dodecyl sulphate

SDS-PAGE - Sodium dodecyl sulphate polyacrylamide gel electrophoresis

sIgA - Secretory IgA

TAE - Tris-acetate-EDTA

TARFs - Tumor necrosis factor receptor-associated factors

TCA - Trichloroacetic acid

TE - Tris-EDTA

TGF-β - Transforming growth factor beta

TLR - Toll-like receptor

ThyA - Thymidylate synthase A

TNF - tumor necrosis factor

TYG - Tryptone-yeast extract-glucose

Acknowledgements

First and foremost I would like to thank Dr. Song F. Lee and Dr. Scott A. Halperin for their advice and endless support during my Masters program. I would also like to thank Dr. Jun Wang and Dr. Jean Marshall for serving on my committee and providing valuable input. Special thanks to Dr. Wang's lab for their kind help on tissue culture experiments, Dr. Robert L. White for the use of his freeze-dryer, Carrie Philips for her demonstration of mouse bone marrow cell isolation and bone marrow-derived dendritic cell culturing, Cynthia Tram for her help on FACS analysis, and Lauren Davey for her protein purification experience. Thanks to Naif Jalal, and other present and past members of our lab for their endless support during the past three years. This study was supported by an IWK Graduate Student Scholarship.

Chapter 1. Introduction

1.1 Mucosal membrane

The mucous membrane consists of one or more layers of epithelial cells and lines the surface of oropharyngeal cavity, respiratory tract, gastrointestinal tract, and urogenital tract, as well as exocrine glands, the inner ear, and conjunctiva surface of the eye (Mayer, 2003; Holmgren & Czerkinsky, 2005). As an interface between the host and the outside environment, a variety of defence mechanisms have evolved to prevent mucosal invasion and damage by pathogens and toxins (Holmgren & Czerkinsky, 2005). The epithelial layers serve as a physical barrier preventing direct contact of foreign antigens with the internal environment. The epithelial cells and mucosal associated glands produce mucus that is rich in glycoproteins, antimicrobial peptides, and secretory IgA that can prevent the attachment and penetration of the foreign antigens including food particles, airborne matter, particulate matter and pathogenic microorganisms (Neutra *et al.*, 2001). In addition, a highly specialized innate and adaptive mucosal immune system provides constant immune surveillance of the external environment and protects the host from potential pathogen invasion (Mayer, 2003; Holmgren & Czerkinsky, 2005; Neutra & Kozlowski, 2006).

1.2 The mucosal immune system

The mucosal immune system has three major tasks: protect the mucosal membrane from colonization by harmful microbial pathogens, prevent the penetration of infectious and immunogenic components through the mucosal membrane, and prevent the development of an immune response against harmless antigens (Mayer, 2003; Holmgren & Czerkinsky, 2005; Neutra & Kozlowski, 2006; Woodrow *et al.*, 2012). This

specialized local immune system is characterized by functionally and anatomically divided inductive sites and effector sites, the presence of lymphocytes that are phenotypically distinct from those found in the systemic lymphoid tissues, and the presence of IgA as the major antibody isotype (Mayer, 2003).

The mucosa-associated lymphoid tissues (MALT) and mucosal draining lymph nodes (LNs) represent the mucosal inductive sites, where antigen-specific immune responses are initiated. The effector sites are the regions where antibody production and cell-mediated immune responses occur (Brandtzaeg *et al.*, 2008). The MALT is characterized as a highly compartmentalized immunological system that functions independently from the systemic immune system. It is scattered along mucosal linings. MALT can be further divided into the gut-associated lymphoid tissue (GALT), such as the Peyer's patches, the appendix, and solitary follicles, the nasopharynx-associated lymphoid tissue (NALT) that includes the tonsils and adenoids at the entrance of the aerodigestive tract, and the bronchus-associated lymphoid tissue (BALT). There are also several potential MALT that are less well characterized such as the salivary-gland-or duct-associated lymphoid tissue (SALT / DALT), conjunctiva-associated lymphoid tissue (CALT), lachrymal drainage-associated lymphoid tissue (LDALT), Eustachian tube-associated lymphoid tissue (TALT), and larynx-associated lymphoid tissue (LALT) (Brandtzaeg *et al.*, 2008).

All MALT contain functional compartments including follicles, interfollicular regions, subepithelial dome regions, and follicle-associated epithelium. B cells, T cells and a variety of antigen presenting cells (APCs), such as macrophages and dendritic cells (DCs) accumulate in these functional compartments of MALT (Brandtzaeg, 2009). To

initiate an immune response, antigens can be either transported from the outer surface of mucosal membrane to the subepithelial dome region of the MALT by specialized epithelial cells known as 'M' cells, which are located within the follicle-associated epithelium, and then captured by the antigen-presenting cells (APCs). In addition, antigens can also be directly captured by the APCs from the mucosal surface (Holmgren & Czerkinsky, 2005; Brandtzaeg *et al.*, 2008). The captured antigens are then presented to the conventional T cells located in the interfollicular regions of MALT. Then, some of these antigen-loaded APCs further migrate to the draining lymph node with subsequent T-cell recognition. The types of immune response induced in mucosal tissues are affected by many factors including the nature of antigens, the state of APCs involved, and the local cytokine and chemokine environment (Holmgren & Czerkinsky, 2005). The intestinal dendritic cells in steady state are hyporesponsive and maintain immune tolerance in the gut by inducing regulatory T cell responses against food antigens and commensal microorganisms, thereby preventing unnecessary inflammation and hypersensitivity (Iwasaki & Kelsall, 1999; Pabst & Mowat, 2012). The $CD103^+$ DCs from the intestine lamina propria are found to carry antigens to gut-draining mesenteric lymph nodes and potent in inducing the generation of Foxp3+ regulatory T cell responses (Pabst & Mowat, 2012). Under normal steady-state conditions, some commensal bacteria are recognized by certain Toll-like receptors (TLRs) such as TLR2 expressed on APCs cell and epithelial cell surface, and this interaction seems to be crucial for maintenance of homeostasis in the gut epithelium (Rakoff-Nahoum *et al.*, 2004; Round & Mazmanian, 2010; Perez-Lopez *et al.*, 2016).

On the other hand, APCs recognize a variety of bacterial, viral, fungal, and protozoal molecular patterns as 'danger signals' through pattern recognition receptors (PRRs), which include toll-like receptors, lectin, selectins, integrins, NOD-like receptors, and retinoic acid-inducible protein-1 (RIG-I)-like receptors (Dwivedy & Aich, 2011). Signalling through these receptors up regulates the expression of MHC and co-stimulatory molecules, such as CD40, CD80, and CD86. The activated NFκB pathway also leads to the production of proinflammatory cytokines, such as TNF, IL-1, IL-6 and IL-12 (Novak *et al.*, 2008; Dwivedy & Aich, 2011). These activated APCs tend to induce the development of both humoral and cell-mediated immune responses (Holmgren & Czerkinsky, 2005). Certain adjuvants and proinflammatory conditions at the mucosal site are also recognized by APCs as 'dangers signals', which can lead to APCs activation.

1.2.1 Humoral mucosal immune response

The production of secretory IgA (sIgA) in mucosal secretions such as mucus and saliva is the typical mucosal humoral response upon infection or mucosal immunization (Holmgren & Czerkinsky, 2005). sIgA is secreted into mucosal secretions as dimeric or multimeric molecules (van Egmond *et al.*, 2001). The dimerization or multimerization, together with a high degree of glycosylation, are believed to contribute to the protease resistant property of sIgA, which makes these antibodies specifically suited for functioning in mucosal secretions (van Egmond *et al.*, 2001; Holmgren & Czerkinsky, 2005). The high affinity sIgA can function as neutralizing antibodies by agglutinating bacteria and bacterial products (Hutchings *et al.*, 2004). The low-affinity sIgA promotes immune exclusion that shields the mucosal surface from direct contact with pathogens

(van Egmond *et al.*, 2001).

Upon mucosal infection or immunization, the conventional B (B-2) cells in the follicles of MALT or regional LNs are believed to be responsible for the generation of high-affinity IgA antibody response through a canonical T cell dependent pathway (van Egmond *et al.*, 2001; Cerutti, 2008). In the interfollicular regions of MALT, DCs present the captured antigen to $CD4^+$ T cells, which leads to $CD4^+$ T cell priming. The antigen-primed $CD4^+$ T cells trigger B cell class switch from IgM to IgA through a CD40-dependent pathway involving cognate T cell–B cell interactions in the germinal center of MALT (Cerutti, 2008). The local expression of cytokines such as TGF-β, IL-4, IL-6 and IL-10 are also thought to be important for B cell IgA class switching (Cerutti, 2008).

The majority of the antigen-primed effector CD4+ T cells and the IgA-expressing effector B cells and plasma cells leave the inductive sites and migrate through the lymphatics and bloodstream into major effector tissues, such as the lamina propria of the gut, the upper respiratory tract, the female reproductive tract, or acinar regions of exocrine glands. The adhesion molecules and chemokines expressed on the surface of mucosal effector T cells and IgA-expressing B cells mediate this preferential migration to mucosal effector sites (Brandtzaeg & Johansen, 2005; Griffith *et al.*, 2014). In addition, a small fraction of the stimulated antigen-primed effector CD4+ T cells and the IgA-producing effector cells also migrate to the systemic compartment (Brandtzaeg & Johansen, 2005; Brandtzaeg *et al.*, 2008). In secretory effector sites, the effector B cells undergo terminal differentiation into plasma cells that produce dimeric IgA (Brandtzaeg & Johansen, 2005). The dimeric IgA is then exported as secretory IgA. The antigen-primed T cells mainly migrate to the epithelium of the mucosal effector sites and expand

to memory or effector T cells, which can further interact with effector B cells (Brandtzaeg & Johansen, 2005; Griffith *et al.*, 2014).

Furthermore, there is a shared expression of adhesion and chemokine receptors of cells at the different mucosal effector sites, which are complementary to the adhesion molecules and chemokines expressed by effector T cells and IgA-expressing B cells. This allows the activated IgA-producing B cells in the mucosal inductive sites to migrate to distant mucosal epithelia and provide protection to distant mucosal surfaces. This is known as the common mucosal immune system, which generates a protective mucosal response from distant sites (Mestecky, 1987).

In mice, low affinity IgA is mainly expressed via B-1 cells induced in a T-cell-independent pathway. B-1 cells are specialized B-cell subsets that are ontogenically, phenotypically and genotypically distinct from the conventional B (B-2) cell (Baumgarth, 2010). In adult animals, B-1 cells are mainly present in the pleural and peritoneal cavities (Hayakawa *et al.*, 1985). In addition, the B-1 cells are also found in secondary lymphoid tissues, mucosal sites, and the omentum (Ansel *et al.*, 2002). In steady state, the B-1 cells are responsible for the production of a large proportion of the "natural" low-affinity IgM that present lifelong in normal individuals. These cells can be activated by various stimuli including certain carbohydrates, TLR agonists such polysaccharides or lipopolysaccharides, cytokines (e.g. IL-5, IL-10 and IL-15), and commensal bacteria (Ansel *et al.*, 2002; Thurnheer *et al.*, 2003). Upon stimulation, the activated B-1 cells can rapidly migrate from the pleural and peritoneal cavities through RLNs to effector sites, where they differentiate and secrete large amounts of IgM or/and undergo class switch preferentially towards IgA in a $CD4^+$ T-cell and CD40L-independent manner (Murakami

et al., 1994; Ha *et al.*, 2006). This B-1 cell derived low-affinity IgA response is generated much quick than that the high-affinity IgA response derived from B-2 cells, therefore contributes to a major portion of the secretory IgA production on mucosal surface and functions as a early immune defense in the gut mucosa and in the respiratory track (Cerutti, 2008). In addition, mucosal dendritic cells capture the T cell-independent antigens such as polysaccharides or lipopolysaccharides in a non-degradative endocytic pathway. These antigens are then recycled to the dendritic cell plasma membrane and presented to B-1 cells (Baumgarth, 2010). Furthermore, the bacterial TLR ligands have recently been shown to induce DCs release of soluble class-switch-inducing factors related to CD40L, including B-cell activating factor (BAFF) and a proliferation-inducing ligand (APRIL), which have potent IgA-inducing functions (Herzenberg *et al.*, 1986).

1.2.2 Cell-mediated mucosal immune response

In addition to the humoral response, the induction of a mucosal cytotoxic T lymphocyte (CTL) response has been reported after mucosal infection or immunization. The presence of a mucosal cytotoxic T cell response is essential for immune clearance of pathogens in mucosal infections by viruses, intracellular bacteria and parasites (Holmgren & Czerkinsky, 2005). The mucosal CTL response is predominantly induced by wild-type or attenuated viruses and bacteria in mucosal tissues (Sheridan *et al.*, 2014; Pennington *et al.*, 2016; Keselman *et al.*, 2016). Moreover, oral or nasal administration of soluble proteins and peptides with certain adjuvants, such as cholera toxin (CT) and *E. coli* related enterotoxins, can promote mucosal CTL development (Chamcha *et al.*, 2015; Meyer *et al.*, 2015; Iwasaki, 2016; Singh *et al.*, 2016).

Upon infection or immunization, the antigen-loaded DCs either activate the naïve T cells present at the site of infection/immunization, or migrate to interfollicular regions of MALT or RLNs and cross-present the captured antigens to $CD8^+$ T cells, which leads to antigen specific $CD8^+$ T cell priming (Holmgren & Czerkinsky, 2005). Some of the antigen-bearing DCs are able to migrate to distant lymphoid organs and prime naive CD8 T cells after mucosal immunization (Hervouet *et al.*, 2013). With the help of inflammatory signals, antigen-loaded DCs and $CD4^+$ T cell (Krummel *et al.*, 2016), antigen-experienced $CD8^+$ T cells then differentiate into effector or memory T cells (Krummel *et al.*, 2016). Activated effector $CD8^+$ T cells in MALT preferentially migrate towards mucosal effector sites, where they further differentiate into effector and memory $CD8^+$ T cells (Krummel *et al.*, 2016; Griffith *et al.*, 2014).

1.3 Mucosal vaccines

Most infectious pathogens enter the host via a mucosal surface. It is now common understanding that the local mucosal immune responses are important for the protection against infections initiated at mucosal surfaces (Mayer, 2003; Holmgren & Czerkinsky, 2005; Neutra & Kozlowski, 2006; Woodrow *et al.*, 2012). Protective mucosal immune responses are most efficiently induced by antigens administrated at the mucosal surfaces, not by the antigens injected directly into the host body. Therefore, mucosal vaccines may be the ideal for preventing infections at the route of entry (Holmgren & Czerkinsky, 2005; Neutra & Kozlowski, 2006; Rhee *et al.*, 2012; Woodrow *et al.*, 2012). Ideally, mucosal vaccination would be done by topical application, which dose not involve the use of a needle and is easier to administer than parenteral doses. Mucosal surfaces have a

higher tolerance to bacterial by-products such as endotoxin, which lowers the risk of side effects of the mucosal vaccines compared to traditional injectable vaccines (Neutra & Kozlowski, 2006; Woodrow *et al.*, 2012).

Unlike parenteral vaccines that have been developed and optimized since 1796, mucosal vaccines have only started receiving attention for the past few decades. Until now, only a few mucosal vaccines have been approved in the market, such as the oral vaccine against poliovirus, *Salmonella typhi*, *Vibrio cholerae,* and rotavirus, as well as a nasal vaccine against influenza virus (Neutra & Kozlowski, 2006; Fujkuyama *et al.*, 2012; Rhee *et al.*, 2012). The physical and biological features of the mucosal membrane present difficulties in the development of effective mucosal vaccines. Antigens are often diluted in mucosal secretions, become trapped in mucus, and are degraded by proteases or nucleases (for DNA vaccines). In the digestive track, most vaccine antigens that are delivered in soluble form are destroyed by the low pH of the stomach and the large quantity of digestive enzymes in the intestine (Lycke, 2012). As well, the efficiency of antigens crossing the mucosa is expected to be low. It is also hard to control the dosage of the vaccination to optimize the immunization outcomes. Moreover, the mucosal immune system possess potent tolerance mechanisms to prevent the immune system from overreacting to the many environmental antigens, which makes it hard to induce a strong immune response against mucosally delivered antigens (Mayer, 2003; Holmgren & Czerkinsky, 2005; Neutra & Kozlowski, 2006; Woodrow *et al.*, 2012). Taken together, the type of vaccine antigens, dosage of the vaccine antigens, the type of adjuvants, antigen delivery regiment, and the immunization site have critical effects on whether a mucosal vaccine can induce a robust local and systemic immune response.

1.4 Mucosal vaccine delivery to mucosal membrane in the oral cavity

The development of mucosal vaccines has been extensively focused on the gastrointestinal, nasal, and pulmonary route, whereas vaccine administration to the mucosal surface in the oral cavity has received relatively less attention (Amorij *et al.*, 2012). Several features of the oral cavity make it an attractive immunization site compare to other mucosal surfaces. As the entryway of the gastrointestinal and respiratory tracts, the mucosal immune system in the oral cavity plays an indispensible role in the first line of defense against antigen invasion. The neutral pH and relatively low levels of proteases in the oral mucosa results in longer stability of the vaccine antigens (Sudhakar *et al.*, 2006). In addition, the excellent accessibility of the mucosal tissues in the oral cavity is another asset for immunization (Kraan *et al.*, 2014).

In humans, Waldeyer's ring that includes tonsils, tubal tonsils, adenoids and lingual tonsil is considered the MALT (Rui-Qing Wu *et al.*, 2014). The main effector sites are the epithelium, lamina propria and salivary glands (Novak *et al.*, 2008). On the other hand, the MALTs are much simpler in mice compared to those in humans, mainly because rodents lack tonsils. Instead of having multiple inductive sites, the cervical lymph node serves as the regional lymph node in mice. In addition, the oral cavity is covered with stratified squamous epithelium (Kraan *et al.*, 2014) and M cells are not present (Song *et al.*, 2009; Nagai *et al.*, 2015). The initiation of an immune response in the oral cavity is heavily reliant on antigen uptake by the dendritic cells resident in the epithelium layer and their sequentially maturation and migration to RLNs (Hovav, 2013). Therefore, the dendritic cell compositions and nature make mucosal regions in the oral cavity suitable for vaccine delivery.

1.4.1 Dendritic cell compositions in different mucosal regions of oral cavity

The ability of local dendritic cells to take up antigens from sites of infection or immunization sites and subsequently mature and migrate to RLNs is essential for the initiation of an immune response (Hovav, 2013). In the oral cavity, the tissue resident dendritic cells are mainly conventional DCs, which can be further categorized into at least four phenotypically different subpopulations: langerhans cells (LCs, $CD11c^+$ $CD11b^+$ Ep-CAM^+, and CD207 (langerin)$^+$ $CD103^-$), the resident interstitial dendritic cells (iDCs, $CD11c^+CD11b^+$and Ep-CAM^-. langerin$^-$ $CD103^-$) (Le Borgne *et al.*, 2006; Chalermsarp & Azuma, 2009; Aramaki *et al.*, 2011; Nudel *et al.*, 2011), langerin-expressing resident interstitial dendritic cells ($CD103^+ln^+$iDCs) (Bursch *et al.*, 2007; Nagao *et al.*, 2009; Aramaki *et al.*, 2011; Del Rio *et al.*, 2010), and langerin$^-CD103^+$ iDCs ($CD103^+$iDCs) (Nudel *et al.*, 2011). In addition, $CD11c^{int/lo}$ langerin$^-$ iDCs are recruited from the circulation to the mucosal sites upon stimulation (Aramaki *et al.*, 2011). A brief summary of the subsets of dendritic cells in the oral cavity and their distribution is shown in Table 1.

The LCs and iDCs represent the major DC subset in the buccal, sublingual, and gingival mucosa (Le Borgne *et al.*, 2006). Upon immunization or infection, the activated resident iDCs express high levels of CD80, CD86, MHC II, CD273 and CD274 as well as moderate level of CD205. The iDCs, including both the resident and recruited iDCs are the main cell population in the oral mucosa responsible for antigen uptake and presentation to both $CD4^+$ and $CD8^+$ T cells in the RLNs (Le Borgne *et al.*, 2006; Nudel *et al.*, 2011; Hovav, 2013). The tissue resident iDCs migrate rapidly into the RLNs after the buccal or sublingual surface application of hapten dibutyl phthalate (DBP)/FITC

Table 1 Dendritic cell subsets in the murine oral mucosa

DC subsets	Cellular markers[1]					Distribution[2]
	CD11c	CD11b	Ep-CAM	Langern/CD207	CD103	
LCs	+	+	+	+	-	Buccal, Sublingual, Gingiva
Resident iDCs	hi	+	-	-	-	Buccal, Sublingual, Gingiva
Recruited iDCs	int/ low	+	-	-	-	Buccal, Sublingual, Gingiva
$CD103^+$ iDCs	+	+	-	-	+	Buccal, Gingiva
$CD103^+Ln^+DCs$	+	+	+	+	+	Buccal
pDCs	ND	ND	ND	ND	ND	Sublingual
Macrophage-like cell	-	+	-	-	-	Buccal, Sublingal, Gingiva

Abbreviation: DC: dendritic cell; LCs: Langerhans cells; iDC: interstitial DC; Ln^+DC, Langerin-expressing iDC; pDCs, pDCs: plasmacytoid DCs; Ep-CAM: epithelial cell adhesion molecule; ND, not defined.

[1] Expression of cellular markers: "+" indicates the expression; "hi" indicates the high expression; "int" indicates intermediate expression; "low" indicates the low expression; "-" indicates no expression.

[2] Indicates the location that the cells are naturally existed.

(Aramaki *et al.*, 2011; Nudel *et al.*, 2011). The peak level of the resident iDCs in the RLNs occurs at 24 hour after stimulation, but diminishes immediately (Chalermsarp & Azuma, 2009; Aramaki *et al.*, 2011). Sublingual immunization of OVA with CT as adjuvant induces a rapid migration of antigen-bearing iDCs to RLNs and can be detected as early as 6 hour (Song *et al.*, 2009). The newly recruited iDCs, expressing intermediate levels of CD86, CD273 and CD274, migrate into the RLNs at a constant rate and maintain at a high cell number in the RLNs up to 4 days after buccal or sublingual DBP/FITC painting. This cell subpopulation functions similarly to resident iDCs and is believed to compensate for the function of resident iDCs at later time points (Chalermsarp & Azuma, 2009; Aramaki *et al.*, 2011).

Upon stimulation, the resident LCs in the buccal and sublingual mucosa migrate slowly to the RLNs and reach a peak level at 96 hour after stimulation, with limited expression of CD80, CD86, CD273 and CD274 (Aramaki *et al.*, 2011; Nudel *et al.*, 2011). The role of LCs in the immune response is controversial. In the oral cavity, the LCs is best known for its property to generate immune tolerance. In a plasmid DNA buccal and sublingual immunization study, the depletion of LCs led to an increase $CD4^+$ T cell responses and better antibody production, but a reduced $CD8^+$ T cell response (Romani *et al.*, 2010; Upadhyay *et al.*, 2013). Moreover, in the absence of LCs, mice infected with *P. gingivalis* showed a reduced number of T regulatory cells, an increased number of activated high numbers of $CD4^+$ T cell and enhanced IFN-γ production (Arizon *et al.*, 2012).

Both $CD103^+ln^+$iDCs and langerin$^-CD103^+$ iDCs are mainly found in gingiva mucosal tissue. The function of langerin$^-CD103^+$ iDCs is not clear. Upon stimulation, the

$CD103^+ln^+$iDCs in the mouse gingiva slowly migrate to RLNs and only show limited antigen-presenting properties (Aramaki *et al*., 2011; Nudel *et al*., 2011). However, the actual function of the $CD103^+ln^+$iDCs in the oral cavity remains unclear. The similar DC type has been characterized in other organs including skin (Bursch *et al.*, 2007), lungs (Belz *et al.*, 2004; Sung *et al.*, 2006), and intestine (Welty *et al.*, 2013). In the skin and lungs, $CD103^+ln^+$iDCs represent the migratory DCs population that is able to cross-present viral and self-antigens in RLNs. In the intestine, the $CD103^+$ DCs migrate to the RLNs for the induction of T regulatory cells (Coombes *et al.*, 2007; Sun *et al.*, 2007; Matteoli *et al.*, 2010) and are required for Th17 development in the lamina propria (Welty *et al.*, 2013).

In addition to the four major DCs subpopulations, a macrophage-like ($CD11b+CD11c^-$) cell population is found mainly in the sublingual mucosa. This cell population is believed to play an important role in generating immune tolerance through sublingual infection or immunization (Zhang *et al.*, 2014; Tanaka *et al.*, 2016). In an OVA sensitized allergic asthma mouse model, activation of $CD11b^+$ cells significantly reduced asthma symptoms after OVA challenge (Mascarell *et al*., 2011). A recent study showed that repeated administration of antigen at sublingual mucosa led to a significant reduction of iDCs number (Zhang *et al.*, 2014). Plasmacytoid dendritic cells (pDCs) that are mostly found in the bloodstream were also recruited into the sublingual area upon infection (Hovav, 2013).

Taken together, the mucosal resident iDCs and newly recruited iDCs play an important role in initiating an immune response in oral cavity. The abundant number of the dendritic cells in the buccal and sublingual mucosa suggests that these two mucosal

sites are the ideal immunization sites in oral cavity. Although the LCs and iDCs are also present in the gingival region, the cell counts are relatively low compared with the buccal and sublingual region (Troy, 1984; Arizon *et al.*, 2012). In addition, the gingival region is covered by thin layer of masticatory mucosa, which lacks submucosa and is bound directly to alveolar bone via the lamina propria (Kraan *et al.*, 2014). The cell composition and numbers, as well as the epithelium structure in gingival region, make it not suitable for vaccination compare to the buccal and sublingual mucosal region.

1.4.2 Buccal and sublingual vaccine development

As mentioned above, the macrophage-like $CD11b^{+}CD11c^{-}$ cells are present predominantly in the sublingual mucosa, and are thought to be critical in antigen uptake and induction of immune tolerance (Mascarell *et al.*, 2008; Novak *et al.*, 2008). This makes the sublingual mucosa an attractive site for clinical tolerance induction over other sites (Moingeon & Mascarell, 2012). The sublingual route has been widely used as an immunotherapy site for treatment of allergic hypersensitivity (Shim *et al.*, 2013). For example, sublingual immunotherapy in allergen-sensitized mice reduces the allergic symptoms as well as the allergen-specific nasal lavage and serum IgE levels upon allergen challenge (Brimnes *et al.*, 2007; Kildsgaard *et al.*, 2007). Sublingual immunotherapy for asthma has been extensively tested in clinical trials in the United States and Europe (Viswanathan & Busse, 2012).

In recent years, many studies have investigated the ability of sublingual immunization to induce an immune response against infections. Of all the mucosal vaccine delivery strategies, mucosal vaccines administered via the sublingual route are

most successful with live attenuated vaccines and inactivated vaccines (Kraan *et al.*, 2014). Live attenuated vaccines include genetically engineered live bacteria or viruses strains that are less virulent than the pathogenic parent strains. This vaccine approach provides a high level of antigen exposure and the microorganism itself can serve as the vaccine adjuvant, which promotes the induction of a protective immune response (Lycke, 2012). Mice immunized with live-attenuated influenza virus plus adjuvant on sublingual mucosa were protected against influenza virus challenge as well as cross-protected against different influenza virus subtypes (Song *et al.*, 2008; Park *et al.*, 2012).

Inactivated vaccines include non-living, whole-cell or component vaccines (Lycke, 2012). Recently, the human papillomavirus 16L1 protein vaccine (Cho *et al.*, 2010), respiratory syncytial virus (RSV) G protein fragment vaccine (Kim *et al.*, 2012), and subunit influenza vaccine (Pedersen *et al.*, 2011; Murugappan *et al.*, 2014) have been tested in mice via sublingual immunization with additional adjuvants, and high levels of antigen specific mucosal IgA and systemic IgG responses were reported. Sublingual immunization with non-living whole-cell vaccines, including formalin-inactivated influenza virus vaccine (Song *et al.*, 2008) and a *Salmonella* vaccine (Huang *et al.*, 2008) with CT as an adjuvant induced enhanced mucosal IgA antibody levels, and antigen specific CTL responses.

The buccal mucosal tissue is rich in iDCs and LCs and has the highest dendritic cell count compared to other mucosal in the oral cavity. This makes the buccal mucosa an attractive site for immunization. The development of vaccines administered via the buccal route has focused on DNA vaccines whereas only a few studies have involved protein-based vaccines. Intramucosal injection of recombinant plasmid DNA coding for

viral antigens, such as the measles virus haemagglutinin (Etchart *et al.*, 1997) and HIV-1 antigen (Lundholm *et al.*, 1999; Ma *et al.*, 2014) induced antigen specific CTL responses and antigen-specific IgA and IgG responses in different animal models. In addition, surface application of the bilayer films containing plasmid DNA on the buccal mucosal surface of rabbits led to serum antigen-specific IgG production (Cui & Mumper, 2002).

In the few studies with protein antigen, buccal intramucosal injection of OVA protein induced a strong mucosal and systemic antibody response (Ma *et al.*, 2014). The human papillomavirus (HPV) long peptide injected intramucosally in the buccal mucosal region induced an antigen specific $CD8^+$ T cell response even without adjuvant (Yang *et al.*, 2016). Also, buccal surface and intramucosal immunization of measles virus nucleoprotein induced a protective $CD4^+$ and $CD8^+$ response as well as a systemic IgG response in mice (Etchart *et al.*, 2001).

1.4.3 Live-bacteria as vaccine delivery vehicle via the sublingual and buccal route

Although live-attenuated vaccines have shown promising results when administered via the sublingual route, the safety issue and vaccine stability are still the main concerns associated with this type of vaccine (Lycke, 2012; Woodrow *et al.*, 2012). Inactivated vaccines were developed as an alternative approach, which are more stable and safer than live-attenuated vaccine (Lycke, 2012). As summarised above, a variety of inactivated vaccine antigens successfully induced a antigen-specific IgA, IgG, and CTL response administered via the sublingual and buccal route with co-administration of a potent mucosal vaccine adjuvant such as CT and *E. coli* heat-labile toxin (Lycke, 2012; Rhee *et al.*, 2012).

Genetic engineering techniques have allowed the development of genetically attenuated pathogens, as well as commensal bacteria as live vaccine vestor to deliver heterologous antigens (Da Silva *et al.*, 2014). The use of commensal bacteria as vaccine vectors has a number of advantages over attenuated bacteria. Most of the commensal bacteria are natural colonizers of the mucosal surface (McGhee *et al.*, 1992). Therefore, these bacteria are easily administered topically, which make them cost efficient, and they should be well-tolerated by the host (Medina & Guzmán, 2001; Lee, 2003). This strategy of using live commensal bacteria as vaccine delivery vehicles has emerged over the past two decades, however, it has not been very well studied in the context of sublingual and buccal immunization.

1.4.4 *Streptococcus gordonii* as a vaccine vector

Streptococcus gordonii is a commensal bacterium and a pioneer organism in the human oral cavity, colonizing the oral mucosa and tooth surface. It can be detected in the oral cavity of infants by 6 months of age and remains as part of the oral microbiota throughout life (Carlsson *et al.*, 1970). In addition, *S. gordonii* is able to colonize the oral cavity of mice, rats, and monkeys (Medaglini *et al.*, 1997). Our lab has demonstrated that recombinant *S. gordonii* can colonize the nasal cavity, pharynx, trachea, and oral cavity of BALB/c mice (Lee, 2003; Knight *et al.*, 2008). The recombinant *S. gordonii* recovered from colonized mice were positive for the expression of heterologous antigens (Oggioni *et al.*, 1995; Lee, 2003). Furthermore, *S. gordonii* is naturally competent for genetic transformation permitting easy genetic manipulation (Pozzi & Wells, 1997). Developing a recombinant *S. gordonii* strain via chromosomal integration rather then via plasmid

vectors provides stability of genetic construct in the engineered strain, which is important for a live vaccine vector (Pozzi & Wells, 1997).

In 1995, Medaglini's group successfully demonstrated the oral colonization of recombinant *S. gordonii* in the mouse oral cavity and showed the induction of both a mucosal and systemic immune response against the antigen (Medaglini *et al.*, 1995). A variety of antigens, such as the Ag5.2 protein from hornet venom (Medaglini *et al.*, 1995), E7 protein of HPV type 16 (Medaglini *et al.*, 1997; Oggioni *et al.*, 1999), gp-120 of HIV-1 (Di Fabio *et al.*, 1998; Oggioni *et al.*, 1999), measles virus protein (Maggi *et al.*, 2000), and the gp-120 coupled with LTB (Maggi *et al.*, 2002) have been successfully constructed and expressed individually or as a group of proteins on the surface of *S. gordonii* and proved to be immunogenic in animal immunization. Furthermore, several studies showed that oral colonization of recombinant *S. gordonii* could induce the effective protection against the infection (Medaglini *et al.*, 2001; Wang *et al.*, 2013). For example, a recent study has shown that intranasal immunization with recombinant *S. gordonii* expressing the M6-Sj-F1 (*Schistosoma japonicum*) fusion protein on the bacterial surface induced a strong serum IgG, serum IgA, and saliva IgA response against Sj-F1, and the immunized animals were protected from *S. japonicum* (Wang *et al.*, 2013). In our laboratory, we have successfully constructed a recombinant *S. gordonii* RJM4 expressing the N-terminal 179-amino acid fragment of S1 subunit of pertussis toxin (PT) as a SpaP/S1 fusion protein. Oral colonization of the recombinant *S. grodonii* induced a PT and SpaP specific salivary IgA response in mice (Lee *et al.*, 2002b).

Another approach to expressing heterologous antigens by *S. gordonii* is to have the antigen released into the culture medium as a secreted protein (Lee *et al.*, 2002a; Lee

et al., 2002b). Having the protein antigen secreted instead of expressed on the cell surface may minimize the immune response against the recombinant bacterial strain even after long term colonization because the heterologous antigen is not associated with the vector bacterium once secreted. Our laboratory has successfully constructed several heterologous antigens that were secreted by *S. gordonii*, such as a S1S3FHA fusion protein (Lee *et al.*, 2002b), a single chain variable fragment (scFv) of antibody against complement receptor 1 (anti-CR1-HA) (Knight *et al.*, 2008), and several FHA fusion proteins (Lee, unpublished data). Moreover, oral colonization of recombinant *S. gordonii* secreting anti-CR1 was able to induce antibody response against the HA tag (Knight *et al.*, 2008).

Although using *S. gordonii* as a vaccine vector has shown promising results, there are still many challenges in the development of *S. gordonii* based live oral mucosal vaccines. The secreted antigens are more easily diluted by mucus and salivary flow making it hard to predict the efficiency of secreted antigens being captured by local dendritic cells (Neutra & Kozlowski, 2006). In addition, the secreted protein antigens alone or coupled with adjuvant has to be able to induce APC activation upon being captured, which is essential for inducing an immune response at a mucosal surface (Huub *et al.*, 2015). Therefore, improving the immunogenicity of the protein antigens secreted by recombinant *S. grodonii*, and the efficiency of antigen uptake are two main focus in the development of an effective *S, gordonii* based live oral mucosal vaccine.

1.5 Targeting antigen to dendritic cells

Antigen-targeting is an approach that can deliver antigens using antibodies or

ligand that are specific for receptors expressed on the surface of DCs. It has the potential to reduce the required dose of antigen to obtain a protective immune response and increase the efficiency of the vaccine antigen by avoiding contact with non-targeted cells (Kastenmüller *et al.*, 2014). In addition, this approach allows antigen to target certain receptors expressed only by specialized DCs subsets to induce the specific immune response (Macri *et al.*, 2016).

The antigens can be coupled to the targeting antibodies or ligands by chemical conjugation or by genetic means as a recombinant antibody/ligand-antigen fusion gene construct (Caminschi & Shortman, 2011). Chemical conjugation has been found to have several side reactions that may reduce the efficiency of the complex, while using recombinant antigen-antibody/ligand fusion protein produce a more reliable product (Lehmann *et al.*, 2016). The recombinant fusion protein approach also allows one to know the exact number of antigen molecules coupled and allows better control of the endotoxin concentration in the fusion protein preparation (Lehmann *et al.*, 2016).

Since the antigen targeting approach was successfully tested *in vitro* aimed at the Fc receptor and MHC molecule in 1987 (Snider & Segal, 1987), there are now over 100 dendritic cell-targeting studies published with a broad range of DCs surface molecules. The MHC molecule, co-stimulatory factor CD40, multi-lectin receptor DEC 205, C-type lectin receptor DCAR1 and Clec9A, mannose receptor1 (CD206), DC specific ICAM3 grabbing non-integrin (DC-SIGN or CD209), complement receptor 1 (CR-1) as well as XC-chemokine receptor 1 (XCR1) are the most commonly studied surface receptors expressed on the dendritic cell surface (Macri *et al.*, 2016).

Among the above DCs surface molecules, DEC 205 and Clec9A are the most

studied. Targeting a variety of antigens to mice and human dendritic cells via anti-DEC 205 IgG monoclonal antibodies was found to elicit a strong antigen specific T cell activation *in vitro* (Birkholz *et al.*, 2010; Tsuji *et al.*, 2011). In addition, targeting antigen to DCs via anti-DEC 205 antibodies together with anti-CD40 antibodies as the dendritic cell activation agent induced the proliferation and differentiation of antigen-specific $CD8^+$ and $CD4^+$ T cells in mice (Hawiger *et al.*, 2001; Bonifaz *et al.*, 2002; Mahnke *et al.*, 2005; Boscardin *et al.*, 2006). It was reported by several groups that targeting antigens to mouse DCs via anti-Clec9A *in vivo* with and without anti-CD40 antibodies induced both $CD4^+$ T cell dependent antigen specific antibody response and $CD8^+$ T cell response (Caminschi *et al.*, 2008; Joffre *et al.*, 2010). A recent study in non-human primates showed that immunization with rat anti-Clec9A antibodies alone gave a strong anti-rat IgG antibody response (Li *et al.*, 2015).

It is worth noting that dendritic cell activation upon antigen targeting is essential for inducing antigen specific immune responses. In the presence of anti-CD40 antibodies, delivery of antigen via DEC 205 leads to T cell expansion, production of IFN-γ, export of T cells to peripheral tissues, and generation of a protective immune response (Bonifaz *et al.*, 2002; Bonifaz *et al.*, 2004; Neubert *et al.*, 2014). In contrast, delivery of antigens to DCs via anti-DEC 205 alone leads to the deletion of MHC class I–restricted T cells (Bonifaz *et al.*, 2002) and activation of regulatory T cells (Mantegazza *et al.*, 2008), resulting in the generation of T-cell tolerance. In some cases, delivering antigen to dendritic cells via anti-Clec 9A antibody led to activation of $Foxp3^+$ T cells, when the anti-CD40 antibody was absent (Joffre *et al.*, 2010). In fact, anti-CD40L antibody has been used extensively as a dendritic cell activation agent to induce a protective immune

response. For example, the CD40L-adjuvanted simian immunodeficiency virus (SIV) DNA vaccine induced enhanced antiviral humoral and cellular immunity, which conferred protection against a pathogenic SIV (Kwa *et al.*, 2014). Intranasal immunization with liposome encapsulated anti-CD40 antibodies and the peptide corresponding to a CTL epitope of influenza A virus nucleoprotein (NP) induced a mucosal CTL response, which reduced virus replication in the lung (Ninomiya *et al.*, 2002). Dendritic cell activation induced by anti-CD40 antibodies *in vivo* was found to correlate with the efficacy of peptide-based anti-tumor vaccines (Diehl *et al.*, 1999). Furthermore, the presence of anti-CD40 antibodies in the administration of tolerogenic peptide vaccine converted the immune tolerance into strong CTL response (Diehl *et al.*, 1999).

The critical role the CD40 cell signaling plays in the generation of a potent immune response upon vaccination indicates that CD40 on the dendritic cell surface is an attractive target for antigen delivery.

1.5.1 CD40 and CD40L

Murine CD40 is a 48 kDa type I transmembrane protein that belongs to the tumour necrosis factor (TNF) receptor superfamily. It contains a 21- amino acid (aa) leader sequence, a 193-aa-extracellular domain, a 22-aa transmembrane domain, and a 90-aa intracellular domain (62 aa in human) (van Kooten & Banchereau, 2000). CD40 is highly conserved between human and murine species sharing 62% amino acid identity for the entire coding sequence and 78% identity in the intracellular extension. The C-terminal 32 aa of human CD40 are identical to the mouse sequence. All 22 extracellular

cysteines are conserved between human and mouse, suggesting that CD40 from human and mouse are folded into the same protein structure (van Kooten & Banchereau, 2000). CD40 was first identified on the B cells surface, but is now known to be expressed by a variety of immune cells, including dendritic cells, macrophages, monocytes, and platelets, as well as different types of stoma cells includes myofibroblasts, fibroblasts, and epithelial and endothelial cells (van Kooten & Banchereau, 2000; Bishop & Hostager, 2003; Ma & Clark, 2009).

The ligand of CD40, known as CD154 or CD40L, is a type II transmembrane protein that also belongs to the TNF superfamily. The full size CD40L ranges from 32 kDa to 39 kDa depends on post-translational modifications. Human CD40L and mouse CD40L has 78% aa identity for the whole molecule, 75% identity in the extracellular domain, 96% in the transmembrane region and 81% in the cytoplasmic domains (van Kooten & Banchereau, 2000). The expression of CD40L is primarily restricted to T cells. Under certain inflammatory conditions, expression of CD40L can also be detected on macrophages, dendritic cells, activated B cells, platelets, mast cells, basophils, eosinophils, and NK cells (Karpusas *et al.*, 1995). The extracellular domain of CD40L can be found as a soluble form released by activated T cells (Graf *et al.*, 1995). The soluble form of CD40L exhibits similar functions and level of activities to the membrane-anchored form (Mazzei *et al.*, 1995). The CD40L monomers can naturally self-assemble around a threefold symmetry axis to form a noncovalent homotrimer that binds three receptor molecules (Fanslow *et al.*, 1994; Pullen *et al.*, 1999).

The binding of CD40L and CD40 has a strong effect on cell activities and plays an essential role in the survival of different types of cells (van Kooten & Banchereau,

2000). Upon binding of CD40L, CD40 clusters on the cell surface and induces the recruitment of adapter proteins known as tumor necrosis factor receptor-associated factors (TRAFs) to the CD40 cytoplasmic tail (Bishop *et al.*, 2007). To date, at least five TRAFs (1, 2, 3, 5, and 6) are known to associate with CD40 signalling. In dendritic cells, the recruitment of TRAFs after CD40 ligation leads to the expression of genes involved in cytokine production, co-stimulatory molecules expression and other maturation markers. The major TRAF recruited by dendritic cells upon CD40 signalling activation is TRAF6. The recruitment of TRAF6 results in the activation of p38 MAPK and JNK leading to the production of cytokines, such as TNF, IL-12p40 and IL-6 (Quezada *et al.*, 2004). As the result of the CD40 signalling, the dendritic cells mature and stimulate naïve T cells resulting in T cell activation and differentiation (Kooten & Banchereau, 1997).

It is well known that CD40 signalling on B cells plays an essential role in germinal center formation, immunoglobulin isotype switching, somatic hypermutation of the Ig, and plasma cell and memory B cell formation (Kooten & Banchereau, 1997). A defect of CD40L is responsible for X-linked hyper-IgM syndrome (X-HIM). Affected individuals are incapable of producing immunoglobulins of the IgG, IgA and IgE isotypes (Disanto *et al.*, 1993; Bajorath *et al.*, 1995). The mutation of S128 and E129 on the human CD40L in X-HIM patients prevents the binding of the CD40L to CD40 (Bajorath *et al.*, 1995). In addition, the mutation of Y145 and K143 of CD40L also significantly reduced its binding ability to CD40 compared to the wild type CD40L (Bajorath *et al.*, 1995).

1.5.2 Antigen targeting to CD40 via CD40L

The ability of CD40 signalling to induce dendritic cell to become fully competent antigen presenting cells ready for efficient antigen presentation and T cell priming, makes CD40 an excellent candidate for antigen-targeting. In additions, targeting antigen to CD40 using antibody constructs or CD40L can also facilitate the internalization of the delivered antigen to early-endosomes (Cohn *et al.*, 2013), which further facilitates antigen uptake upon targeting.

To date, antigens delivered to DCs via CD40 have been studied with protein based, DNA based, and virus based vaccine formulations. Subcutaneous, intraperitoneal and intravenous injections have been the most common administration method. Administering DCs treated with CD40-targeted tumor antigen, or direct intraperitoneal injection of the vector plasmid in mice has resulted in high levels of tumor-specific CTL responses against tumor antigen expressing cells (Williams *et al.*, 2012). CD40L has also been used to target the gp100 melanoma tumor antigen to dendritic cells. DNA vaccination with the SPD-gp100-CD40L plasmid together with plasmid coding for IL-12 and GM-CSF significantly reduced tumor growth and increased mice survival in a B16-F10 melanoma model (Gupta *et al.*, 2015). Similar results have also been reported in virus-based vaccination and protein-based vaccination models. Targeting Her-2/neu- or HPV type 16 E6/E7 adenoviruses to CD40 on DCs via CD40L results in an enhanced CTL response against human Her-2/neu- and HPV16 E6/E7-expressing tumors and improved tumor growth inhibition (Kim *et al.*, 2010). Immunization with nanoparticles (NP)-CD40L that co-encapsulated tumor antigen and TLR2 ligand Pam3Csk4 via subcutaneous injections induced antigen-specific $CD8^+$ T cell responses and enhanced

tumor control as well as prolonged survival of tumor-bearing mice (Rosalia *et al.*, 2015). Fusion proteins consisted of the anti-human CD40 antibody and a string of five highly conserved $CD4^+$ and $CD8^+$ T-cell epitope-rich regions of HIV-1 Gag, Nef and Pol induced the expansion of the antigen specific memory $CD4^+$ and $CD8^+$ T cells in HIV-infected patients' PBMC and DCs-T-cell co-cultures *in vitro* (Flamar *et al.*, 2013). Similar results have been reported in other studies that targeted different HIV antigens to DCs via CD40-CD40L interaction (Melchers *et al.*, 2011; Gupta *et al.*, 2014). Furthermore, in Hatzifoti and Heath's study, CD40 monoclonal antibody conjugated to a peptide of virus haemagglutinin, or a whole, killed virus vaccine and a split virus vaccine was more immunogenic than the antigen alone control group (Hatzifoti & Heath, 2007). Recently, Yin's group demonstrated that targeting antigen to CD40 induced an increase in the expansion of antigen-specific $CD8^+$ T cells by up to four fold compared with using other targeting receptors and was about 1000 times more efficient then using uncoupled antigen (Yin *et al.*, 2016).

The above examples clearly indicate that antigen targeting to CD40 is a promising approach to elicit an enhanced immune response.

1.6 Hypothesis and objective

Given findings indicating that targeting antigen to CD40 on dendritic cells via CD40L or anti-CD40 antibody can induce a protective immune response, this could be an excellent approach to enhance the immune response elicited by mucosal immunization in the oral cavity.

To the best of my knowledge, there are few studies that test this approach in

protein-based vaccines and it has not been tested in protein-based mucosal vaccination. Moreover, antigen targeting to CD40 has not been tested in any form in oral mucosal immunization.

1.6.1 Hypothesis

I hypothesized that targeting antigen to dendritic cells in oral mucosa via CD40-CD40L interactions can elicit an enhanced immune response.

1.6.2 Objective

To test the hypothesis, four objectives were designed.

Objective 1: To deign and construct DNA coding for the fusion protein containing the antigen and extracellular domain of the mouse CD40L as well as the DNA coding for the control proteins and clone them into *E. coli* and/or *S. gordonii* for protein expression.

Objective 2: To purify biological active antigen-targeting fusion proteins from either *E. coli* cell and/or *S. gordonii* culture supernatant and perform *in vitro* characterization.

Objective 3: To test the ability of the antigen-targeting fusion protein to induce an immune response in mouse oral cavity compared with the control protein.

Objective 4: To test the approach of targeting antigens to CD40 via CD40LS with *S. grodonii* based oral live mucosal vaccine.

Chapter 2: Materials and Methods

2.1 Bacteria and growth conditions

Bacterial strains used in this study are listed in Table 2.

2.1.1 *Escherichia coli*

E. coli strains were cultured aerobically in Luria-Bertani (LB) broth (1% tryptone, 0.5% yeast extract, and 1% NaCl, w/v) or Super Broth (1% MOPS [morpholinepropane-sulfonic acid], 3% tryptone, 2% yeast extract, w/v) at 37°C with shaking at 180 rpm. The parent strains of *E. coli* SG13009 and XL1-blue were grown in the presence of 50 μg/ml of kanamycin (BioShop, Burlington, ON) and 10 μg/ml tetracycline (Sigma-Aldrich, Oakville, ON, Canada), respectively. Recombinant *E. coli* carrying pComb3X or pQE-30 plasmid were grown in the presence of 100 μg/ml of ampicillin (BioShop) in addition to kanamycin or tetracycline. Cultures at late exponential phase of growth were stored in 1 ml aliquots in 25% (v/v) glycerol at -80℃ as stocks.

2.1.2 *Streptococcus gordonii*

All *S. gordonii* strains were cultured in tryptone-yeast extract-glucose (TYG) broth (1% tryptone, 0.25% yeast extract, 1% glucose and 1% K_2HPO_4, w/v) at 37°C and 5% CO_2 without shaking. *S. gordonii thyA::erm* mutant was grown in the presence of 20 μg/ml of thymidine (BioShop) and 10 μg/ml of erythromycin (BioShop). *S. gordonii* carrying OVA fusion protein genes were cultured without antibiotics. The overnight cultures were stored in 1 ml aliquots in 25% (v/v) glycerol at -80℃ as stocks.

Table 2 Bacterial strains used in this study

Bacterial strain	Characteristics	Source
S. gordonii		
S. gordonii thyA::ermAM	*thyA* gene interrupted by *ermAM* cassette	Lee *et al*., 2016
S. gordonii HppG (PRN-CD40LS)	HppG strain carrying *prn-cd40ls* gene	This study
S. gordonii DL1 (OVA-CD40LS)	DL1 strain carrying *ova-cd40ls* gene	This study
E. coli		
E. coli XL1-blue	Alpha complementation	Stratagene
E. coli XL1-blue (pComb3X OVA-CD40LS)	Carries pComb3X containing *ova-cd40ls* gene	This study
E. coli XL1-blue (pComb3X OVA-CD40LS$\Delta_{142\text{-}146}$)	Carries pComb3X containing *ova-cd40ls$\Delta_{142\text{-}146}$* gene	This study
E. coli XL1-blue (pComb3X rOVA)	Carries pComb3X containing *ova* gene	This study
E. coli XL1-blue (pQE-30 OVA-CD40LS)	Carries pQE-30 containing *ova-cd40ls* gene	This study
E. coli XL1-blue (pQE-30 rOVA)	Carries pQE-30 containing gene coding the C-terminus OVA	This study
E. coli SG13009	Contains pREP4 repressor plasmid	Qiagen
E. coli SG13009 (pComb3X OVA-CD40LS)	SG13009 strain carries pComb3X containing *ova-cd40ls* gene	This study
E. coli SG13009 (pComb3X OVA-CD40LS$\Delta_{142\text{-}146}$)	SG13009 strain carries pComb3X containing *ova-cd40ls$\Delta_{142\text{-}146}$* gene	This study

Table 2 Bacterial strains used in this study (continued)

Bacterial strain	Characteristics	Source
E. coli SG13009 (pComb3X rOVA)	SG13009 strain carries pComb3X with gene coding the C-terminus OVA	This study
E. coli SG13009 (pQE-30 OVA-CD40LS)	SG13009 strain carries pQE-30 containing *ova-cd40ls* gene	This study
E. coli SG13009 (pQE-30 rOVA)	G13009 strain carries pQE-30 containing gene coding the C-terminus OVA	This study

2.2 Agarose gel electrophoresis

DNA was electrophorezed on 0.8% (w/v) agarose gels in TAE buffer (Tri-acetate-EDTA buffer, 40 mM Tris base, 1 mM EDTA, and 0.1% (v/v) glacial acetic acid). The gel was placed in an electrophoresis tank filled with 1 X TAE buffer containing 0.5 μg/ml of ethidium bromide (Sigma-Aldrich) and run at 125 volts for 45 minutes and then examined under UV light using the UVP BioDoc-It Imaging System (Upland, CA, USA).

2.3 Polymerase chain reaction (PCR)

All genes used in this study were amplified by Taq DNA polymerase (New England Biolabs, ON, Canada). The 100 μl PCR reaction was set up in a 0.2 ml PCR tube by mixing the DNA template, primers, DNA polymerase, deoxyribonucleoside triphosphates (dNTP's), reaction buffer, and sterilized dH_2O. The volumes and final concentration of each component are listed in Tables 3. The conditions of PCR, performed in a Eppendorf Mastercycler EP S thermo-module, are described in Tables 4.

2.4 Construction of fusion protein genes

The primers used in this study are listed in Table 5. Plasmids constructed or used in this study are listed in Table 6. All enzymes used in this study were purchased from New England Biolabs. All restriction reactions were preformed at 37℃ for 1 h except for SfiI (50℃ for 1 h).

The construction of OVA fusion protein genes is depicted in Figure 1. Briefly, the DNA coding for the C-terminus fragment of OVA (rOVA) was amplified from pOVA-003 using primers SL1048/SL1049. The BamHI-restricted *ova* gene and similarly-

Table 3 PCR reactions with Taq DNA polymerase

Ingredients	Final concentration	Volume (µl) in 100 µl reaction
10 µM forward primer	0.5 µM	5
10 µM reverse primer	0.5 µM	5
10 x ThermoPol® Buffer (New England BioLabs)	1 x	10
dNTP mix (1 mM of each)	15 µM	1.5
Taq DNA polymerase (New England BioLabs, 5000 units/ml)	0.025 unit/µl	0.5
DNA template		1
H_20		77

Table 4 Thermocycling conditions for PCR

Steps	Temperature	Time
Initial Denaturation	95°C	1 min
30 Cycles	94°C	20 sec
	50°C	20 sec
	72°C	1 min/kb
Final Extension	72°C	5 min
Hold	4°C	

Table 5 Primers used in this study[1]

Primer	Nucleotide sequence	Description
SL 556	aatcgagctcagaggtgatgaggaccct c	Forward primer mouse CD40LS mutated BamHI, SstI
SL 626	gcgtgaattcttaatggtgatggtgatggt gctg	Revers primer of histidine tag, stop codon, SfiI
SL 655	ttggccgccctggcctcagagtttgagta agccaaaa	Revers primer of mouse CD40LS, stop codon, SfiI
SL 841	caggcatgcgaatcttggatcaatcctt	Forward primer for *S.gordonii thyA*+promoter, SphI
SL 1048	cctggcccaggcggccatgttgcctgat gaagtc	Forward primer for C-terminus region of Ovalbumin, SfiI
SL 1049	cctggccggcctggccggatcctggatg gtcagccctaa	Reverse primer of C-terminus region of ovalbumin, BamHI, SfiI
SL 1060	tacgaattcgttcaacagaagcagtctc	Reverse primer for 5' fragment of *sgo 1142*
SL 1092	cggactagtaccatgaaaabcaacttg	Reverse primer of CD40LS at A141, SpeI
SL 1093	Cggactagtggcccactgtagaacg	Forward primer of CD40LS at T147, SpeI
SL 1206	tacggatccatgttgcctgatgaag	Forward primer of OVA C-terminus, HindIII
SL 1207	tacaagctttggatggtcagccctaa	Reverse primer of OVA C-terminus, BamHI

[1] All primers were synthesized by Alpha DNA (Montréal, Québec).

Table 6 Plasmids used in this study

Plasmid	Characteristics	Source
pSec FHA-CD40LS-HA-1	pDL 276 plasmid backbone with streptococcal replication origin removed, HA tag removed, *xyl/tetO* promoter, SpaP signal sequence, *fha-cd40ls* fusion protein gene, kan^R	Lee *et al*., Unpublished
pOVA-003	Plasmid contains whole ovalbumin gene	Lee *et al*., Unpublished
pComb3X	Bacterial expression vector, *lacZ* promoter, OmpA signal sequence, C-terminus 6X His and HA tag, two SifI cloning sites, amp^R	(Barbas *et al.*, 2001)
pComb3X OVA-CD40LS	*lacZ* promoter, OmpA signal sequence, *ova-cd40ls* fusion protein gene, C-terminus 6X His and HA tag, amp^R	This study
pComb3X OVA-CD40LS$\Delta_{142\text{-}146}$	*LacZ* promoter, OmpA signal sequence, *ova-cd40ls*$\Delta_{142\text{-}146}$ fusion protein gene, C-terminus 6X His and HA tag, amp^R	This study

Table 6 Plasmid DNA used in this study (continued)

Plasmid	Characteristics	Source
pComb3X rOVA	*LacZ* promoter, OmpA signal sequence,*rova fragment* protein gene, C-terminus 6X His and HA tag, amp^R	This study
pComb3X PRN-CD40LS	*lacZ* promoter, OmpA signal sequence, *prn-cd40ls* fusion protein gene, C-terminus 6X His and HA tag, amp^R	This study
pQE-30	Bacterial expression vector, T5 promoter, N-terminus 6X His tag, BamHI and Hind III cloning sits, amp^R	Qiagen
pQE-30 OVA-CD40LS	T5 promoter, N-terminus 6X His tag, *ova-cd40ls* fusion protein gene, amp^R	This study
pQE-30 OVA-CD40LS$\Delta_{142\text{-}146}$	T5 promoter, N-terminus 6X His tag, *ova-cd40ls*$\Delta_{142\text{-}146}$ fusion protein gene, amp^R	This study
pQE-30 *r*OVA	T5 promoter, N-terminus 6XHis tag, *ova fragment* protein gene, amp^R	This study

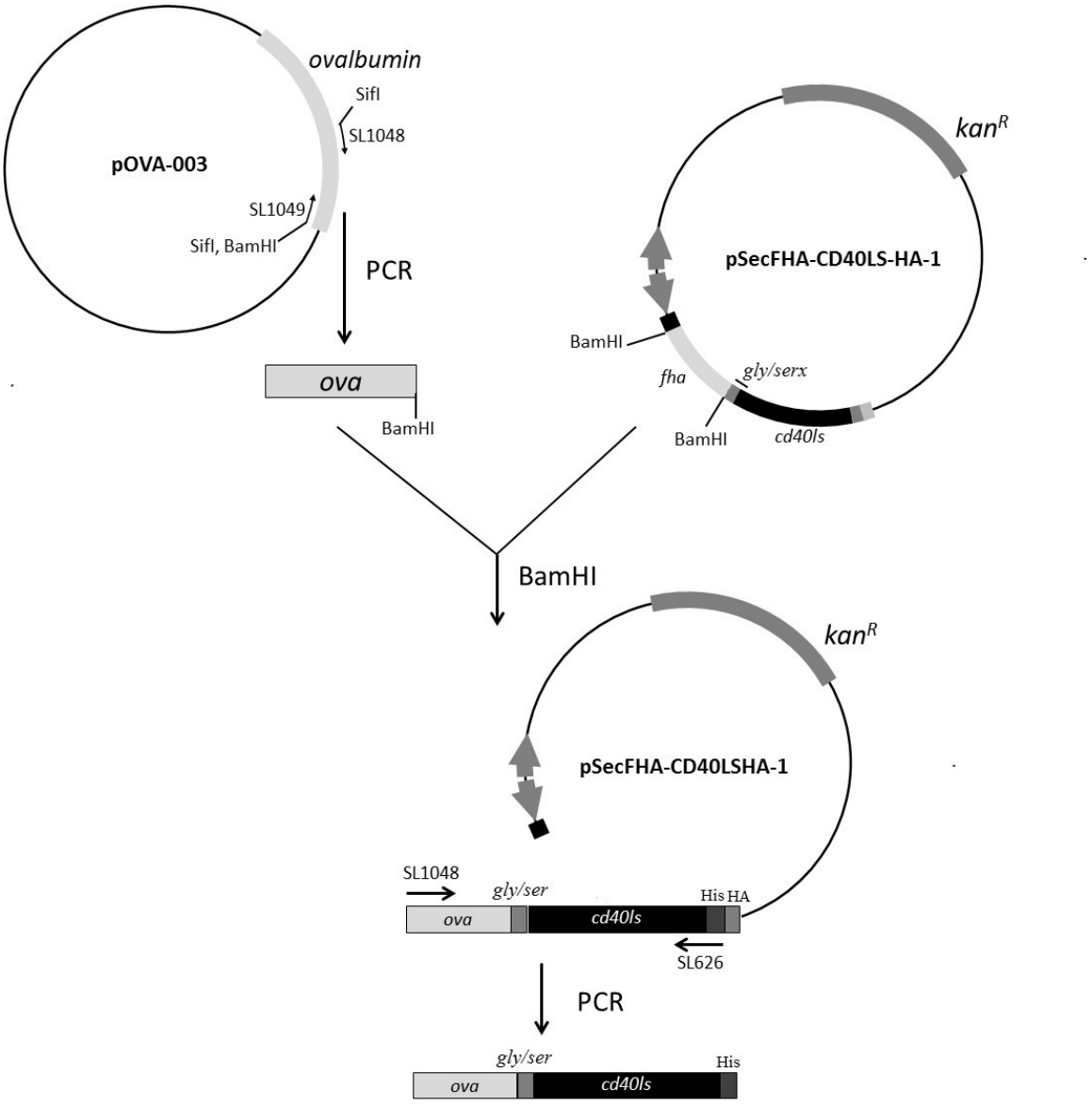

Figure 1 Construction of OVA-CD40L fusion protein gene

The *fha* gene was removed from the pSecFHA-CD40LS-HA-1 by BamHI digestion. The remaining plasmid backbone was ligated with BamHI restricted *ova.* The *ova-cd40ls* gene was then amplified by PCR. The intact *ova-cd40ls* gene consists of *ova*, *gly/ser* protein linker sequence (*gly/ser*), *cd40ls* and 3'end his tag sequence. Primers used for DNA construction and verification are indicated.

restricted pSecFHA-CD40LS-HA-1 were run on a 0.8% agarose gel and purified from the gel using the Mini Plus™ Plasmid DNA Isolation Kit (DNA Land Scientific, LA, USA) and subsequently ligated using T4 DNA ligase at room temperature for 16 h. The OVA-CD40LS fusion protein gene was then amplified from the ligated DNA by PCR with primers SL1048/SL626.

The *ova-cd40lsΔ*$_{142\text{-}146}$ gene, which contained the mutant *cd40ls* was constructed by deleting the DNA coding for 5 amino acids (amino acid residues #142 to #146 of mouse CD40L) from CD40LS (Figure 2). Briefly, DNA fragments before and after the deletion site were amplified from pComb3X OVA-CD40LS using primers SL1048/SL1093, and SL1092/SL626, respectively. Primers SL1093 and SL1092 introduced a new SpeI restriction site into the 'before' and 'after' DNA fragments. The two gene fragments were then restricted by SpeI (37℃, 1 h), and ligated. The mutated fusion protein gene was amplified from the ligation product by PCR with primers SL1048/SL626. The mutation was conformed by restriction analysis with SpeI.

2.5 Cloning gene constructs into *E. coli*

2.5.1 Transformation of $CaCl_2$-induced competent *E. coli* cells

Competent *E. coli* cells were prepared using $CaCl_2$ treatment. Two ml of overnight culture of *E. coli* XL1-blue (or SG13009) was added to 90 ml of LB broth containing appropriate antibiotics, and incubated until the OD_{600nm} of the culture reached 0.35. The cells were harvested by centrifugation at 10 000 x g for 10 min at 4℃. The cell pellet was washed with 100 ml of cold transformation buffer #1 (10 mM Tris, 150 mM NaCl, pH 7.5). The cells were gently re-suspended in 100 ml of cold transformation

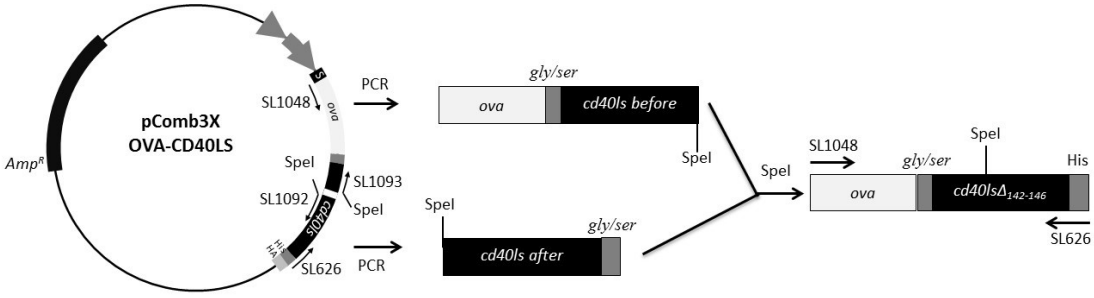

Figure 2 Construction of OVA-CD40LSΔ$_{142\text{-}146}$ DNA structures

The fusion protein gene construct consists of *ova*, gly/ser protein linker sequence (*gly/ser*), *cd40ls* $\Delta_{142\text{-}146}$ with SpeI restriction site ~200 bp away from 5' end of *cd40ls* $\Delta_{142\text{-}146}$, and the sequence for his tag. S: leading sequence; *cd40ls* before: *cd40ls* gene fragment before the deletion site; *cd40ls* after: cd40ls gene fragment after deletion site. Primers used for DNA construction and verification are shown.

buffer #2 (50 mM $CaCl_2$) and incubated on ice for 45 min. The cells were collected by centrifugation and re-suspended in 6 ml of transformation buffer #2 with 20% glycerol. The competent cells were divided into 220 µl aliquots and stored at -80℃.

Transformation was performed according to the method described by (Sambrook *et al.*, 1989). Briefly, 200 µl of *E. coli* competent cells and 100 µl of cold transformation buffer #3 (10 mM Tris, 50 mM $CaCl_2$, 10 mM $MgSO_4$, pH 7.5) were added to the DNA and incubated on ice for 45 min. The cells were then heat shocked at 37℃ for exactly 2 minutes followed by incubation at room temperature for 10 minutes. Five hundred µl of LB broth was added and the cells were incubated at 37℃ for 1 hour. The cells were then inoculated onto four LB agar plates containing the appropriate antibiotics and incubated overnight.

2.5.2 Plasmid DNA isolation from *E. coli*

One and a half ml of an overnight culture was centrifuged at 10 000 x g, 10 minutes, 4℃. The cell pellet was re-suspended in 100 µl of GTE buffer (50 mM glucose, 25 mM Tris-HCl, pH 8.0, and 10 mM EDTA). One hundred and eighty six µl of sterilized dH_2O with 1 µl of RNase (10 µg/µl) was added to the cell suspension and mixed by vortexing. Fourteen µl of lysis solution (10 µl 20% (w/v) SDS [sodium dodecyl sulfate], 4 µl 10 M NaOH) was then added and the cell suspension was inverted to mix once followed by 5 min incubation at room temperature. After that, 150 µl of cold potassium acetate (KAc) solution (60% of 5 M KAc, 11.5% of glacial acetic acid, and 28.5% of dH2O, v/v) were added and gently mixed with the cell lysate. The samples were then incubated on ice for 10 minutes and centrifuged for 5 minutes at 14,000 x g. The

resulting supernatant was transferred to a new microtube. The DNA was extracted once with chloroform. After centrifugation (10 000 x g, 5 min, 4℃), the top layer was collected into a new tube and the DNA was precipitated by adding 1 ml of cold 95% ethanol containing 2.5% KAc. The samples were incubated at -80℃ for 30 minutes and centrifuged (14 000 x g, 10 min, 4℃). The pellets were washed with 70% ethanol. The plasmid was vacuum-dried and dissolved in 20 µl of TE buffer (10 mM Tris-HCl, pH 7. 1 mM EDTA, pH 8).

2.5.3 Cloning fusion protein gene constructs into *E. coli*

The PCR amplified fusion protein genes were extracted with chloroform and cut with SfiI. The similarly restricted pComb3X or pQE-30 plasmids and fusion protein gene were gel purified and ligated. The ligated product was transformed into *E. coli* XL 1-blue cells. After 24 h, individual colonies were grown in 2 ml LB containing appropriate antibiotics and the plasmid from each colony was isolated and analyzed by restriction analysis and PCR. The plasmids with correct insert genes were isolated from the recombinant *E. coli* XL 1-blue and transformed into *E. coli* SG13009 for protein expression.

2.6 Expression of recombinant protein by *E. coli*

2.6.1 Small-scale recombinant protein production

Two ml of LB broth with appropriate antibiotics was inoculated with 20 µl of frozen stock culture of the recombinant *E. coli* and incubated. The next day, 100 µl of the overnight culture was added to one ml of fresh LB and incubated for 3 h. Then, 1 mM of

isopropyl-β-D-thiogalactoside (IPTG) was added to induce protein expression. After 3 h, the cells were collected by centrifugation at 10 000 x g at 4℃ for 10 min and boiled in 100 µl 1X SDS-PAGE sample buffer (5% (v/v) β-mercaptoethanol, 5% 0.5 M (w/v) Tris-HCl buffer (pH 8), 0.07 M SDS, 10% glycerol (v/v), and 0.6 mM bromophenol blue) for 5 min. After centrifugation at 10 000 x g for 3 min at 4℃, 2-5 µl of the boiled sample was used for sodium dodecyl sulfate polyacrylamide gel electrophoresis (SDS-PAGE) and western blotting analysis.

For analysis of proteins in *E. coli* cell lysate, the cell pellet was re-suspended in 0.2 ml phosphate-buffered saline (PBS) (8.7 mM Na_2HPO_4, 1.5 mM $NaH_2PO_4 \cdot H_2O$, 145 mM NaCl, 5 mM $MgCl_2 \cdot 6H_2O$). The cells were sonicated to 90% cell breakage and then centrifuged at 18 000 x g at 4℃ for 30 minutes. The supernatant was transferred into a new 1.5 ml microtube as the soluble fraction of *E. coli* cell lysate. The pellet, which was the insoluble fraction of *E. coli* cell lysate, was re-suspended in 200 µl 1 X SDS-PAGE sample buffer. Sixteen µl of the soluble and insoluble fractions was used for SDS-PAGE and western blotting.

2.6.2 Large-scale recombinant protein production

One hundred ml of super broth medium was inoculated with 100 µl of frozen stock culture of recombinant *E. coli* SG13009 and incubated overnight. The overnight culture was added into 900 ml fresh super broth and incubated until the culture reached mid-exponential phase of growth. Then protein expression was induced with I mM IPTG.

After 3 h IPTG induction, cells were collected by centrifugation at 10 000 x g at 4℃ for 10 min and stored at -80℃. The next day, the cell pellet was re-suspended in 10

ml PBS with 1 mM phenylmethanesulfonyl fluoride (PMSF). The cells were then sonicated. The insoluble protein fraction was collected by centrifugation at 27 000 x g at 4 °C for 30 minutes and the supernatant was discarded. The pellet was then re-suspended in 15 ml equilibration buffer (50 mM $NaH_2PO_4•H_2O$, 300 mM sodium chloride, 10 mM imidazole, pH 7) containing 8 M urea. After overnight incubation at 4℃, the insoluble materials were removed by centrifugation at 27 000 x g at 4 °C for 30 minutes and the supernatant was collected into a new tube. This centrifugation processes was repeated until a clear protein solution was obtained.

2.7 Cloning fusion protein gene constructs into *S. gordonii*

2.7.1 Construction of gene delivery constructs

The fusion protein gene was cloned into *S. gordonii* based on a delivery system *using* thymidylate synthase (ThyA) as a selection marker. ThyA is an enzyme that catalyzes the conversion of dUMP to dTMP and is essential for bacteria survival (Ahmad *et al.*, 1998). In order to deliver the fusion protein gene onto the chromosome of *S. gordonii*, a delivery gene construct consisting of the fusion protein gene and the *thyA* gene was constructed following the method described by Lee, *et al* (2016). The delivery gene constructs consisted of the intact *thyA* gene, gene of interest, and the gene fragment immediately downstream of *thyA* (5' fragment of *sgo1142*), and a *xyl/tetO* promoter. The recipient strain, *S. gordonii thyA::ermAM* mutant is a thymidine auxotroph and cannot survive without exogenous thymidine in the culture medium. Upon transformation, the transformants were selected in thymidine-free conditions. Following transformation, the fusion protein gene would integrate into the chromosome of *S. gordonii thyA::ermAM*

mutant through a double crossing-over event.

In this study, a previously constructed delivery gene construct (Lee *et al.*, 2016) was restricted with SfiI to remove the unwanted insert gene. Then, the PCR product of the recombinant protein gene was restricted with SfiI and ligated with the *thyA* gene and the *xyl/tetO* promoter-5'*sgo1142* (Figure 3). The whole gene construct was obtained from the ligated DNA by PCR with primers SL841/SL1060. The PCR product was then examined by agarose gel electrophoresis, extracted with chloroform and used for transformation.

2.7.2 Transformation of *S. gordonii thyA::ermAM*

Transformation of *S. gordonii* cells was performed using the protocol developed by (Perry & Kuramitsu, 1981). Four ml of TYG broth containing 5% (v/v) heat-inactivated fetal bovine serum (FBS, Invitrogen, Burlington, ON, Canada) and 10 µg/ml thymidine (transformation medium) were inoculated with 30 µl of frozen *S. gordonii thyA::ermAM* culture and incubated. The next day, 4 ml of pre-warmed transformation medium was inoculated with 100 µl of the overnight culture and incubated for 90 minutes. Then, 750 µl of the culture were transferred to a 1.5 ml microtube containing the PCR product and the culture was incubated for 30 min. Additional 750 µl of pre-warmed transformation medium was then added and the culture was incubated for another 90 minutes. The culture was then centrifuged and 1 ml of supernatant was discarded. The cell pellet was re-suspended in the remaining 500 µl supernatant and 100 µl of the suspension were plated onto TYG agar plates without antibiotic and thymidine. After 24-48 h incubation, colonies were replica-plated onto TYG agar plate with and without

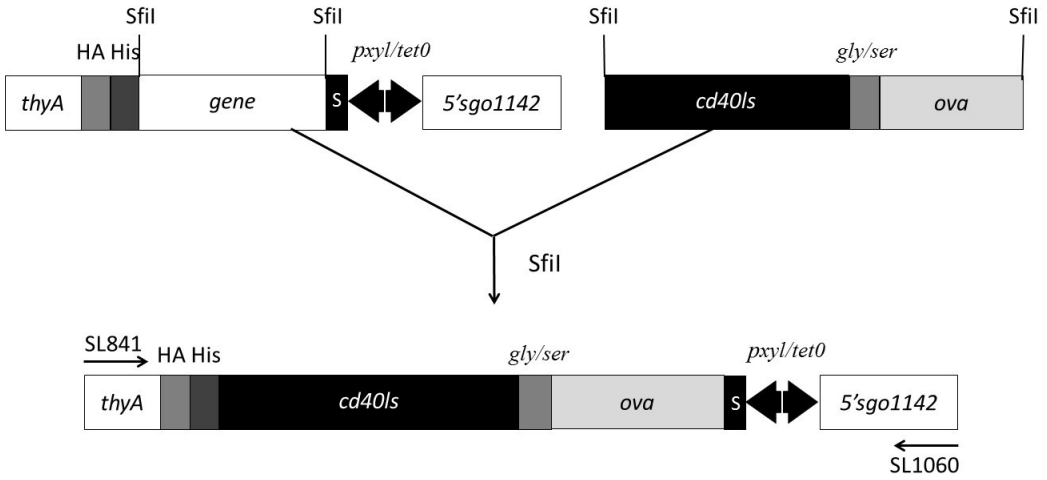

Figure 3 Construction of gene delivery construct for *S. godonii*

The gene delivery construct consisted of the complete *thyA* gene with 3' end HA tag and 6 x His, gene to be delivered, a signal sequence (S), *xyl/tetO* promoter gene (*xyl/tetO*), and a fragment of the *sgo1142* gene. The *ova-cd40ls* gene was ligated to the delivery construct via two rare-cutting SfiI sites. *gly/ser*: DNA coding for the gly/ser protein linker. Primers used for DNA construction and verification are indicated.

erythromycin. Colonies that were erythromycin-sensitive and thymidine-prototrophic were grown and chromosomal DNA were extracted and analyzed by PCR.

2.7.3 Chromosomal DNA extraction from *S. gordonii*

To extract chromosomal DNA, 1 ml of overnight *S. gordonii* culture was centrifuged (10 min, 10 000 x g, 4℃). The cells were re-suspended in 200 ul of TE buffer and 200 ul of chloroform, and 400 μm-glass beads (70 mg) was added. The tube was vortexed vigorously for 1 min and centrifuged at 10 000 x g, 4℃ for 5 min. The top (aqueous) layer containing the chromosomal DNA was collected into a new microtube. For PCR screening, 1 μl of the DNA extract was used as DNA template.

2.8 Analysis of recombinant protein production by *S. gordonii*

For screening purposes, proteins from 1 ml of *S. gordonii* culture supernatant were concentrated by trichloroacetic acid (TCA) precipitation. One ml of the culture supernatant was mixed with 0.4 ml of 20% (w/v) TCA (BioShop) and incubated on ice for 40 min. The precipitated proteins were collected by centrifugation at 10 000 x g, 4℃, 10 min and washed with 1 ml cold acetone. The proteins were dissolved in 20 μl of 1 X sample buffer and analyzed by SDS-PAGE and western blotting.

For protein purification purpose, 10 ml of TYG was inoculated with 50 μl of frozen culture of *S. gordonii* and grew overnight. Then, 1 liter fresh TYG was inoculated with the 10 ml overnight culture and 10 ng/ml (final concentration) of tetracycline was added to induce protein production overnight. Culture supernatant was obtained from the induced *S. gordonii* culture by centrifugation at 10 000 x g, 4℃, 10 min and proteins in

the culture supernatant was precipitated by 50% saturated ammonium sulphate at 4℃, overnight. The precipitated proteins were collected by centrifugation at 10 000 x g, 4℃, 10 min and dissolved in 10 ml PBS. The solution was dialyzed against 1 liter of PBS at 4℃ with 3 changes of buffer. The protein samples were stored on ice at 4℃ until purification.

2.9 Sodium dodecyl sulfate polyacrylamide gel electrophoresis (SDS-PAGE) and Western immunoblotting

SDS-PAGE was performed according to the protocol developed by (Laemmli, 1970). Protein samples were mixed with 1X sample buffer, boiled for 5 min, and then centrifuged at 10 000 x g for 5 min. Protein samples were analyzed on 15% SDS-PAGE gels. SDS-PAGE was conducted at 200 V for 45 minutes in a mini Trans-Blot cell (BioRad Laboratories, Mississauga, ON, Canada). The gels were stained with Coomassie Brilliant Blue staining solution (0.1% (w/v) coomassie brilliant blue R 250, 50% (v/v) isopropanol, 10% (v/v) glacial acetic acid, 40% (v/v) H_2O). The concentration of the purified fusion protein was determined by comparison with bovine serum albumin (BSA, Sigma-Aldrich) standards on the same gel using Image J software (National Institutes of Health, Bethesda, MD).

Western immunoblotting was performed according to the method described by Tobin *et al.,* (1979). Antibodies used are given in Table 7. After electrophoresis, the gel was placed on a piece of nitrocellulose membrane (0.45 μM) that was pre-wetted with 1 X transfer buffer (0.025 M Tris base, 0.192 M glycine, 0.1% SDS (w/v), 20% methanol (v/v)) and then sandwiched between two pieces of filter paper. Proteins were transferred onto the nitrocellulose membrane at 200 mA for 1 hour and then the membrane was

blocked with 1% (w/v) gelatin in PBS with 0.1% (v/v) tween (PBST). The membrane was then incubated with the primary antibody at 4℃. The next day, the membrane was washed five times with PBST and then incubated with the alkaline phosphatase conjugated secondary antibody for 1 hour at room temperature. The blots were then washed five times with PBST and developed with 33 µl of 5-bromo-4-chloro-3-indoyl phosphate (BCIP) (50% (w/v) BCIP in dH2O) and 66 µl of nitroblue tetrazolium (NBT) (50% (w/v) NBT, 70% (v/v) dimethyl-formamide) in 10 ml of alkaline phosphatase buffer (0.01 mM $MgCl_2$•$6H_2O$, 0.1 M NaCl, and 0.2 M Tris-HCl, pH 9.8). The immunoblots were covered with aluminum foil and developed at room temperature on a rocker until the desired band intensity was obtained.

2.10 Protein purification

Fusion proteins expressed by *E. coli* or *S. gordonii* were purified or attempted to be purified via different approaches depends on the properties of the fusion proteins. The purified fusion proteins were then quantified via SDS-PAGE and Image J analysis. Aliquots of the purified protein were freeze-dried for long-term storage at -20℃.

2.10.1 Nickel affinity chromatography

In this study, His60 Ni superflow resin (Clontech, CA, USA) and Profinity™ IMAC resin (BioRad Laboratories) were used to purify his-tagged recombinant protein from *E. coli*. The His60 Ni superflow resin was used for the purification of rOVA and OVA fusion protein produced by *E. coli* from the pComb3X expression vector, as well as the PRN-CD40LS from *S. gordonii*. The IMAC resin was used for the purification of

Table 7 Antibodies used in western blotting

Antibody	Characteristics	µg/ml	Dilution	Source
Rabbit anti-OVA	Polyclonal, whole antiserum	NA	1:1000	Sigma-Aldrich
Goat anti-rabbit IgG	Polyclonal, against the whole IgG, Alkaline phosphatase conjugate	NA	1:3000	Sigma-Aldrich
Mouse anti-His	Monoclonal	1000	1:2000	Abm
Goat anti-mouse IgG	Polyoclonal, against the whole IgG, Alkaline phosphatase conjugate	NA	1:3000	Sigma-Aldrich
Rat anti-mouse CD40L biotin	Monoclonal, Biotinylated	500	1:500	R&D
ExtrAvidin	Alkaline phosphatase conjugate	NA	1:60000	Sigma-Aldrich

rOVA and OVA-CD40LS produced by *E. coli* from the pQE-30 expression vector. To pack a nickel affinity column, a thin layer of cotton was placed into a 10 ml syringe. The syringe was then filled with three ml of either the His60 Ni superflow resin or the IMAC resin. A piece of short plastic tubing was connected to the syringe and a clamp was used to control the liquid flow.

Three refolding approaches were used to refold the purified recombinant protein from nickel affinity column chromatography. The first approach was to refold the protein by stepwise dialysis following purification under denatured condition (Figure 4A). The His60 Ni superflow resin or IMAC Resin column was first equilibrated with 10 column volumes of equilibration buffer (300 mM NaCl, 50 mM $NaH_2PO_4 \bullet H_2O$, 10 mM imidazole, pH 7) containing 8 M urea. The protein sample was then passed through the column three times and the final flow-through was collect as unbound fraction. The column was washed with 20 ml equilibration buffer with 8 M urea. Endotoxin was then removed by washing the column with 20 ml of 0.1% (v/v) Triton X-114 in equilibration buffer with 8 M urea. The Triton X-114 was then removed from the column with 20 ml of endotoxin free wash buffer (300 mM NaCl, 50 mM $NaH_2PO_4 \bullet H_2O$, pH 7, 40 mM imidazole) with 8 M urea. The his-tagged recombinant protein was then eluted with 10 ml cold elution buffer containing 8 M urea and collected in 1 ml fractions. The protein concentration in each fraction was examined by SDS-PAGE and image J analysis. The fractions were then combined and the denatured fusion protein was refolded (renatured) by stepwise dialysis under endotoxin-free conditions. Briefly, the combined fractions were dialyzed against 500 ml of 6 M urea in PBS (urea-PBS) for 4 h at 4℃ followed by 500 ml of 4 M urea-PBS for 4 h. Then the protein was dialyzed against 500 ml 2 M

A

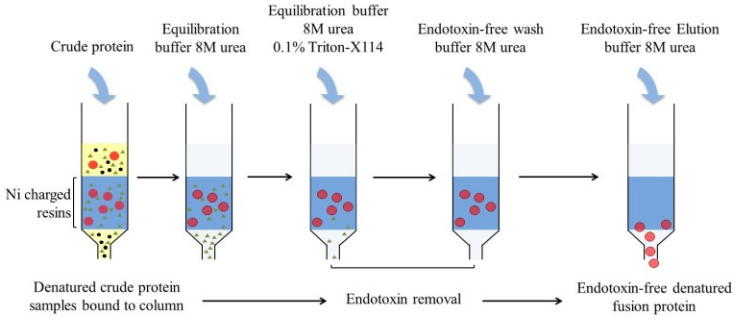
Crude protein
Equilibration buffer 8M urea
Equilibration buffer 8M urea 0.1% Triton-X114
Endotoxin-free wash buffer 8M urea
Endotoxin-free Elution buffer 8M urea
Ni charged resins
Denatured crude protein samples bound to column
Endotoxin removal
Endotoxin-free denatured fusion protein

B

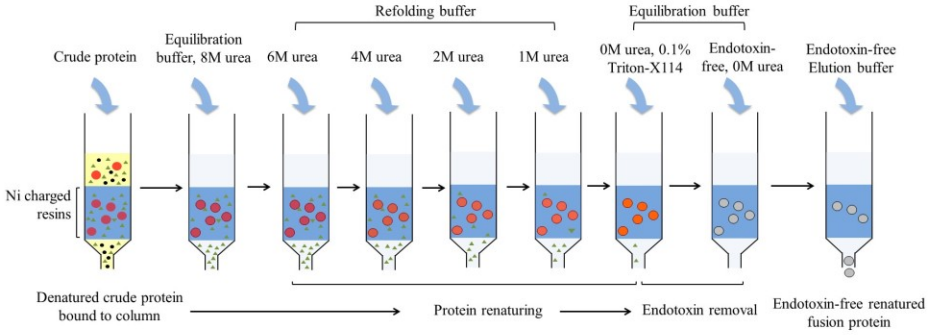
Refolding buffer
Equilibration buffer
Crude protein
Equilibration buffer, 8M urea
6M urea
4M urea
2M urea
1M urea
0M urea, 0.1% Triton-X114
Endotoxin-free, 0M urea
Endotoxin-free Elution buffer
Ni charged resins
Denatured crude protein bound to column
Protein renaturing
Endotoxin removal
Endotoxin-free renatured fusion protein

C

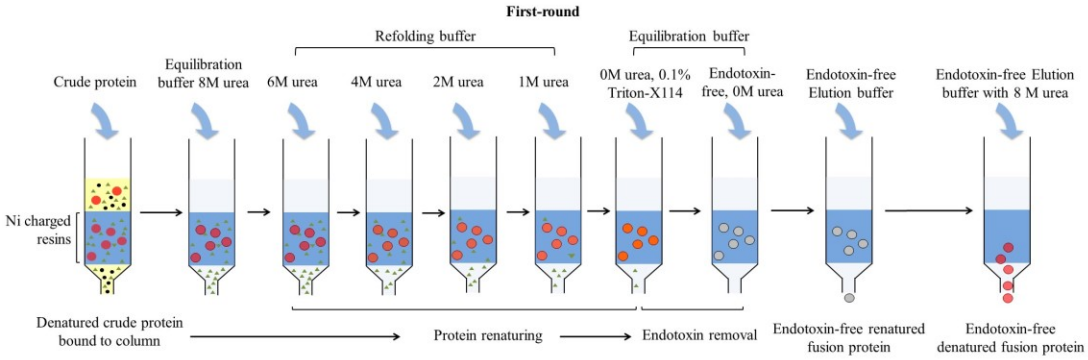
First-round
Refolding buffer
Equilibration buffer
Crude protein
Equilibration buffer 8M urea
6M urea
4M urea
2M urea
1M urea
0M urea, 0.1% Triton-X114
Endotoxin-free, 0M urea
Endotoxin-free Elution buffer
Endotoxin-free Elution buffer with 8 M urea
Ni charged resins
Denatured crude protein bound to column
Protein renaturing
Endotoxin removal
Endotoxin-free renatured fusion protein
Endotoxin-free denatured fusion protein

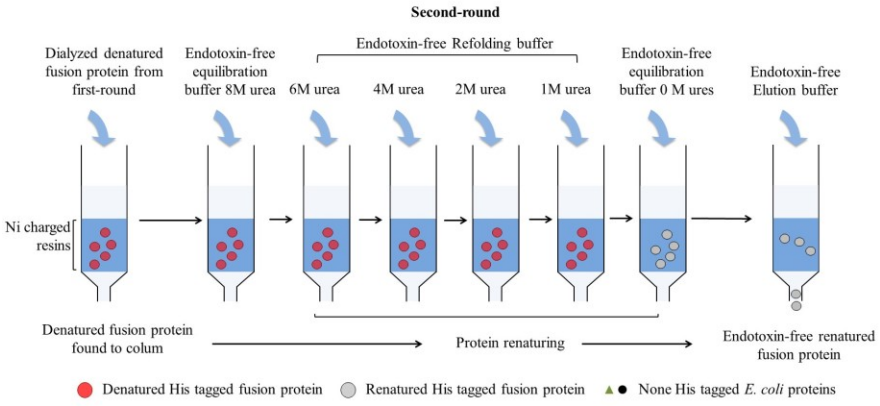
Second-round
Endotoxin-free Refolding buffer
Dialyzed denatured fusion protein from first-round
Endotoxin-free equilibration buffer 8M urea
6M urea
4M urea
2M urea
1M urea
Endotoxin-free equilibration buffer 0 M ures
Endotoxin-free Elution buffer
Ni charged resins
Denatured fusion protein found to colum
Protein renaturing
Endotoxin-free renatured fusion protein
Denatured His tagged fusion protein
Renatured His tagged fusion protein
None His tagged E. coli proteins

Figure 4 Purification of his-tagged fusion proteins by nickel affinity column chromatography coupled with endotoxin removal

His-tagged fusion proteins were purified (A) under denatured condition, (B) with on-column refolding, or (C) with “two-rounds” on-column protein refolding approaches.

urea-PBS for 4 h at 4℃. Finally, the protein was dialyzed against 1 liter of PBS at 4℃ to remove the residual urea. Any precipitates were removed from the refolded protein sample by centrifugation at 10 000 x g, 4℃, 15 min. SDS-PAGE coupled with Image J analysis was used to estimate the concentration of the refolded fusion protein.

The second approach was to purify the recombinant protein via on-column protein refolding (Figure 4B). The His60 Ni superflow column was first equilibrated with 10 x column volume of equilibration buffer containing 8 M urea. The crude protein sample was passed through the column three times and the final flow-through was collect as the unbound fraction. The column was washed with 5 ml of equilibration buffer with 8 M urea. The fusion proteins were then refolded on the column by washing the column sequentially with 5 ml aliquots of refolding buffers (300 mM NaCl, 50 mM $NaH_2PO_4•H_2O$ pH 7, 10 mM imidazole, 1 mM oxdized glutathione, 3 mM reduced glutathione) containing decreasing concentrations (6 M, 4 M, 2 M, 1 M) of urea. Then the column was washed with 20 ml of cold equilibration buffer with 0.1% (v/v) TritonX-114 to remove the endotoxin. The remaining TritonX-114 was washed off from the column with another 20 ml cold endotoxin-free equilibration buffer. The refolded protein was eluted with 10 ml endotoxin-free elution buffer (300 mM NaCl, 50 mM $NaH_2PO_4•H_2O$ pH 7, 300 mM imidazole) and collected in 0.5 ml fractions.

The third approach used was a ‘two-rounds’ on-column protein refolding (Figure 4C). The ‘first-round’ purification was the same as the on-column protein refolding described above except that an IMAC resin column was used. Following elution, the protein remained on the column after purification was eluted with 30 ml of endotoxin-free elution buffer with 8 M urea and collected as 8 M urea protein eluate. Then, the

eluted protein was dialyzed against 1 liter of equilibration column buffer containing 8 M urea but no imidazole to remove the imidazole from the sample. The same column used in the first run was equilibrated with endotoxin-free equilibration buffer containing 8 M urea and the dialysed protein was applied to the column and refolded on the column as described above under endotoxin-free condition. The column was then washed with 20 ml equilibration buffer. The recombinant protein was eluted with 10 ml elution buffer and collected in 0.5 ml fractions.

2.10.2 Hydrophobic interaction chromatography

Phenyl-sepharose column chromatography was used to purify recombinant proteins based on the hydrophobic properties of the proteins. In this study, this column chromatographic method was used mainly for protein on-column refolding purpose (Figure 5). The recombinant proteins were first isolated from the crude *E. coli* cell lysate by nickel affinity column chromatography under denatured and endotoxin-free condition as described above. NaCl was then added to the isolated denatured protein sample to a final concentration of 2 M, which allow the proper binding of the protein to the column resin. The column containing 10 ml phenyl-sepharose resin (GE Healthcare Life Science, Mississauga, ON, Canada) was equilibrated with 30 ml of 50 mM Tris-HCl buffer, pH 7, 2 M NaCl and 8 M urea. The protein sample was passed through the column twice and the flow-through was collected as the unbound fraction. The protein was refolded on the column by washing sequentially with 10 ml aliquots of 2 M NaCl, 50 mM Tris-HCl buffer (pH 7) containing decreasing concentrations (6 M, 4 M, 2 M, 1 M) of urea. The protein was eluted with 50 mM Tris-HCl buffer with a stepwise pH gradient from 7 to 11

with 1 pH unit increments. For the purification of proteins from endotoxin-free sample, the column was prewashed with 30 ml of 0.1% (v/v) TritonX-114 in 50 mM Tris-HCl buffer, pH 7, followed with 30 ml endotoxin-free 0.5 mM (w/v) Tris-HCl buffer, pH 7.

2.10.3 Preparation of endotoxin-free equipment and buffers

All glassware and equipment made with metal used in this study were baked overnight in an oven at 185℃ to remove the endotoxin contamination. For the equipment that was heat sensitive, such as pH electrode, endotoxin was removed by washing with 0.1% (v/v) 0.1% TritonX-114 followed by washing with endotoxin-free water. Endotoxin was also removed from dialysis tubings as follow: dialysis tubings were washed with 250 ml 0.1% TritonX-114-H_20 with slow stiring at 4℃ for at least 4 h. Then the tubings were washed with 250 ml endotoxin-free water with slow stiring at 4℃. The endotoxin-free water was changed at least twice during the final washing step. To prepare endotoxin-free buffers, chemicals were weighed in to pre-baked grass beaker or new plastic falcon tubes and dissolved in endotoxin-free water.

2.11 Cells

2.11.1 Generation of bone marrow-derived dendritic cells

Bone marrow-derived dendritic cells (BMDCs) were generated from female BALB/c mice following the method described by (Lutz *et al.*, 1999) with modifications. On day 0, femurs and tibiae were cleaned of surrounding muscle tissues and the intact bones were left in 70% ethanol for 10 sec and washed with sterile PBS. Then both ends of the bones were cut with a scalpel and the marrow was flushed out with PBS using a

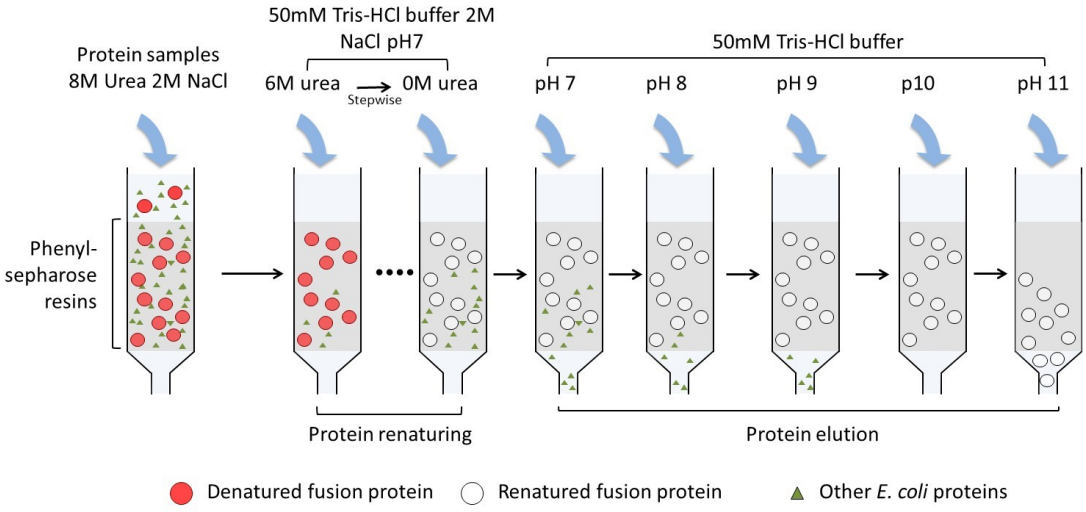

Figure 5 Protein refolding on hydrophobic interaction chromatography

syringe with a 26-gauge needle. The marrow was mixed by vigorous pipetting and then passed through a 70 μm-pore-size cell strainer (Corning incorporated, Corning, NY, USA) to obtain a suspension with mostly single cells. The cells were seeded at 0.2 million per ml of RPMI medium with L-glutamine (Wisent Bioproducts, QC, Canada) supplemented with 10% heat-inactivated FBS, 2% HEPES (Wisent Bioproducts), 1% penicillin-streptomycin (Wisent Bioproducts), 0.003% (v/v) β-mercaptoethanol (Sigma-Aldrich), and 10 ng/ml of recombinant murine granulocyte macrophage colony-stimulating factor (rmGM-CSF, Sigma-Aldrich) in 10 cm tissue culture dishes (15 ml/dish) (Corning Inc., Corning, NY, USA). Cells were incubated at 37°C with 5% CO_2. On day 3, an equal volume of fresh growth medium was added to each plate. On day 6, half of the culture from each plate was collected, centrifuged, and the cell pellet was re-suspended in 15 ml fresh growth medium, and then returned to the original plate. On day 8, the non-adherent cells were suspended in the culture medium by repeated pipetting and then transferred into 50 ml falcon tube. The cells were then collected by centrifugation (1500 rpm, 10 min, 4°C) and used for subsequent experiments.

2.11.2 BMDCs stimulation

BMDCs (1 ml/well, 1 x 10^6 cells) were seeded in Costar® 24-well, flat-bottomed cell culture plates (Corning). The cells were stimulated with 0.5 μg and 0.25 μg of native or heat-inactivated fusion protein in triplicates. The heat-inactivation treatment was done by heating the protein samples in a boiling water bath for 5min. Plates were incubated for 24 h at 37℃, 5% CO_2. The culture supernatants were collected for cytokine ELISA and the cells were detached from the bottom of the plate with a cell scraper and collected by

centrifugation. The cells were then used for flow cytometry analysis.

2.11.3 Preparation of spleen cells

Mice were euthanized and the spleens were placed in 0.5 ml RPMI with 5% FBS (RPMI-FBS). Each spleen was then transferred to a sterile petri dish containing 5 ml of RPMI-FBS. The spleen was then mashed between two frosted glass slides and the slides were then rinsed with 5 ml RPMI-FBS. The cell suspension was transferred to a 50 ml falcon tube and the petri dish was washed with 10 ml of RPMI-FBS. To eliminated red blood cells, the cells were centrifuged (1500 rpm, 10 min, 4°C) and re-suspended in 4 ml ACK buffer (150 mM NH_4Cl, 10 mM $KHCO_3$, and 0.1 mM EDTA) and incubated at room temperature for exactly 5 minutes. Then, 20 ml of RPMI-FBS was added to stop lysis. After centrifugation (1500 rpm, 10 min, 4°C), the cells were re-suspended in 10 ml growth medium (RPMI medium with L-glutamine supplemented with 10% heat-inactivated FBS, 2% HEPES, 1% penicillin-streptomycin, and 0.003% β-mercaptoethanol) and were passed through a 40 µm cell strainer to obtain a single cell suspension. The cells were then counted using a hemocytometer and used for subsequent experiments.

2.11.4 Splenocytes stimulation

Splenocytes were seeded (1 x 10^6 cells/well) in Costar® 96-well, flat-bottomed cell culture plates (Corning). The cells were stimulated with 20, 10, and 1 µg/ml of purified rOVA, or 200 ng/ml of OTII peptide (AnaSpec, Inc, Fremont, CA, USA) in triplicate. The plates were incubated for 72 h at 37℃. The culture supernatants were then

collected for cytokine ELISA.

2.12 Enzyme-linked immunosorbent assay (ELISA)

Antibodies used are listed in Tables 8 and 9.

ELISAs were used to test the function of fusion proteins in binding to human CD40 and the detection of OVA-specific antibodies in sera and saliva. For the human CD40 binding assay, Costar® medium binding 96-well flat-bottom polystyrene microtiter plates (Corning) were coated with 0.1 μg/well of human CD40 (GenScrit, NJ, USA) in 0.2 M sodium phosphate buffer, pH 7, at 4℃. The next day, the plates were blocked with 1% BSA in PBST for 1 h at 30℃, and then the fusion proteins (100 ng/well) were added in duplicate. The plates were incubated at 4°C overnight and then washed with PBST, and the bound fusion proteins was detected with the rabbit anti-OVA antibody and alkaline phosphatase conjugated goat anti-rabbit IgG.

For the detection of OVA-specific antibodies in sera and saliva, 96-well flat-bottom polystyrene microtiter plates were coated with 100 ng/well of ovalbumin (Sigma-Aldrich) in 0.2 M sodium phosphate buffer, pH 7 and incubated at 4℃. The next day, the plates were washed twice with PBST and blocked with 1% (w/v) gelatin in PBST for 2 h at room temperature. Two-fold diluted sera or saliva were then added and the plates were incubated at 4℃ overnight. IgG antibodies were detected with the alkaline phosphatase-conjugated goat anti-mouse IgG. IgA antibodies were detected with the biotinylated goat anti-mouse IgA, followed by ExrAvidin-alkaline phosphatase conjugate. IgM antibodies were detected with the alkaline phosphatase-conjugated goat anti-mouse IgM. All antibodies used for OVA-specific antibodies detection were diluted in PBST. The ELISA

Table 8 Antibodies used in binding ELISA and antibody ELISA

Antibody	Characteristics	μg/ml	Dilution	Source
Rabbit anti-OVA	Polyclonal, whole antiserum	NA	1:1000	Sigma-Aldrich
Rabbit anti-mouse IgM	Polyclonal, μ-chain specific	NA	1:30000	Sigma-Aldrich
Goat anti-rabbit IgG	Polyclonal, against the whole IgG, alkaline phosphatase conjugate	NA	1:3000	Sigma-Aldrich
Mouse anti-IgG_1	Monoclonal	1000	1:8000	Southern Biotechology
Mouse anti-IgG_{2a}	Monoclonal	1000	1:8000	Southern Biotechology
Mouse anti-IgA Biotin	Monoclonal, Biotinylated	500	1:8000	Southern Biotechology
Rat anti-mouse CD40L biotin	Monoclonal, Biotinylated	500	1:500	R&D
Goat anti-mouse IgG	Polyoclonal, against the whole IgG, alkaline phosphatase conjugate	NA	1:3000	Sigma-Aldrich
Goat anti-mouse IgM	Polyoclonal, against the whole IgM, alkaline phosphatase conjugate	NA	1:3000	Sigma-Aldrich
ExtrAvidin	Alkaline phosphatase conjugate	NA	1:60000	Sigma-Aldrich

Table 9 Antibodies used in cytokine ELISA

Antibody	Clone	Characteristics	µg/ml	Dilution	Source
Anti-mouse IL-6	6B4 IGH 54	Capture Ab	500	1:500	eBioscience
Anti-mouse IL-6 Biotin	MP5-32C11	Detection Ab	500	1:500	eBioscience
Anti-mouse TNF-alpha	TN3-19.12	Capture Ab	500	1:250	eBioscience
Anti-mouse TNF-alpha Biotin	Polyclonal	Detection Ab	500	1:500	eBioscience
Anti-mouse IFN-γ	XMG1.2	Capture Ab	500	1:1000	eBioscience
Anti-mouse IFN-γ Biotin	R4-6A2	Detection Ab		1:500	eBioscience
Anti-mouse IL-13	eBio13A	Capture Ab	500	1:250	eBioscience
Anti-mouse IL-13 Biotin	eBio1316H	Detection Ab	500	1:500	eBioscience

plates were developed with 1 mg/ml *p*-nitrophenyl phosphate (pNPP) in diethanolamine buffer (10% (v/v) diethanolamine, 1 mM $MgCl_2$, pH 9.8) and read with a microplate reader (Synergy HT; BioTeK®, USA) at 405 nm. The titers of antibodies were expressed as the reciprocal of the dilutions that produced an A_{405} reading 0.05 higher than that of the preimmune samples.

For the quantification of total serum IgM, 96-well plates (Maxisorp, Nunc Thermo scientific, US) were coated with capture antibodies for mouse IgM diluted in PBS and incubated at 4℃. The next day, the plates were washed twice with PBST and then blocked with 2% (w/v) BSA in PBS for 2 h at room temperature. The plates were washed twice and the diluted serum samples or the standards (mouse IgM) were added. The plates were incubated at 4℃. The next day, the plates were washed 4 times with PBST. The detection antibody that diluted in PBST was then added and the plates were incubated at 4℃ overnight. Then the plates were washed 4 times and developed with pNPP as described above. The mean absorbance (y axis) was plotted against the standard protein concentration (x axis) to create a standard curve. The concentration of the total IgM in each serum sample was then calculated.

Cytokine ELISA was preformed to determine the concentration of the cytokines produced by BMDCs or splenocytes. Briefly, 96-well plates (Maxisorp, Nunc Thermo scientific) were coated with capture antibodies diluted in coating buffer (0.1 M $NaHCO_3$, 0.5 M NaCl, pH 9.6), and incubated at 4℃. The next day, the plates were washed twice with wash buffer (PBS with 0.05% Tween 20) and then blocked with 2% (w/v) BSA in PBS for 2 h at room temperature. The plates were washed twice and samples or standards were added. The plates were incubated at 4℃. The next day, the plates were washed 4

times with wash buffer. The detection antibody diluted in ELISA assay buffer (0.2% BSA in PBS with 0.05% Tween 20 used for TNF and IL-6; 0.1% BSA in PBS with 0.05% Tween 20 used for IFN-gamma and IL-13) was then added. The plates were incubated for 1 h at room temperature and then washed 4 times. The plates were then incubated with streptavidin-horseradish peroxidase (1/200 in 1% (w/v) BSA in PBS) (R&D system, Minneapolis, MN, USA) for 30 min at room temperature. Finally, after 7 washes, substrate (R&D system, Minneapolis, MN, USA) was added and the plates were incubated for 30 min and the colour development was stopped by the addition of 0.3 M H_2SO_4. The plates were read at $A_{450\ nm}$ using a microplate reader (Synergy HT).

2.13 Flow cytometry

To evaluate the expression of cell surface maturation makers, BMDCs were analyzed by flow cytometry after stimulation for 24 h. The information of reagents used in cell surface marker staining is shown in Table 10.

2.13.1 Cell staining

Cells were detached from tissue culture plates using cell scrapers. Cells from each well were transferred into individual 1.5 ml microtubes and then counted. Cells were then seeded in triplicate in a 96 well V-bottom microplates (Corning) at a concentration of 3×10^5 cells/well, which was used for three color staining. The remaining cells from all the treatment groups were combined and seeded at 3×10^5 cells/well. These cells were used for single color staining control, isotype control, and non-staining control. The cells were then washed with 200 µl/well fluorescence-activated

Table 10 Antibodies used for flow cytometry.

Antibody	Clone	Characteristics	µg/ml	Dilution	Source
Anti-mouse CD16/CD32	93	F_C receptor blocker	NA	NA	eBioscience
APC hamster anti-mouse CD11C	HL3		200	1:200	BD biosciences
APC hamster IgG_1, λ1	G235-2356	APC isotype control	200	1:200	BD biosciences
PE hamster anti-mouse CD80 (B7-1)	16-10A1		200	1:100	BD biosciences
PE hamster anti-mouse IgG_{2a},κ	B81-3	PE-isotype control (Hamster)	100	1:100	BD biosciences
PE rat anti-mouse CD86 (B7-2)	GL1		200	1:100	BD biosciences
PE rat anti-mouse IgG_{2a},κ	R35-95	PE isotype control (rat)	100	1:100	BD biosciences
FITC rat anti-mouse I-A/I-E (MHC II)	2G9		500	1:1000	BD biosciences
FITC rat anti-mouse IgG_{2a},κ	R35-95	FITC isotype control	500	1:1000	BD biosciences

cell sorting (FACS) staining buffer (PBS containing 1% (v/v) FBS and 0.1% (w/v) sodium azide) and centrifuged at 1800 rpm, 3 min, 4℃. Anti-mouse CD16/CD3 (F_C blocker) was added at 2 µl/10^6 cells and the cells were incubated on ice for 5 min. After washing twice with FACS staining buffer, the cells from each treatment group were stained with antibodies against CD80, CD86, and MHC II. Singlet of the combined cell was stained for single color stain, isotype control for each color, and non-staining cell control. After 30 min incubation at 4℃ in the dark, the excess antibodies were removed from the plate and the cells were washed twice with FACS staining buffer. Cells were then fixed with 0.5% (v/v) paraformaldehyde solution (200 µl/3 x 10^5 cells) and transferred into conical FACS tubes (Corning incorporated, Corning, NY, USA). The samples were storage at 4℃ in dark and analyzed the next day.

2.13.2 FACS analysis

A BD FACSCalibur™ flow cytometer (Becton Dickinson, San Jose, CA) configured with 488 nm and 633 nm was used to analyze the single cells. Data were analyzed with FCS Express 4 (De Novo Software, CA, USA).

2.14 *In vivo* experiments

2.14.1 Animals

Female BALB/c mice (Charles River Laboratory, St. Constant, QC, Canada), 5 week-old were housed in groups of 5 animals in conventional type II cages containing nesting material along with water and food supply.

2.14.2 Intramucosal injection in oral cavity

Mice were sedated with ketamine-xylazine (60% Ketamine (100mg/ml), 30% Xylazine (100mg/ml), and 10% sterile dH_2O). The freeze-dried OVA-CD40LS and rOVA were dissolved in endotoxin-free water to a final concentration of 50 µg /ml. Another aliquot of OVA-CD40LS, also at a concentration of 50 µg /ml, but contained 2% (v/v) alum as an adjuvant was prepared and incubated at 4℃ overnight. One µg (20 µl) of the protein was injected into the mucosal layer of the left inside corner of the mouth. The control group was injected with 20 µl of PBS. Following injections, the animals were returned to the cage and placed in a supine position.

The animals were immunized on days 1, 14, and 35. On days 0, 13, 20, and 41, blood was collected from each mouse via facial vein bleeding. On days 0 and 40, saliva was collected from the animal. To do this, 40 µl of 0.05 mg/ml carbamylcholine chloride (carbachol) was injected into the peritoneal cavity of the animal to stimulate saliva secretion (Larsson & Olgart, 1989). The secreted saliva was collected by a pipet into a 1.5 microtube on ice. Approximately 150 µl of saliva was collected from each mouse over 5 min. The saliva sample was then centrifuged at 10 000 x g, 4℃ for 10 min. The supernatants were transferred to a new microtube and 50 µl aliquots were made. All saliva samples were stored at -80℃. On day 42, 2 or 3 mice from each group were euthanized and the remaining mice were euthanized on day 43. At euthanasia, blood was collected by cardiac puncture and spleens were recovered for splenocytes stimulation assay.

2.14.3 Lower lip topical application

The protein samples were prepared as described above to a final concentration of 100 μg /ml and carboxymethylcellulose (CMC) (Sigma-Aldrich) was added to each sample to a final concentration of 1.5% (w/v). Ten μl of the above immunogen was pipetted on to the mucosal surface of the lower lip of sedated mice (n=5). The control group received PBS containing 1.5% carboxymethylcellulose. The liquid was then air-dried with a hair dryer set at a cool and low speed setting (ca. 5 min). The area was then sprayed with a layer of oral liquid bandage (3M™ Cavilon™ No Sting Barrier Film, 3M Canada Corporate, London, Ontario) to prevent protein loss. The animals were put back to the cage in a supine position.

Mice were immunized on days 1, 14, 28 and 35. On days 0, 13, 27, and 41, blood was collected from each mouse via facial vein bleeding. On days 0, and 40, saliva was collected from the animal as described above.

2.15 Statistical analysis

Results were analyzed using the student's *t* test. A *P* value of ≤ 0.05 was considered statistically significance.

Chapter 3: Results

In the present study, the immune response elicited by antigen delivery to the oral mucosal surface of mice with and without targeting to CD40 was tested. The antigen selected for this purpose was a C-terminus fragment of ovalbumin, a very well characterized and relatively weak immunogen. To target OVA to CD40, the extracellular domain of mouse CD40L (CD40LS) was genetically fused to the C-terminus fragment of ovalbumin to form a OVA-CD40LS fusion protein. The OVA fragment without targeting molecule (rOVA) served as a control. In addition, a mutant CD40LS was also genetically fused to the OVA fragment creating a potential second control protein. The DNA construct of each of the recombinant proteins was cloned into *E. coli* for protein expression and purification. The *in vitro* and *in vivo* functions of the purified proteins were then investigated. Furthermore, the DNA construct coding for the OVA fusion proteins was also cloned into *S. gordonii* as an initial attempt to test the antigen targeting approach in a live bacteria based mucosal immunization model.

3.1 Construction of rOVA and OVA fusion protein genes

The *ova* gene fragment (360 bp) coding for the C-terminus 120 amino acid residues of ovalbumin (rOVA) containing both the OTI and OTII sequences was successfully amplified from pOVA-003 by PCR (Figure 6A). To construct *ova-cd40ls*, the *ova* gene fragment was ligated to the *cd40ls* gene through a short DNA sequence coding for a protein linker as illustrated in Figure 1. The 867 bp *ova-cd40ls* gene construct was amplified by PCR (Figure 6B). To construct the gene for OVA-CD40LS$\Delta_{142\text{-}146}$, a mutation was introduced into the *cd40ls* by deleting the DNA sequence encoding for the 5 amino acids that appeared to be important for CD40-CD40L

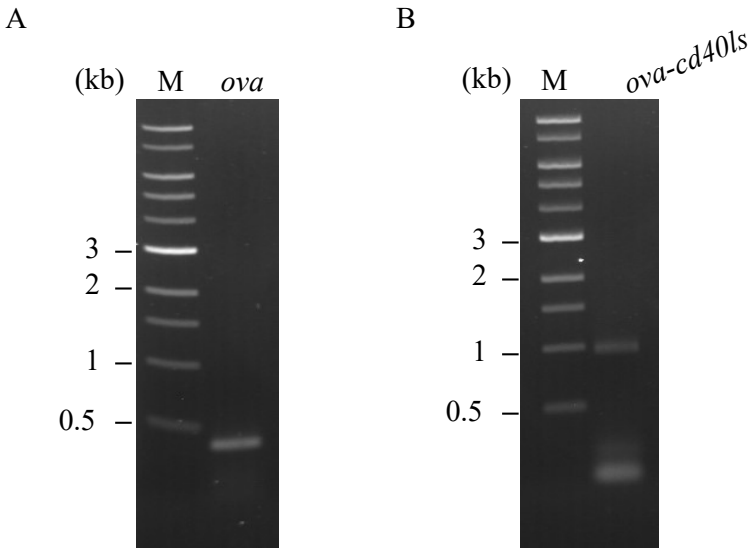

Figure 6 Construction of ova fragment and *ova-cd40ls* DNA

(A) The 360 bp *ova* gene fragment was amplified by PCR from pOVA-003. (B) The 867 bp *ova-cd40ls* gene was amplified from the ligation product by PCR. M: 1 kb DNA ladder (New England BioLabs).

interaction (Bajorath *et al.*, 1995). The ~500 bp gene fragment and the ~400 bp gene fragment before and after the deletion site of *ova-cd40ls* was successfully amplified by PCR (Figure 7A). Then the two fragments were ligated at the SpeI restriction site. The 858 bp *ova-cd40lsΔ$_{142-146}$* gene was obtained by PCR (Figure 7B). The mutation was confirmed by restriction digestion with SpeI. Only *ova-cd40lsΔ$_{142-146}$* could be cut into a ~500 bp and a ~400 bp gene fragments while the *ova-cd40ls* remained uncut by SpeI digestion (Figure 7C).

3.2 OVA fusion protein expression from pComb3X in *E. coli* SG13009

The pComb3X vector contained two SfiI sites for cloning of recombinant protein (Barbas *et al.*, 2001). The expression of the recombinant protein was controlled by the *lac* promoter, which is activated for recombinant protein gene transcription when IPTG was introduced in to the *E. coli* cells. As the results of this IPTG induction, over-expression of the recombinant protein by the *E. coli* is often observed. This plasmid also contains a C terminal 6 x His and HA tags, which allow for protein purification and detection.

The recombinant protein genes, *ova-cd40ls*, *ova-cd40lsΔ$_{142-146}$* and *ova,* were restricted with SfiI and ligated to similarly restricted pComb3X. The ligation product was then transformed into *E. coli* XL1-blue. Single colonies were picked from the transformation plates and allowed to grow overnight. The plasmid DNA was then isolated and analyzed by restriction digestion and PCR. The correct construct, pComb3X OVA-CD40LS, showed two DNA bands, a 3.3 kb vector backbone and a 867 bp *ova-cd40ls* after digestion with SfiI (Figure 8A-1). The *ova* gene fragment (360 bp) in the *ova-cd40ls* gene was amplified from the plasmid DNA by PCR using primer

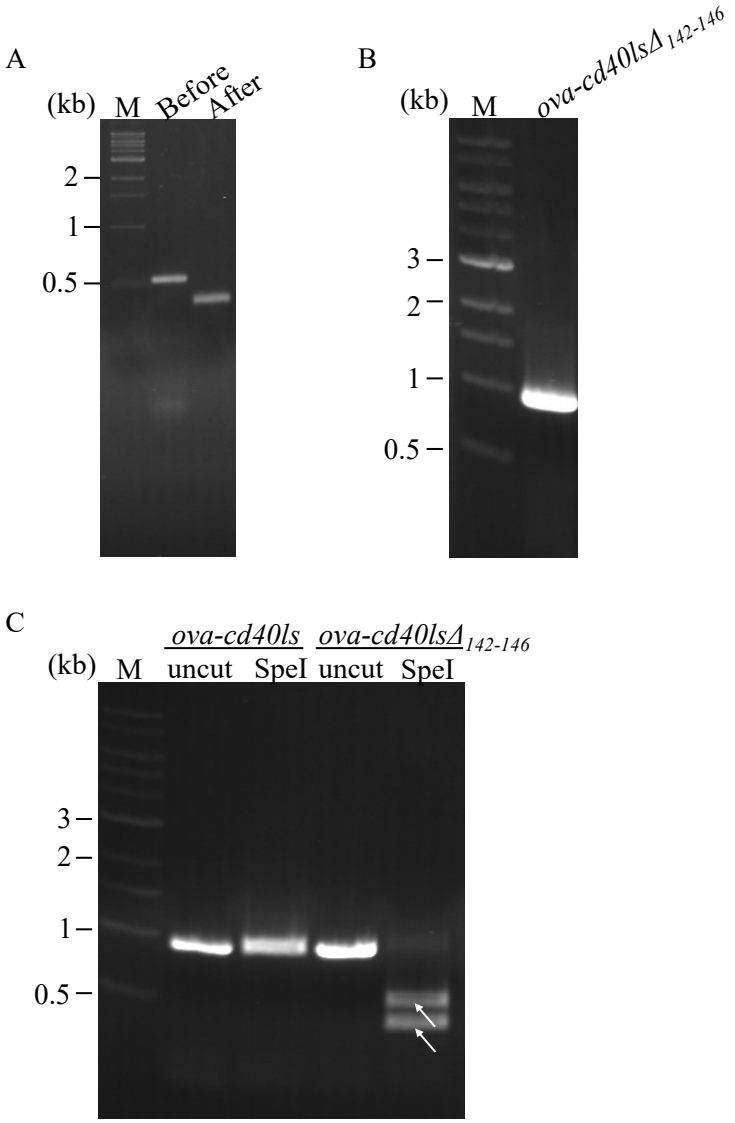

Figure 7 Construction of *ova-cd40lsΔ$_{142-146}$* DNA

(A) The gene fragment before (~500 bp, before) and the after the mutation site (~400 bp, after) were amplified by PCR. The PCR products were then ligated. (B) The *ova-cd40lsΔ$_{142-146}$* gene was amplified by PCR from the ligation product with primer SL1048/SL626. (C) Both *ova-cd40ls* and *ova-cd40lsΔ$_{142-146}$* were restricted with SpeI. Arrows indicated the restriction products. M: 1 kb DNA ladder.

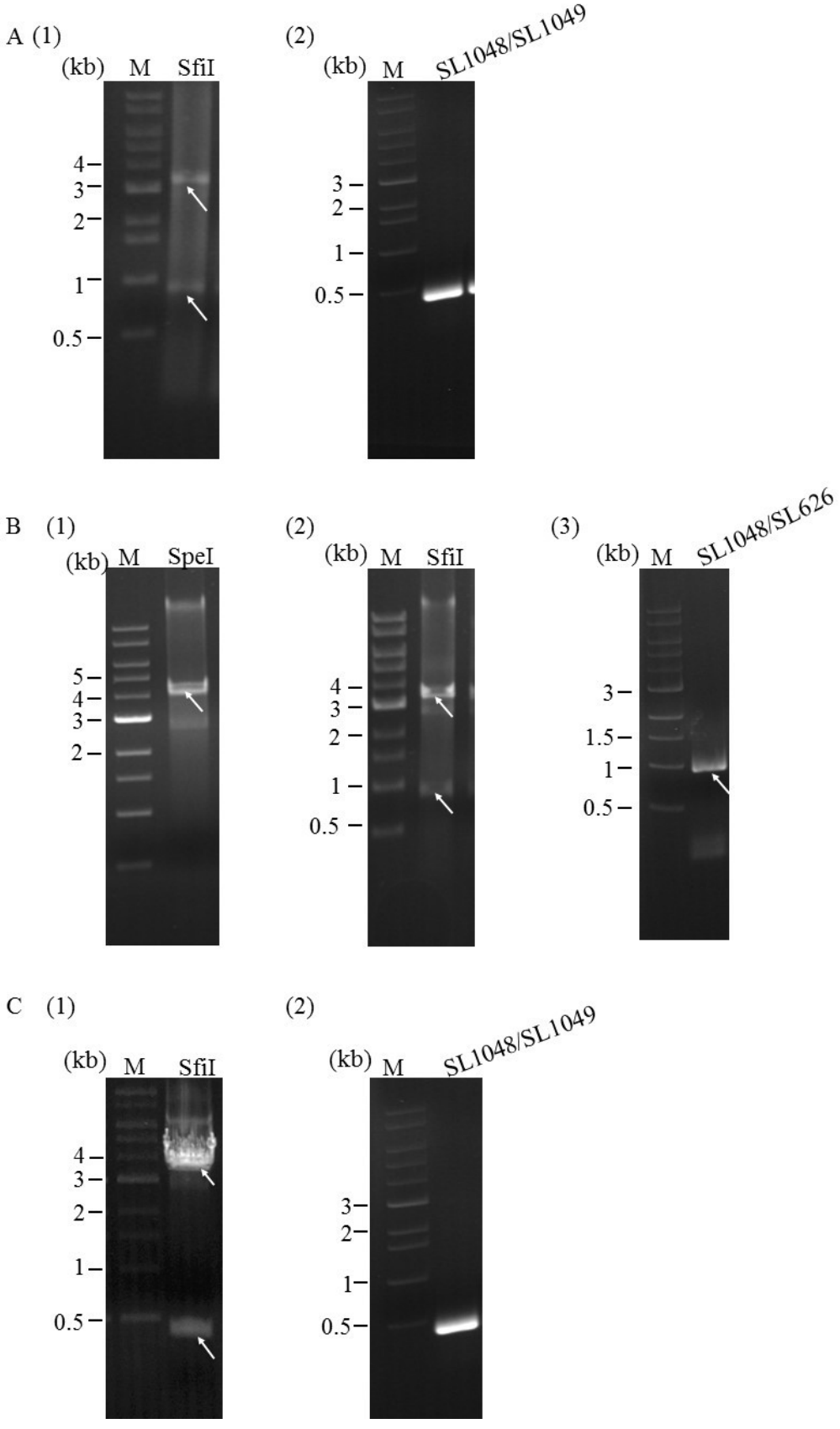
A (1)
(kb) M SfiI
4
3
2
1
0.5
(2)
(kb) M SL1048/SL1049
3
2
1
0.5
B (1)
(kb) M SpeI
5
4
3
2
(2)
(kb) M SfiI
4
3
2
1
0.5
(3)
(kb) M SL1048/SL626
3
1.5
1
0.5
C (1)
(kb) M SfiI
4
3
2
1
0.5
(2)
(kb) M SL1048/SL1049
3
2
1
0.5

Figure 8 Restriction and PCR analyses of pComb3X OVA-CD40LS, pComb3X OVA-CD40LSΔ$_{142\text{-}146}$, and pComb3X rOVA

(A-1) Restriction analysis of pComb3X OVA-CD40LS with Sfi; arrows indicate the 867 bp *ova-cd40ls* and 3.3 kb backbone. (A-2) PCR amplification the 360 bp *ova* gene using SL1048/SL1049. (B-1) Restriction digestion of pComb3X OVA-CD40LSΔ$_{142\text{-}146}$with SpeI; arrow indicates the single cut 4.2 kb plasmid DNA band. (B-2) Restriction digestion of pComb3X OVA-CD40LS$_{\Delta 142\text{-}146}$ with SfiI; arrows indicate the 858 bp *ova-cd40ls$_{\delta 142\text{-}146}$* and the 3.3 kb backbone. (B-3) PCR amplification of *ova-cd40lsΔ$_{142\text{-}146}$* gene from pComb3X OVA-CD40LSΔ$_{142\text{-}146}$ using SL1048/SL626. (C-1) Restriction analysis of the pComb3X OVA with SfiI; arrows indicate the 360 bp *ova* and the 3.3 kb backbone (C-2) PCR amplification of *ova* from pComb3X rOVA using SL1048/SL1049. M: 1 kb DNA ladder.

SL1048/SL1049 (Figure 8A-2).

The correct pComb3X OVA-CD40LSΔ$_{142\text{-}146}$ showed a single DNA band (~4 kb) after restriction with SpeI, which is a unique restriction site located on *ova-cd40lsΔ$_{142\text{-}146}$* (Figure 8B-1). The 858 bp *ova-cd40lsΔ$_{142\text{-}146}$* gene and the 3.3 kb vector backbone were observed following digestion with SfiI (Figure 8B-2). In addition, the *ova-cd40lsΔ$_{142\text{-}146}$* gene was amplified by PCR from the plasmid DNA using SL1048/SL626 (Figure 8B-3).

The correct pComb3X rOVA showed two DNA bands on agarose gel, the 3.3kb vector backbone and 360 bp *ova* after SifI digestion (Figure 8C-1). The *ova* gene was also successfully amplified from pComb3X rOVA (Figure 8C-2).

The above results indicated that the *ova-cd40ls*, *ova-cd40lsΔ$_{142\text{-}146}$* and *ova* gene constructs were successfully cloned into pComb3X plasmid.

The pComb3X OVA-CD40LS, pComb3X OVA-CD40LSΔ$_{142\text{-}146}$ and pComb3X rOVA were transformed to *E. coli* SG13009. Protein expression was confirmed by western blotting using the anti-OVA antibody as the probe. The protein molecular weight of the OVA-CD40LS, OVA-CD40LSΔ$_{142\text{-}146}$, and rOVA was predicted to be 30.8 kDa, 30.4 kDa and 15.5 kDa respectively based on their amino acid sequence. An IPTG-induced protein band was detected with anti-OVA antibody at 35 kDa, 35 kDa, and 15 kDa, which was corresponded to OVA-CD40LS, OVA-CD40LSΔ$_{142\text{-}146}$, and rOVA in the whole cell lysate of *E. coli* SG13009 transformants, repectively (Figure 9A). No IPTG indcued protein was detected in the cell lysate of the parent strain (Figure 9A). The three proteins were mainly found in the insoluble fraction of *E. coli* cell lysate (Figure 9B). Smaller size immunoreactive bands presumably degradation products of the intact recombinant proteins were also detected on the blot. The larger size protein bands

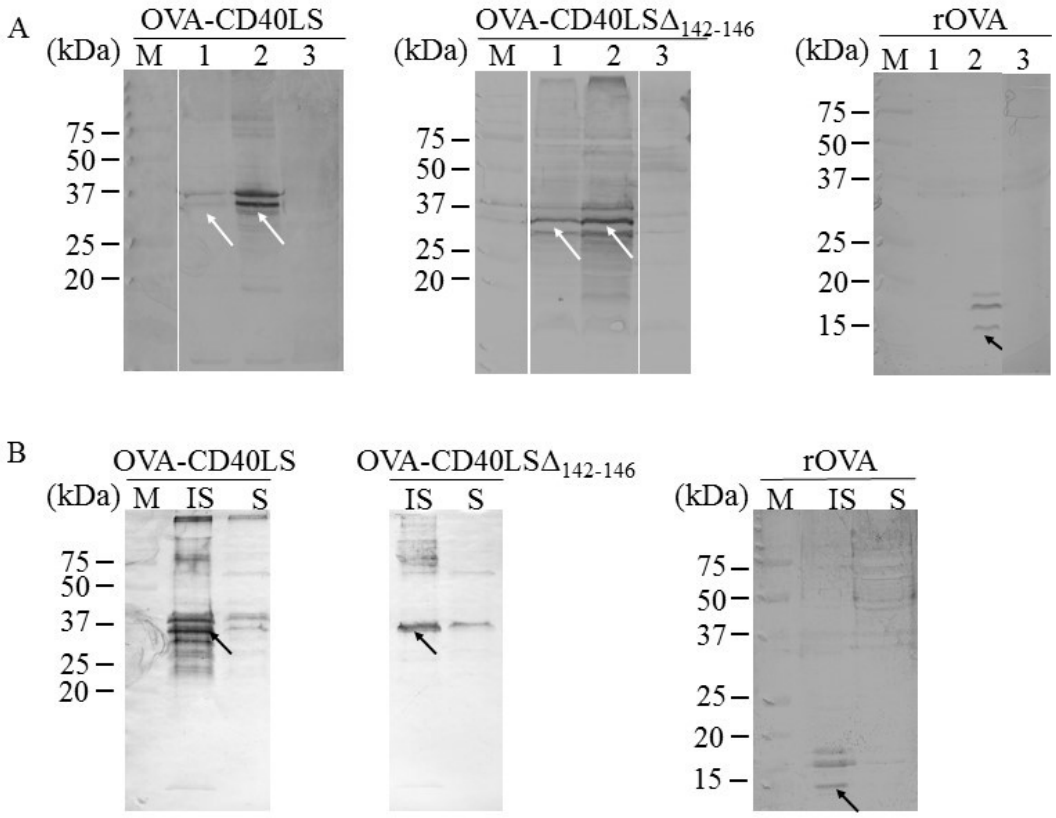

Figure 9 Confirmation of the production of OVA-CD40LS, OVA-CD40LSΔ142-146, and rOVA by *E. coli* transformants with pComb3X expression vector

After induction with IPTG, proteins in the *E. coli* SG13009 cell lysates were detected by western blotting using the anti-OVA antibody. (A) OVA-CD40L, OVA-CD40LSΔ142-146, and rOVA in *E. coli* cell lysates in the absence (lane 1) or the presence (lane 2) of IPTG. The cell lysate of the SG13009 *E. coli* SG13009 parent strain in the presence of IPTG (lane 3) was used as the negative control. (B) OVA-CD40LS, OVA-CD40LSΔ142-146 and rOVA in the insoluble fraction (IS) or the soluble fraction (S). Arrows indicate the OVA fusion proteins and rOVA. M: Pre-stained protein markers (BioRad Laboratories).

detected in both recombinant and parent *E. coli* cell lysates were due to the cross-reactivity of the antibodies (Figure 9). It is worth noting that weak protein bands that correspond to OVA-CD40LS (35 kDa), OVA-CD40LS$\Delta_{142\text{-}146}$ (35 kDa) were also detected in the *E. coli* cell lysate in the absent of IPTG (Figure 9A). The expression of the recombinant proteins without the IPTG induction is possibly due the leaky expression.

3.3 Functionality of partially purified OVA-CD40LS and OVA-CD40LS$\Delta_{142\text{-}146}$

3.3.1 OVA-CD40LS and OVA-CD40LS$\Delta_{142\text{-}146}$ were partially purified and refolded by on-column protein refolding

To obtain the fusion proteins, the insoluble fraction of *E. coli* cell lysate was first solubilized through a protein denaturation process, and then followed by protein purification and refolding. The insoluble fraction of *E. coli* cell lysate was solubilized with 8 M urea and then used for purification by nickel affinity chromatography, using His60 Ni superflow column. The purification profile of each protein was examined by SDS-PAGE. Both OVA-CD40LS and OVA-CD40LS$\Delta_{142\text{-}146}$, bound to the column and were recovered in the eluate (Figure 10A-B). In contrast, the majority of the 15 kDa rOVA remained in the flow through fraction suggesting that the unfolded (denatured) rOVA did not bind to the column. No protein band at 15 kDa was observed in the wash fraction or the eluate (Figure 10C). It is worth noting that a protein band around 15 kDa was co-purified with OVA-CD40LS (Figure 10A), which may be the his-tagged degradation products of the recombinant protein. However, it is also possible that this ~15 kDa protein in OVA-CD40LS eluate represent the *E. coli* proteins that contain multiple histidine residues (Gräslund *et al.*, 2008).

The eluted OVA-CD40LS and OVA-CD40LS$\Delta_{142\text{-}146}$ were then refolded by a

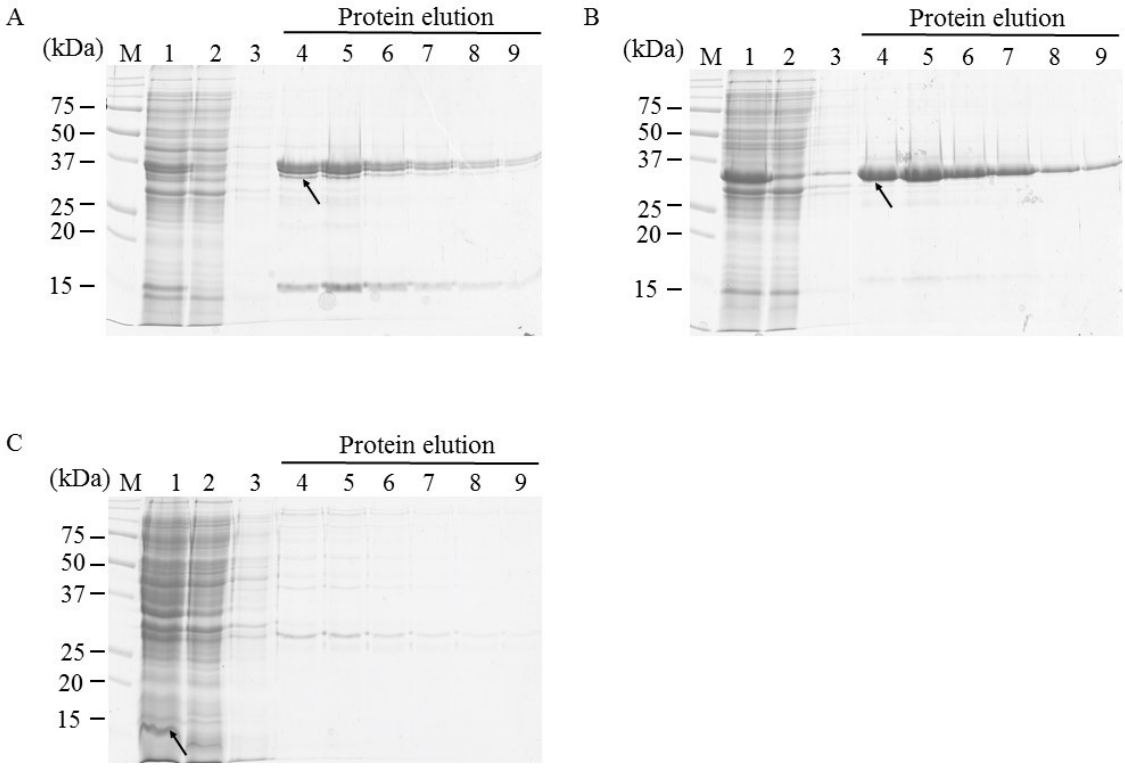

Figure 10 Partial purification of OVA-CD40LS, OVA-CD40LSΔ$_{142-146}$, and rOVA by nickel affinity chromatography under denatured condition

Protein purification profile of (A) OVA-CD40LS, (B) OVA-CD40LSΔ$_{142-146}$, and (C) rOVA analysed by SDS-PAGE. M: Pre-stained protein markers, lane 1: crude proteins from *E. coli* insoluble fraction, lane 2: the flow through, lane 3: combined wash fraction, lane 4-9: eluates. Arrows indicate the recombinant protein.

stepwise dialysis. Unfortunately, the majority of the proteins came out of solution during dialysis (Figure 11), suggesting that the protein did not fold into its native conformation. Only a small portion of each of the fusion protein remained in the solution, which was too dilute for use in functionality tests.

An alternative approach of refolding was pursued. This was by on-column protein refolding which allowed proteins to refold while still bound to the resin. The crude OVA-CD40LS or OVA-CD40LS$\Delta_{142\text{-}146}$ was passed through the His60 Ni superflow column. The unwanted proteins were removed from the column by washing and the bound proteins were refolded by washes containing decreasing concentrations of urea (Figure 4.2). SDS-PAGE analysis showed that the majority of the OVA fusion proteins remained on the column after the refolding process as only a small portion of the OVA-CD40LS or OVA-CD40LS$\Delta_{142\text{-}146}$ was found in the flow through and refolding wash fractions. Although both the OVA-CD40LS and OVA-CD40LS$\Delta_{142\text{-}146}$ were recovered as the major protein component in the eluate, a number of contaminating proteins were also present (Figure 12A-B). Interestingly, the major portion of the OVA-CD40LS remained on the column after elution and could only be recovered under denatured conditions (Figure 12A). The eluted 35 kDa OVA-CD40LS and OVA-CD40LS$\Delta_{142\text{-}146}$ were detected by the anti-OVA antibody confirming their identity (Figure 12C and 12D). These partially purified proteins were named as P-OVA-CD40LS and P-OVA-CD40LS$\Delta_{142\text{-}146}$.

3.3.2 The partially purified OVA-CD40LS and OVA-CD40LS$\Delta_{142\text{-}146}$ were functional *in vitro*

To investigate whether the refolded P-OVA-CD40LS and P-OVA-CD40LS$\Delta_{142\text{-}146}$ were biologically active, the proteins were tested for binding to human CD40 in

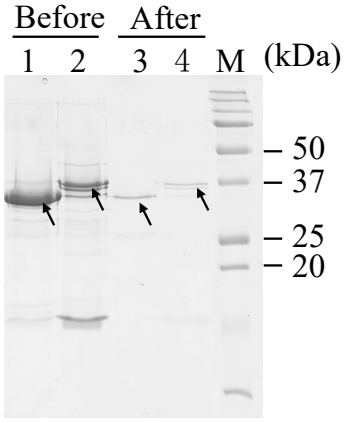

Figure 11 Renaturation of partially purified OVA-CD40LS and OVA-CD40LSΔ$_{142-146}$ by dialysis

SDS-PAGE analysis of the relative amount of OVA-CD40LSΔ$_{142-146}$ (Lane 1 and Lane 3) and OVA-CD40LS (Lane 2 and Lane 4) before and after dialysis. Arrows indicate the fusion proteins. M: Pre-stained protein markers.

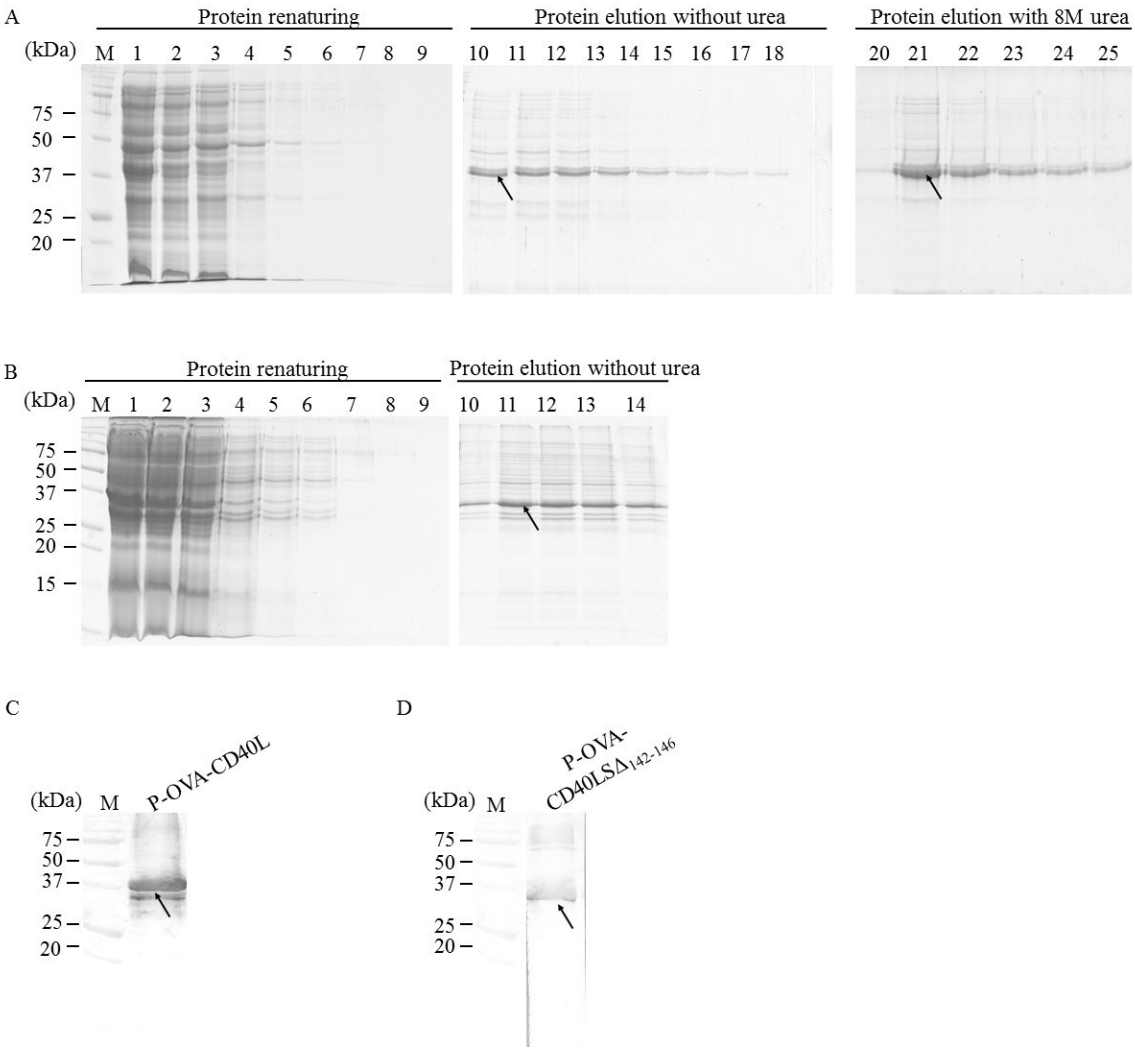

Figure 12 Partial purification and on-column refolding of OVA-CD40LS and OVA-CD40LSΔ$_{142-146}$ from *E. coli* cell lysate

Protein purification profile of (A) OVA-CD40LS and (B) OVA-CD40LSΔ$_{142-146}$ analyzed by SDS-PAGE; arrows indicate the OVA fusion proteins. Western blotting detection of eluted (C) OVA-CD40LS and (D) OVA-CD40LSΔ$_{142-146}$ by the anti-OVA antibody. M: Pre-stained protein markers, lane 1: crude proteins, lane 2: the flow through, lanes 3-7: wash fractions containing 8 M, 6 M, 4 M, 2 M, 1 M urea, respectively. Lanes 8 and 9: 0.1% TritonX-114 wash and the endotoxin-free wash, respectively. Lanes 10-18 (A) or lanes 10-14 (B): eluates without urea. Lanes 19-25 (A): eluates containing 8 M urea.

ELISA. Both fusion proteins showed significantly higher binding to human CD40 compared to the whole ovalbumin (nOVA). P-OVA-CD40LS$\Delta_{142\text{-}146}$ showed a higher binding than P-OVA-CD40L (Figure 13). The biological function of both proteins was then tested in BMDCs stimulation. The TNF and IL-6 level of native P-OVA-CD40LS, native P-OVA-CD40LS$_{\Delta 142\text{-}146}$ and LPS group were significantly higher than the medium control (Figure 14, P<0.0001). In addition, both native P-OVA-CD40LS and native P-OVA-CD40SL$\Delta_{142\text{-}146}$ stimulated TNF and IL-6 production in BMDCs in a dose-dependent manner. Cells stimulated with nOVA or heat-inactivated proteins only produced a basal level of both cytokines (Figure 14). The above results suggested that the P-OVA-CD40LS was biologically active. Interestingly, the P-OVA-CD40LS$\Delta_{142\text{-}146}$ did not show any reduced function compared to P-OVA-CD40LS in both the binding assay and cell stimulation assay.

To further investigate the activity of OVA-CD40LS and OVA-CD40LS$\Delta_{142\text{-}146}$, a better purity of the two proteins was required. Given that the majority of the contaminating proteins could be removed under denatured condition, using a second chromatography column dedicated for protein refolding would be a logical step to obtain pure fusion proteins.

3.4 Purified OVA-CD40LS and OVA-CD40LS$\Delta_{142\text{-}146}$ refolded on hydrophobic column chromatography lacked *in vitro* function

3.4.1 OVA-CD40LS$\Delta_{142\text{-}146}$ but not OVA-CD40LS was purified by phenyl-sepharose column followed by on-column protein refolding

Hydrophobic interaction chromatography separates proteins based on hydrophobicity of proteins. The successful used of hydrophobic interaction chromatography for protein on-column refolding has been reported in several studies

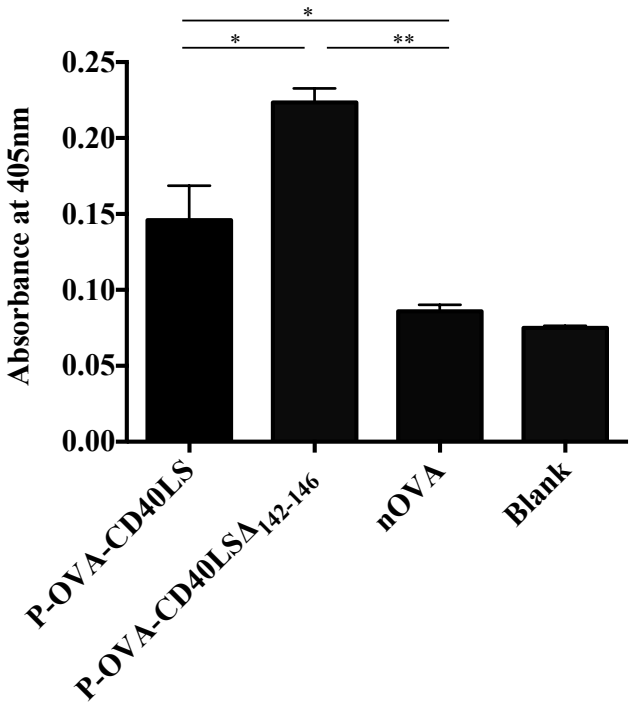

Figure 13 ELISA analysis of the binding of partially purified OVA-CD40LS and OVA-CD40LΔ$_{142-146}$ fusion proteins to human CD40

Plates were coated with recombinant human CD40 (1μg/ml), incubated with P-OVA-CD40L (50 ng), and P-OVA-CD40LΔ$_{142-146}$ (50 ng) or whole ovalbumin (nOVA, 100 ng), detected with rabbit anti-OVA IgG, finally developed with a goat anti-rabbit IgG-AP conjugate with pNPP. Blank: PBST in place of proteins. Data are shown as means ± SD of duplicates. $^{**}P<0.01$, $^{*}P<0.05$.

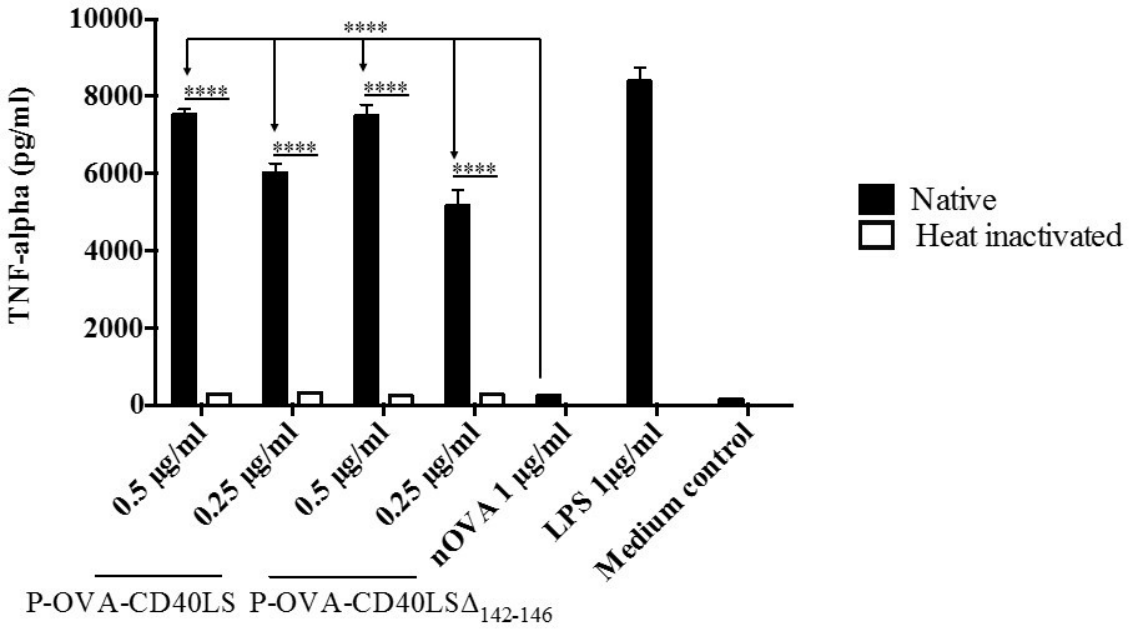
TNF-alpha (pg/ml)
10000
8000
6000
4000
2000
0
****
****
****
****
****
0.5 µg/ml
0.25 µg/ml
0.5 µg/ml
0.25 µg/ml
nOVA 1 µg/ml
LPS 1µg/ml
Medium control
P-OVA-CD40LS
P-OVA-CD40LSΔ142-146
Native
Heat inactivated

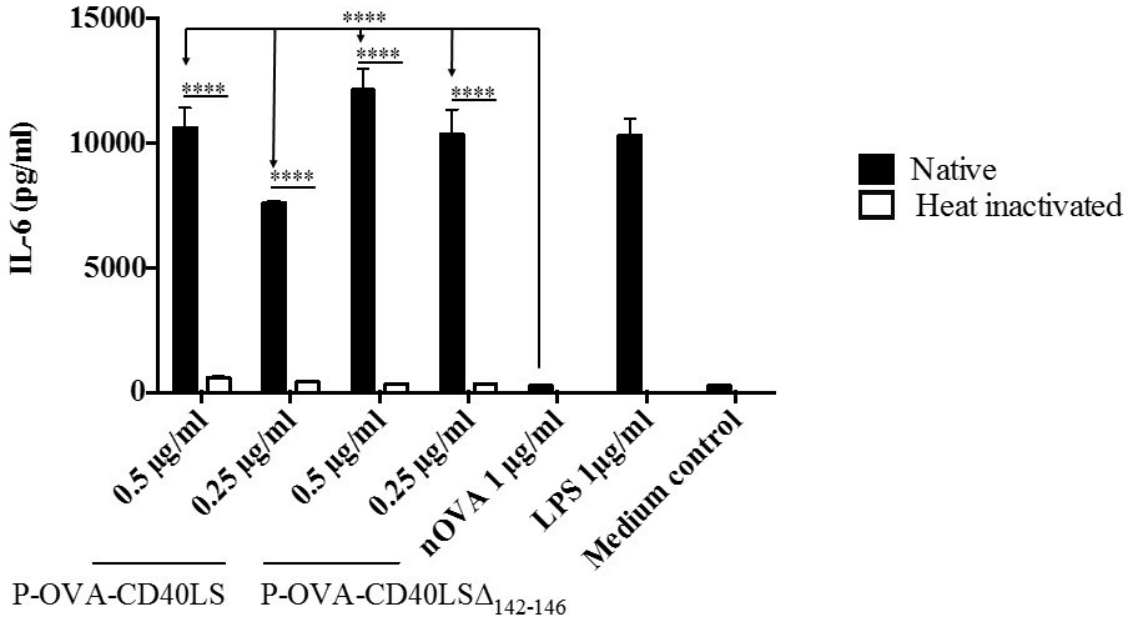
IL-6 (pg/ml)
15000
10000
5000
0
****
****
****
****
****
0.5 µg/ml
0.25 µg/ml
0.5 µg/ml
0.25 µg/ml
nOVA 1 µg/ml
LPS 1µg/ml
Medium control
P-OVA-CD40LS
P-OVA-CD40LSΔ142-146
Native
Heat inactivated

Figure 14 P-OVA-CD40LS, P-OVA-CD40LS$\Delta_{142\text{-}146}$ stimulated TNF and IL-6 production in BMDCs

ELISA analysis of TNF and IL-6 production in mouse BMDCs stimulated with native or heat-inactivated p-OVA-CD40LS, p-OVA-CD40LS$_{\Delta 142\text{-}146}$ or whole ovalbumin molecule (nOVA). BMDCs stimulated with LPS were used as positive control; BMDCs left unstimulated were used as negative control (medium control). Data are shown as means ± SD of triplicates. ****P<0.0001.

(Vallejo & Rinas, 2004; Li *et al.*, 2004; Wang & Geng, 2012). It was chosen as the second column for protein refolding in this study. In addition, the hydrophobic interaction chromatography could also be used to remove the carry over contaminating proteins from the nickel affinity purification. The protein was therefore first isolated from the crude *E. coli* cell lysate by nickel affinity column chromatography under endotoxin-free and denatured condition. The eluted proteins were then pooled and applied to the endotoxin-free phenyl-sepharose column followed by refolding. Protein elution was achieved using an increasing stepwise pH gradient. SDS-PAGE analysis showed that no protein band corresponded to OVA-CD40LS was present in the flow through or refolding wash fractions suggesting that the protein bound to the column. Only a small amount of OVA-CD40LS was recovered in the pH 11 eluate (Figure 15A-1), but not in the pH 8, 9 and 10 eluates (data not shown). Following elution, 10 µl of the resin was boiled for 5 min in SDS-PAGE sample buffer, and a strong protein band at 35 kDa was observed indicating that the majority of the OVA-CD40LS remained tightly bound to the column and could not eluted under the above elution conditions (Figure 15A-2). Reverse dialysis and ultrafiltration were used to concentrate the OVA-CD40LS eluted at pH 11. However, the majority of the proteins were lost during the process (data not shown).

In the case of OVA-CD40LS$\Delta_{142\text{-}146}$, a weak protein band was present in the flow through, 8 M and 6 M urea wash fractions. The OVA-CD40LS$\Delta_{142\text{-}146}$ could not be eluted with pH 8, 9 and 10 (data not shown). A substantial of OVA-CD40LS$\Delta_{142\text{-}146}$ was recovered in the pH 11eluate and detected as the only protein component on SDS-PAGE gels (Figure 15B). The 35 kDa protein band was detected by anti-CD40L and anti-OVA antibodies on western blots confirming the identity of the eluted OVA-CD40LS$\Delta_{142\text{-}146}$

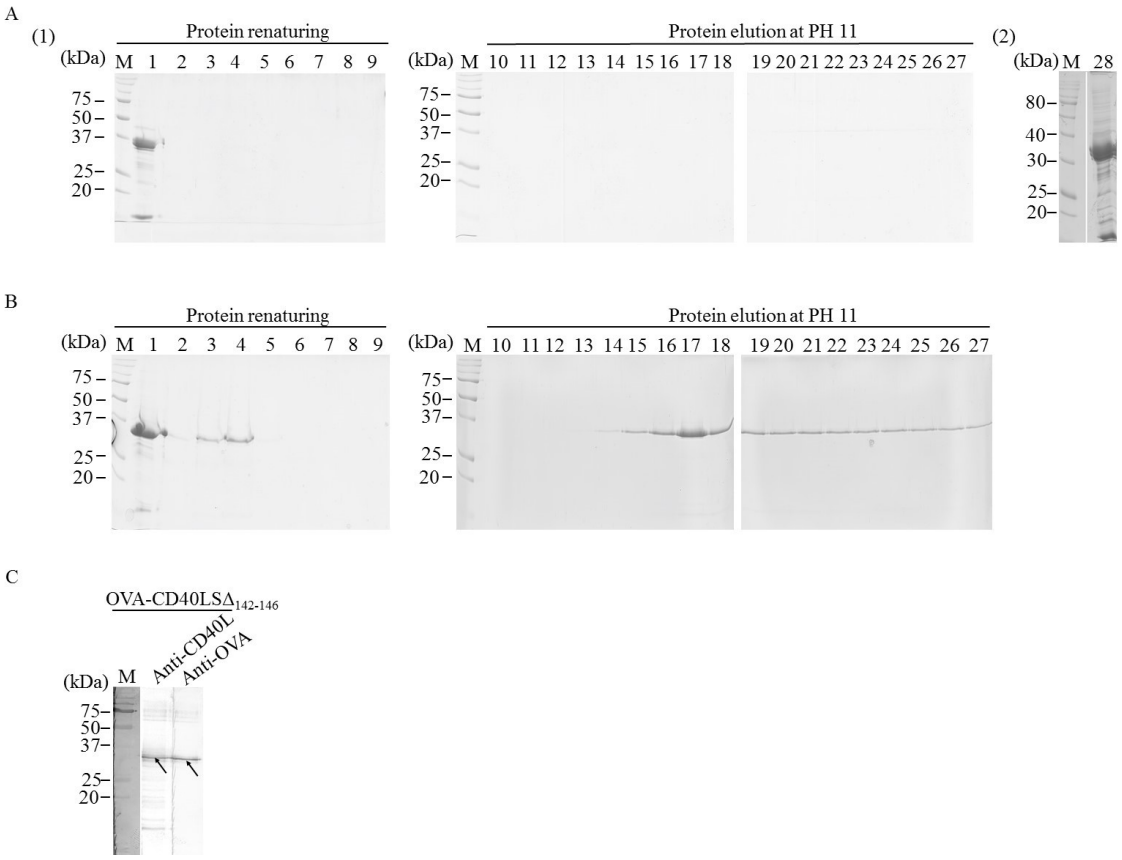

Figure 15 OVA-CD40LSΔ142-146 but not OVA-CD40LS was purified and refolded by phenyl-sepharose column chromatography

SDS-PAGE analysis of (A) OVA-CD40LS and (B) OVA-CD40LSΔ142-146. Proteins were eluted with a stepwise pH gradient from 7 to 11 with 1 pH unit increment, only pH 11 eluates are shown. M: Pre-stained protein markers. Lane 1: total protein. Lane 2: flow through, Lanes 3-8: wash fractions containing 8 M, 6 M, 4 M, 2 M, 1 M and 0 M urea, respectively. Lane 9: NaCl removing wash. Lanes 10-27: protein eluted at pH 11. Lane 28: boiled phenyl sepharose. (C) The identity of the eluted OVA-CD40LSΔ142-146 (arrows) was confirmed by western blotting using anti-CD40L and anti-OVA antibodies as probes.

(Figure 15C). Approximately 466 μg of purified OVA-CD40LSΔ$_{142\text{-}146}$ was obtained from 1 liter of *E. coli* culture. The concentration of the purified OVA-CD40LSΔ$_{142\text{-}146}$ was then estimated to be 118 μg/ml.

3.4.2 Improved expression of OVA-CD40LS and rOVA by pQE-30 expression vector

Given the difficulties in obtaining a pure OVA-CD40LS and rOVA protein, the production of these two proteins was pursued using a different expression plasmid, pQE-30. In this plasmid, protein expression is controlled by the T5 promoter, which allows for protein over-expression upon IPTG induction. In addition, an N-terminal 6 x His tag facilitates protein purification and detection (Barbas *et al.*, 2001).

The *ova-cd40ls* gene was cloned into the modified pQE-30 that has been engineered to contain two SfiI restriction sites. The *ova-cd40ls* gene was obtained from pComb3X OVA-CD40LS by SfiI digestion and then ligated to the SfiI restricted pQE-30. The ligation product was then transformed into *E. coli* XL1-blue. The correct pQE-30 OVA-CD40LS after SfiI restriction showed the expected two DNA bands, the 3.4 kb vector backbone and the 867 bp insert gene (Figure 16A-1). The *ova* gene fragment (360 bp) in *ova-cd40ls* was amplified from pQE-30 OVA-CD40LS by PCR (Figure 16A-2). The above results suggested the *ova-cd40ls* gene construct was successfully cloned into pQE-30 plasmid.

The *ova* gene was obtained from pComb3X rOVA by PCR using primers SL1206/SL1207, which introduced a 5' BamHI restriction site and a 3' HindIII restriction site into the *ova* gene. The gene was then cloned into pQE-30 plasmid through BamHI and HindIII. The ligated DNA was transformed into *E. coli* XL1-blue. The

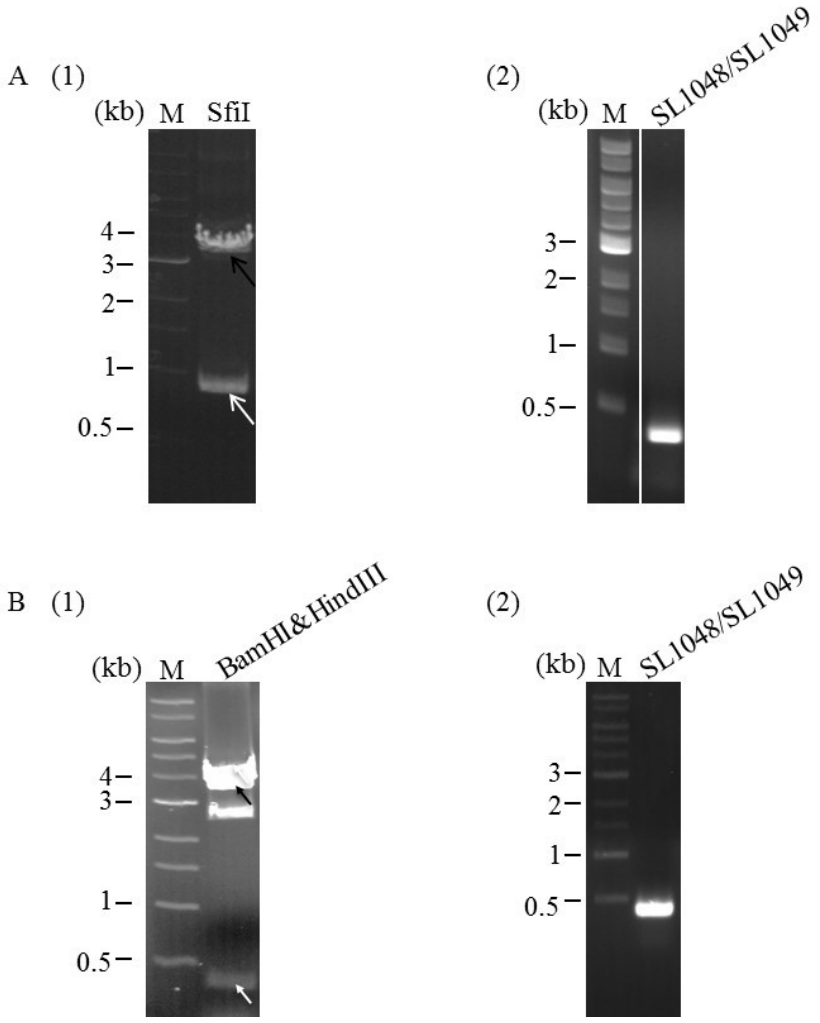

Figure 16 Restriction and PCR analysis of pQE-30 OVA-CD40LS and pQE-30 rOVA

(A-1) Restriction of pQE-30 OVA-CD40LS with SfiI, the arrows indicate the 867 bp *ova-cd40ls* and 3.5 kb plasmid backbone. (A-2) PCR amplification of the 360 bp *ova* gene from pQE-30 OVA-CD40LS with primers SL1048/SL1049. (B-1) Restriction analysis of pQE-30 rOVA with SfiI, arrows indicate the 360 bp *ova* and 3.5 kb backbone. (B-2) PCR amplification of 360 bp *ova* gene from pQE-30 rOVA with primers SL1048/SL1049. M: 1 kb DNA ladder.

correct pQE-30 OVA showed two DNA bands, the 3.4 kb vector backbone and 360 bp *ova* after double digestion by HindIII and BamHI (Figure 16B-1). The 360 bp *ova* gene was also amplified by PCR using primers SL1206/SL1207 (Figure 16B-2). These results suggested the *ova* gene construct was successfully cloned into pQE-30 plasmid.

pQE-30 rOVA and pQE-30 OVA-CD40LS were transformed into *E. coli* SG13009. The production of each protein was confirmed by SDS-PAGE. An IPTG-induced protein band corresponded to OVA-CD40LS (35 kDa) and rOVA (15 kDa) was presented in the recombinant *E. coli* whole cell lysate but not that of the parent the *E. coli* strain (Figure 17 A). Both OVA-CD40LS, and rOVA were mainly found in the insoluble fraction of *E. coli* cell lysate (Figure 17 B).

3.4.3 OVA-CD40LS and rOVA from pQE-30 purified by nickel affinity column chromatography followed by dialysis protein refolding

The insoluble fraction of the *E. coli* cell lysate was prepared for protein purification by nickel affinity column chromatography. OVA-CD40LS was purified from the crude proteins by nickel affinity column under the endotoxin-free and denatured condition. OVA-CD40LS bound efficiently to the column with little remaining in the flow through and wash fractions; the majority of the denatured OVA-CD40LS was recovered in the eluate (Figure 18A). Similar results were obtained with rOVA (Figure 18B). The eluted OVA-CD40LS was refolded by dialysis and the majority of the protein remained soluble after dialysis refolding (Figure 19A). The resulting OVA-CD40LS appeared as a 35 kDa protein band detected by anti-CD40L and anti-OVA antibodies (Figure 19B). The smaller protein bands that were also detected by anti-CD40L and anti-OVA antibody likely were degradation products of OVA-CD40LS. The OVA-CD40LS

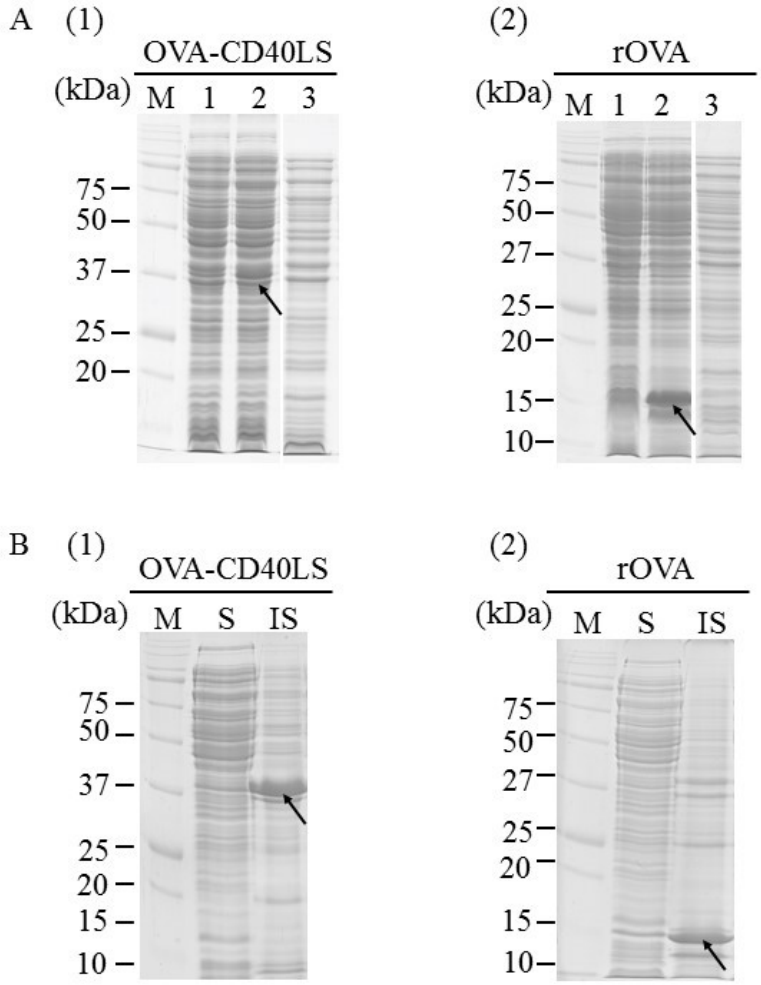

Figure 17 Confirmation of the production of OVA-CD40LS and rOVA by *E. coli* transformants with pQE-30 expression vector

After IPTG induction, proteins in the *E. coli* cell lysate was analyzed by SDS-PAGE. (A) Lysates of cells cultured in the absence (lane 1) or presence (lane 2) of IPTG. IPTG-induced *E. coli* SG13009 parent stain cell lysate (Lane 3). (B) Insoluble fraction (IS) and soluble fraction (S) of recombinant *E. coli* cell lysate. Arrows indicate OVA-CD40LS (A-1 & B-1) and rOVA (A-2 & B-2). M: Pre-stained protein markers.

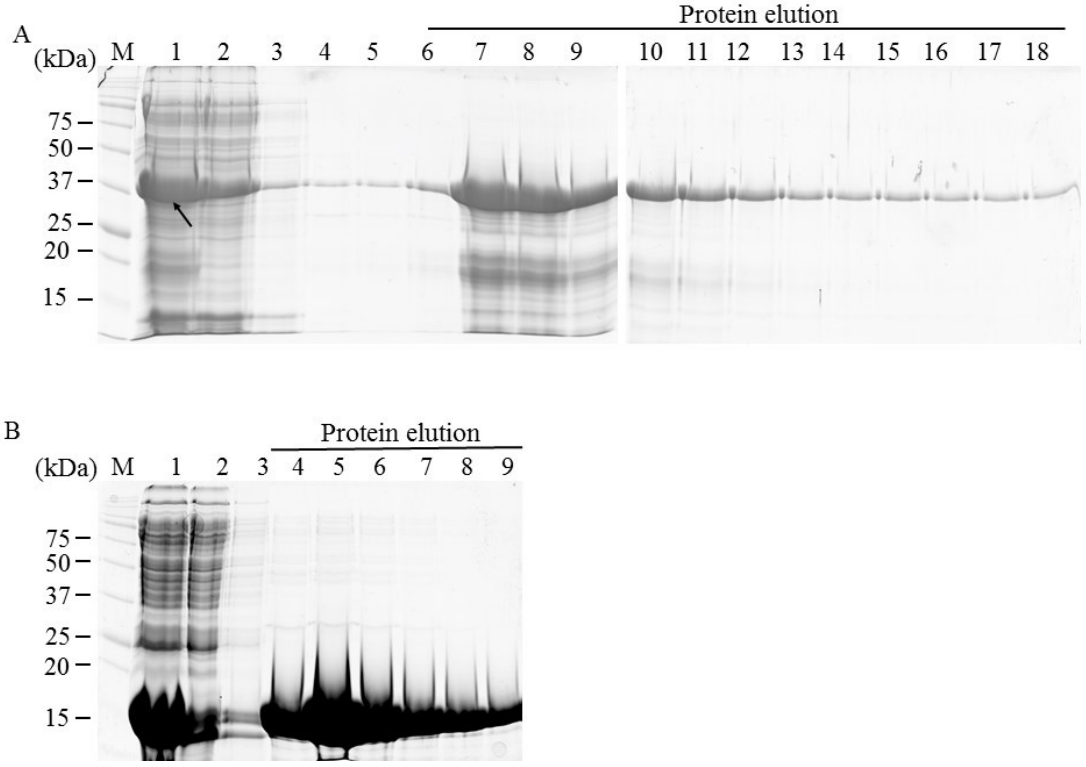

Figure 18 Purification of OVA-CD40LS and rOVA expressed from pQE-30 by nickel affinity chromatography under denatured condition

(A) Protein purification profile of OVA-CD40LS analysed by SDS-PAGE, lane 1: total protein, lane 2: flow through, lanes 3-5: wash fractions, lanes 6-18: eluted protein fractions. (B) Protein purification profile of rOVA analyzed by SDS-PAGE, lane1: total protein, lane2: flow through, lane 3: combined wash fractions, lanes 4-9: eluted protein fraction. M: Pre-stained protein markers.

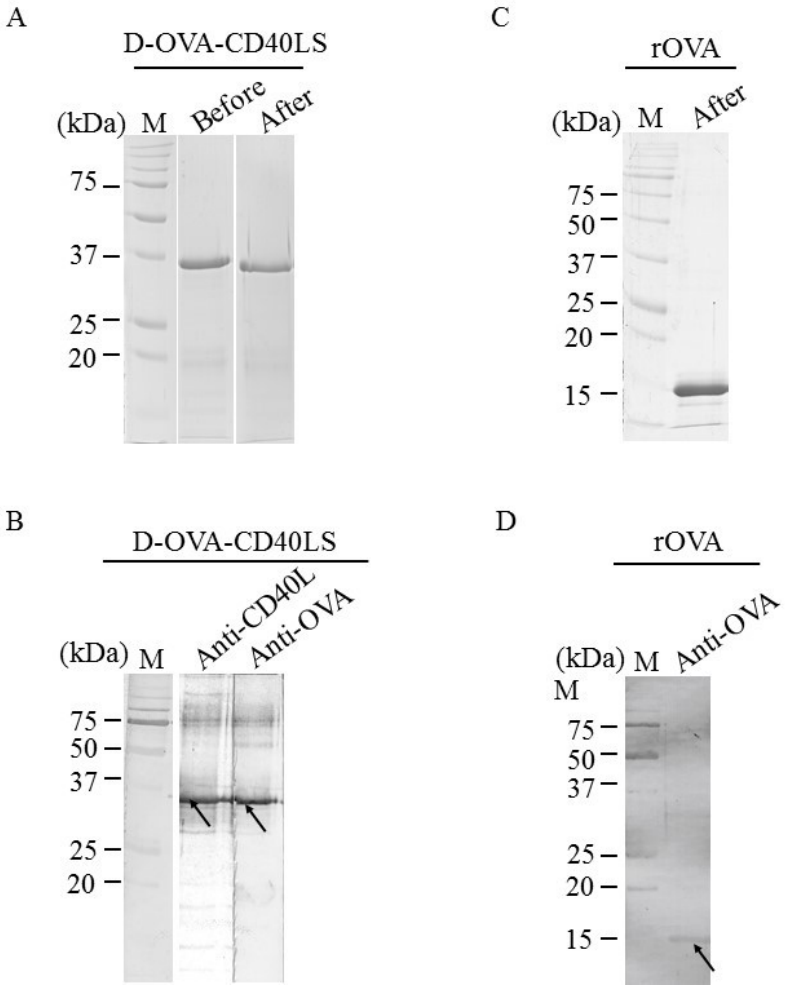

Figure 19 The purified D-OVA-CD40LS and rOVA were renatured by dialysis and analysed with SDS-PAGE and western blotting

(A) SDS-PAGE analysis of the amount of OVA-CD40LS remained in solution before and after dialysis. (B) D-OVA-CD40LS (arrow) after dialysis detected by anti-CD40L and anti-OVA antibodies. (C) SDS-PAGE analysis of the amount of rOVA remained in solution after dialysis. (D) rOVA (arrow) detected by the anti-OVA antibody. M: Pre-stained protein markers.

was named as D-OVA-CD40LS and the final concentration was determined to be 104 μg/ml. Similarly, most of the rOVA remained in the solution after dialysis refolding (Figure 19C). The purified 15 kDa rOVA was recognized by the anti-OVA antibody in western blotting (Figure 19D). Approximately of 11.8 mg of purified rOVA was obtained from 1 liter *E. coli* culture. The final concentration of purified rOVA was estimated to be 219 μg/ml. The protein was then aliquoted as 6 μg/aliquot and freeze-dried.

3.4.4 OVA-CD40LS refolded by dialysis lacked biological activities *in vitro*

The function of the purified D-OVA-CD40LS, OVA-CD40LS$\Delta_{142\text{-}146}$ and rOVA was tested *in vitro*. There was no difference between the binding of D-OVA-CD40LS and rOVA to human CD40 in ELISA (Figure 20) suggesting that the D-OVA-CD40LS could not bind to human CD40. The purified OVA-CD40LS$\Delta_{142\text{-}146}$, on the other hand, showed a higher binding to human CD40 than rOVA and OVA-CD40LS (Figure 20), which was consistent with the partially purified P-OVA-CD40LS$\Delta_{142\text{-}146}$ shown earlier (Figure 13). However, neither D-OVA-CD40LS nor OVA-CD40LS$\Delta_{142\text{-}146}$ could induce TNF or IL-6 production by BMDCs (Figure 21).

The above results suggest that the D-OVA-CD40LS refolded by dialysis was not active. The inconsistent results of the P-OVA-CD40LS$\Delta_{142\text{-}146}$ obtained from nickel affinity chromatography and purified OVA-CD40LS$\Delta_{142\text{-}146}$ obtained from phenyl-sepharose column chromatography in BMDCs stimulation make it hard to determine whether the mutation in CD40LS has resulted in a defective CD40LS that is suitable for use as a control protein. Thus, the OVA-CD40L$\Delta_{142\text{-}146}$ was not included in further investigation.

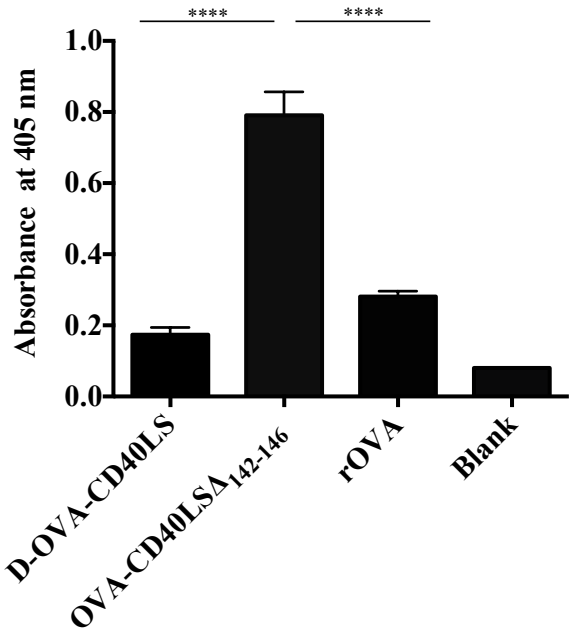

Figure 20 ELISA analysis of the binding of purified D-OVA-CD40L, OVA-CD40LΔ$_{142-146}$, and OVA to human CD40 in ELISA

Plates were coated with recombinant human CD40 (1μg/ml), incubated with D-OVA-CD40L (50 ng), purified OVA-CD40LΔ$_{142-146}$ (50 ng) or purified rOVA (50 ng), detected with rabbit anti-OVA IgG, finally developed with a goat anti-rabbit IgG-AP conjugate with pNPP. Blank: PBST in place of proteins. Data are shown as means ± SD of duplicates. ****P<0.0001.

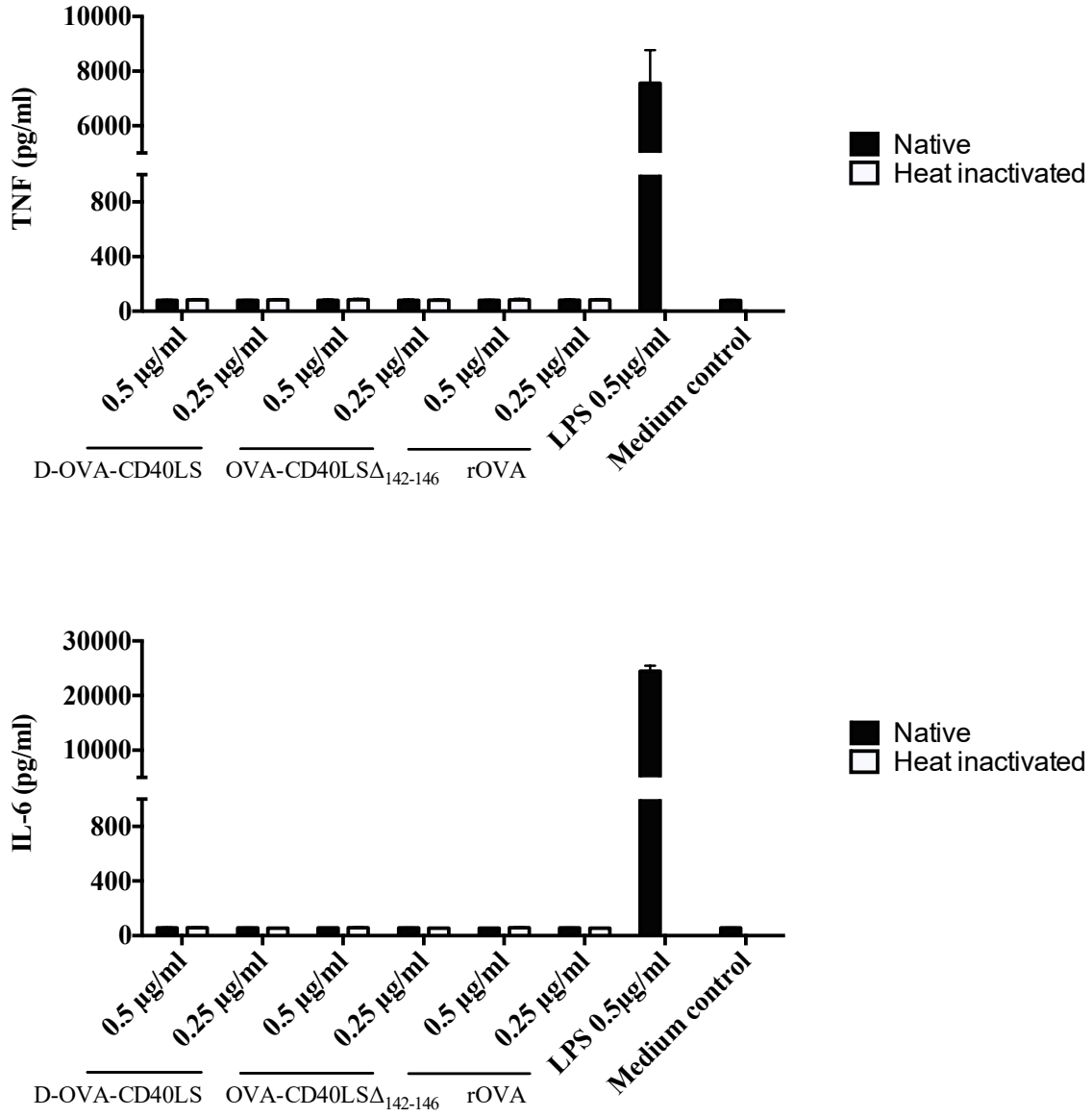

Figure 21 Purified D-OVA-CD40LS and OVA-CD40LSΔ142-146 failed to stimulate cytokine production in BMDCs

ELISA analysis of TNF and IL-6 production in mouse BMDCs stimulated with native or heat-inactivated D-OVA-CD40LS, D-OVA-CD40LS$_{\Delta 142\text{-}146}$ or rOVA. BMDCs stimulated with LPS served as positive control, and BMDCs left unstimulated served as medium control. D-OVA-CD40LS: the purified OVA-CD40LS obtained by dialysis protein refolding. Data are shown as means ± SD of triplicate stimulations.

3.5 OVA-CD40LS purified by 'two-rounds' nickel affinity chromatography and on-column protein refolding was biologically active.

3.5.1 OVA-CD40LS was purified by "two-rounds" on column protein refolding with nickel affinity chromatography

The results described above showed that the partially purified OVA-CD40LS was biologically active *in vitro* but not that refolded by dialysis. The results also showed that only a minor amount of OVA-CD40LS was partially purified with on-column refolding, the majority of the OVA-CD40LS remained bound to the column and could be eluted from the column with imidazole under denatured condition. Based on the above observations, a 'two-rounds' purification approach on the nickel affinity column was developed.

Proteins in the insoluble fraction of the cell lysate of *E. coli* SG13009 carrying pQE-30 OVA-CD40LS was solubilized with urea and passed through the nickel affinity column. After washing, on-column protein refolding, endotoxin removal, and elution, the majority of the OVA-CD40LS remained on the column was eluted with elution buffer containing 8 M urea (Figure 22A). The imidazole in the eluted OVA-CD40LS was removed by dialysis and the protein sample was used for the 'second-round' of purification on the same nickel affinity column. The purification was carried out under endotoxin-free condition. Following washing and on-column protein refolding, OVA-CD40LS was recovered in the eluate as a relatively pure protein (Figure 22B), which was recognized by anti-CD40L and anti-OVA antibodies (Figure 22C). Approximately of 528 μg of purified OVA-CD40LS was obtained from 1 liter of *E. coli* culture. The concentration of purified OVA-CD40LS was then estimated to be 44 μg/ml. The protein was then aliquoted as 6 μg/aliquot and freeze-dried.

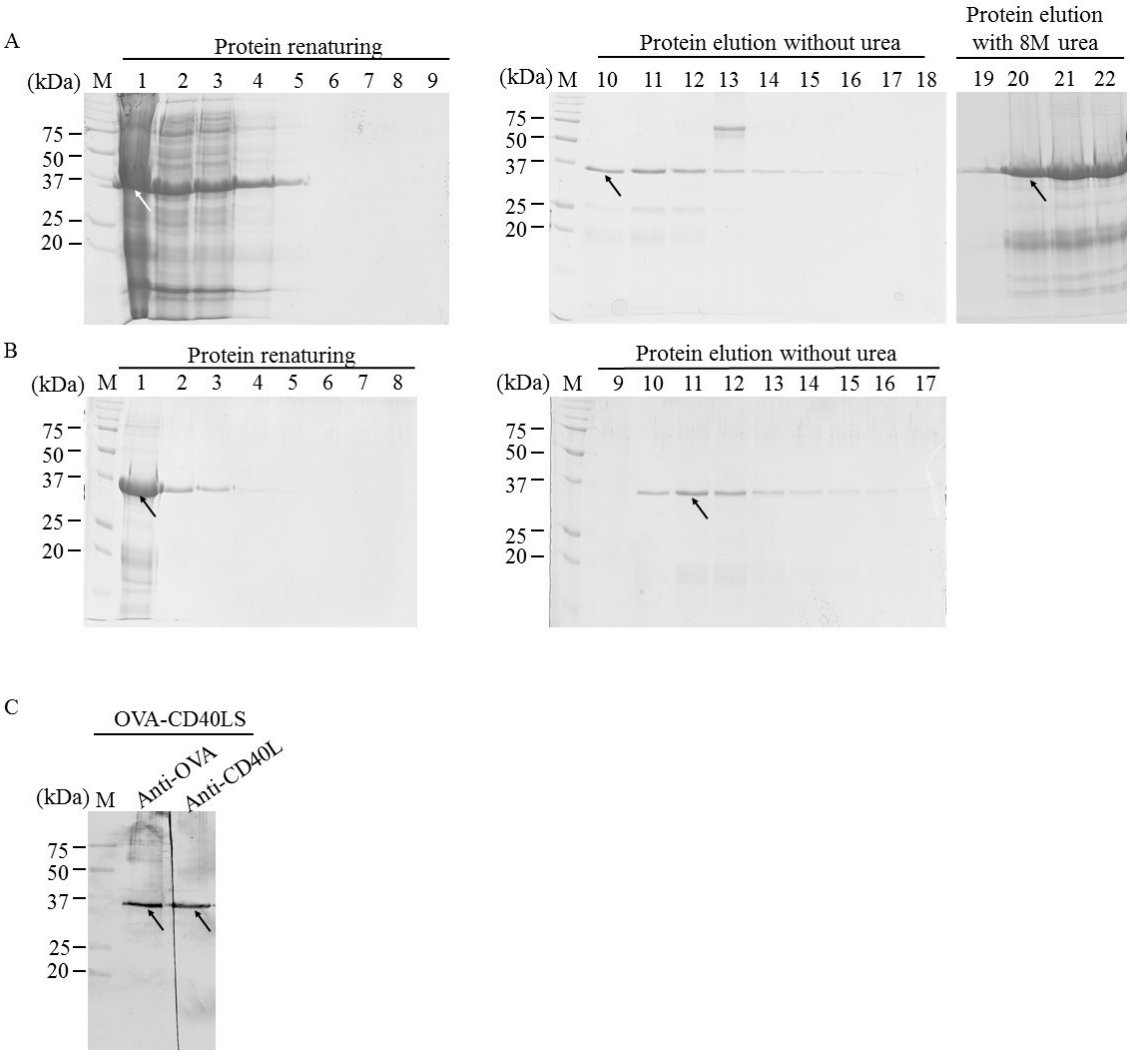
A
Protein renaturing
Protein elution without urea
Protein elution with 8M urea
(kDa) M 1 2 3 4 5 6 7 8 9
(kDa) M 10 11 12 13 14 15 16 17 18
19 20 21 22
75
50
37
25
20
B
Protein renaturing
Protein elution without urea
(kDa) M 1 2 3 4 5 6 7 8
(kDa) M 9 10 11 12 13 14 15 16 17
C
OVA-CD40LS
Anti-OVA
Anti-CD40L
(kDa) M

Figure 22 OVA-CD40LS produced from pQE30 was purified from *E. coli* cell lysate by two rounds of nickel affinity chromatography coupled with on-column protein renaturation

Protein purification profile of OVA-CD40LS was analysed by SDS-PAGE. (A) The denatured OVA-CD40LS was isolated from *E. coli* cell lysate from first round of purification. Total of 30 fractions of 8 M urea was collected, only the first 4 fractions are shown. Lane 1: total protein, lane 2: flow through, lanes 3-7: wash fractions containing 8 M, 6 M, 4 M, 2 M, 1 M of urea, respectively, lane 8: 0.1% TritonX-114 wash, lane 9: endotoxin-free wash, lanes 10-18: 0 M urea elution, lane 19-22: 8 M urea elution. (B) OVA-CD40LS purified and refolded from the second round of purification, lane 1: isolated denatured OVA-CD40LS from first round purification, lane 2: flow through, lanes 3-8: wash fractions containing 8 M, 6 M, 4 M, 2 M, 1 M and 0 M urea, respectively, lanes 9-17: 0 M urea protein elution. (C) Recognition of OVA-CD40LS (arrow) purified from the second round purification by the anti-CD40L and anti-OVA antibodies. M: Pre-stained protein markers.

3.5.2 OVA-CD40LS is functional *in vitro*

The OVA-CD40LS purified from the two-rounds purification approach was tested in CD40 binding ELISA and BMDCs stimulation assay. The purified OVA-CD40LS showed significantly higher binding than that of rOVA (Figure 23) and also showed the ability to stimulate the production of TNF and IL-6 by BMDCs in a dose-dependent manner (Figure 24A). Neither the rOVA nor the heat-inactivated OVA-CD40LS stimulated any cytokine production by BMDCs.

To determine whether OVA-CD40LS was capable of inducing dendritic cell maturation, the expression of CD80, CD86 and MHC II on BMDCs was investigated by flow cytometry. The expression of all three surface makers on BMDCs upon stimulation was showed on Figure 24B. BMDCs stimulated with OVA-CD40LS showed a higher percentage of $CD11C^+CD80^+$ (11.51 ± 0.25 %), $CD11C^+CD86^+$ (24.29 ± 0.90 %), and $CD11C^+MHCII^+$ (32.50 ± 0.61 %) cells out of total cells comparing with BMDCs stimulated with rOVA ($CD11C^+CD80^+$: 9.26 ± 0.17 %; $CD11C^+CD86^+$: 16.56 ± 1.52 %; $CD11C^+MHCII^+$: 26.13 ± 0.54 %) (Figure 24C). The expression of the three surface markers on BMDCs stimulated with heat-inactivated OVA-CD40LS ($CD11C^+CD80^+$: 8.77 ± 0.50 %; $CD11C^+CD86^+$: 12.51 ± 0.99 %; $CD11C^+MHCII^+$: 25.87 ± 0.10 %) were similar to the un-stimulated control ($CD11C^+CD80^+$: 9.23 ± 0.24 %; $CD11C^+CD86^+$: 12.62 ± 0.99 %; $CD11C^+MHCII^+$: 25.91 ± 0.68 %). The mean fluorescent intensity (MFI) values of the groups are shown in Figure 24D.

The above flow cytometry data suggested that the OVA-CD40LS but not rOVA could induce the up-regulation of BMDCs surface marker expression. Therefore, OVA-CD40LS was functional *in vitro* and capable of stimulating BMDCs maturation.

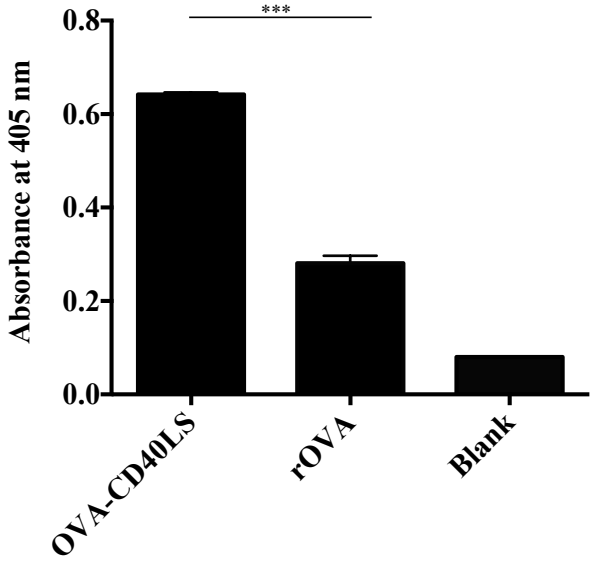

Figure 23 Binding of purified OVA-CD40L to human CD40 in ELISA

Plates were coated with recombinant human CD40 (1μg/ml), incubated with purified OVA-CD40L (50 ng) or rOVA (50 ng), detected with rabbit anti-OVA IgG, finally developed with a goat anti-rabbit IgG-AP conjugate with pNPP. Blank: PBST in place of proteins. Data are shown as means ± SD of duplicates in one experiment. ***P<0.001.

A

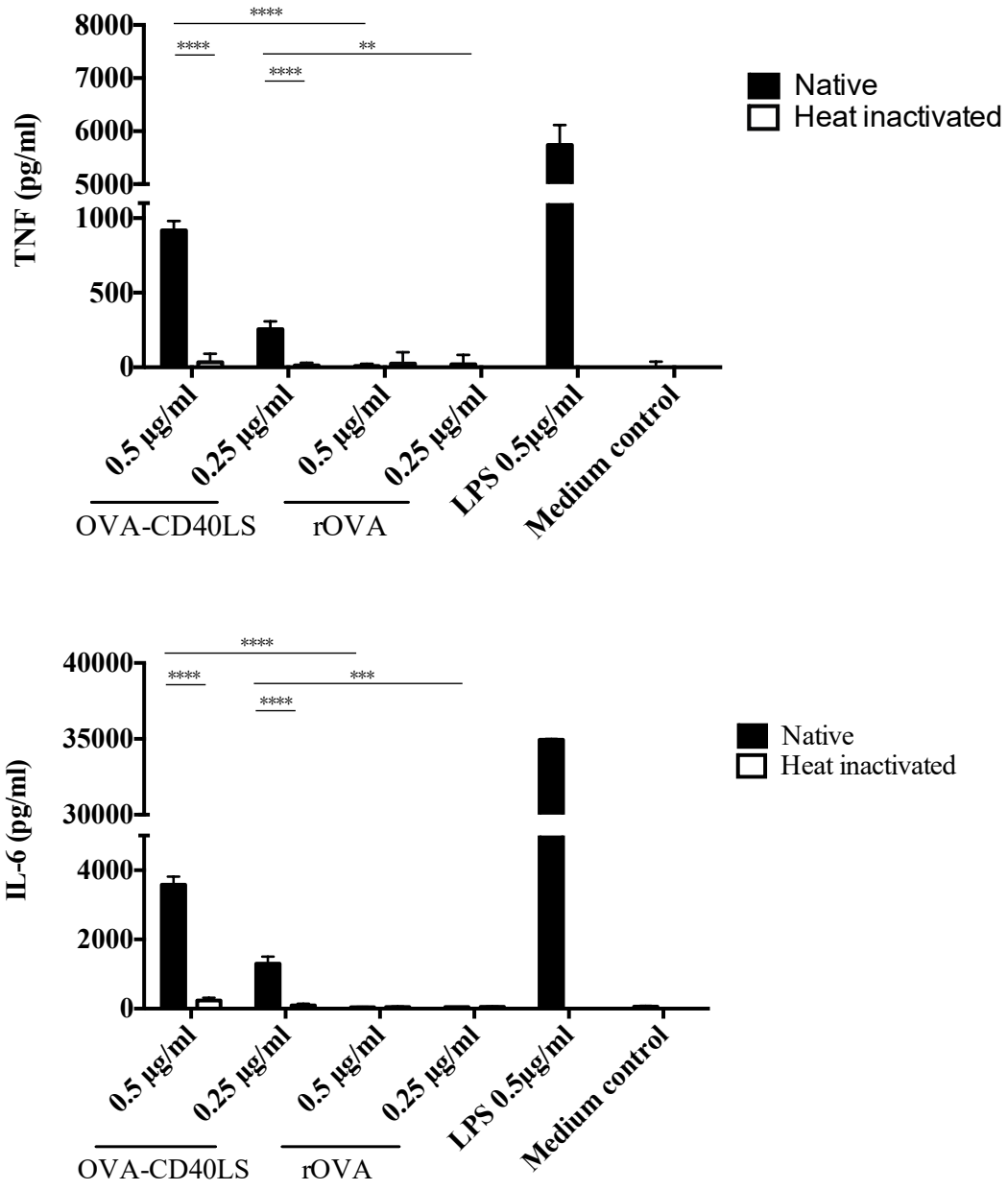
TNF (pg/ml)
8000
7000
6000
5000
1000
500
0
****
****
**
****
Native
Heat inactivated
0.5 µg/ml
0.25 µg/ml
0.5 µg/ml
0.25 µg/ml
LPS 0.5µg/ml
Medium control
OVA-CD40LS
rOVA
IL-6 (pg/ml)
40000
35000
30000
4000
2000
0
****
****
***
****
Native
Heat inactivated
0.5 µg/ml
0.25 µg/ml
0.5 µg/ml
0.25 µg/ml
LPS 0.5µg/ml
Medium control
OVA-CD40LS
rOVA

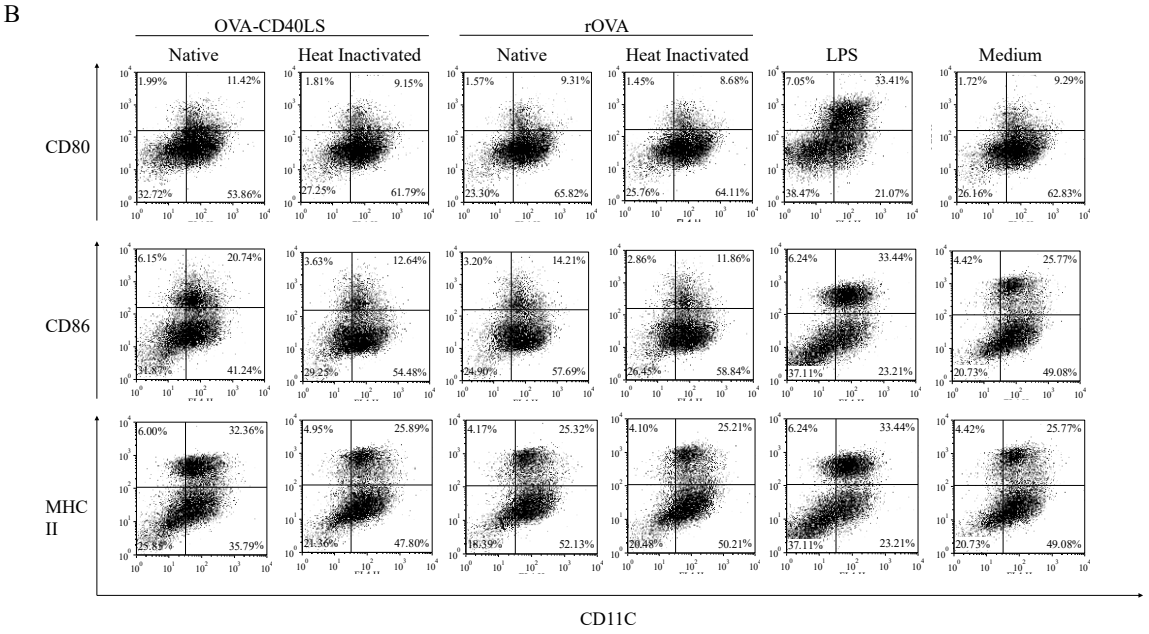
B
OVA-CD40LS
rOVA
Native
Heat Inactivated
Native
Heat Inactivated
LPS
Medium
CD80
CD86
MHC II
CD11C

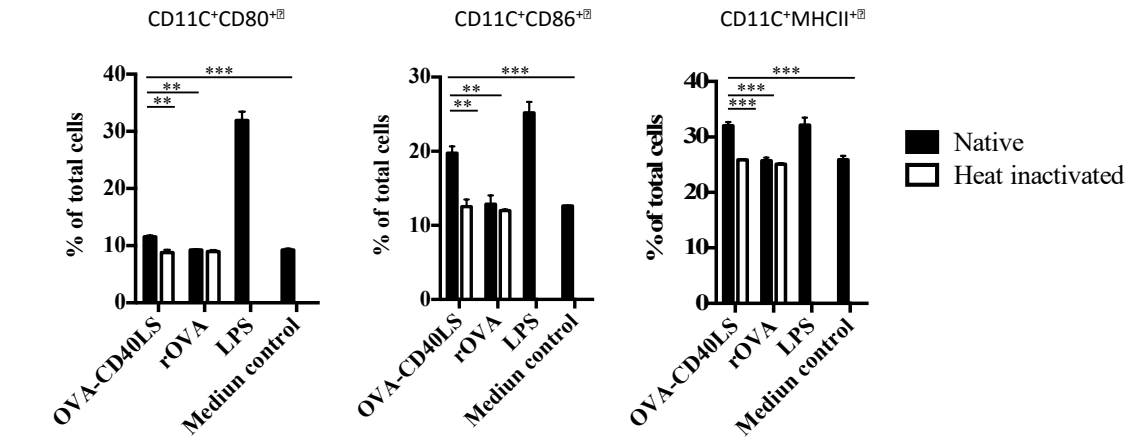
C
CD11C+CD80+
CD11C+CD86+
CD11C+MHCII+
% of total cells
Native
Heat inactivated
OVA-CD40LS
rOVA
LPS
Medium control

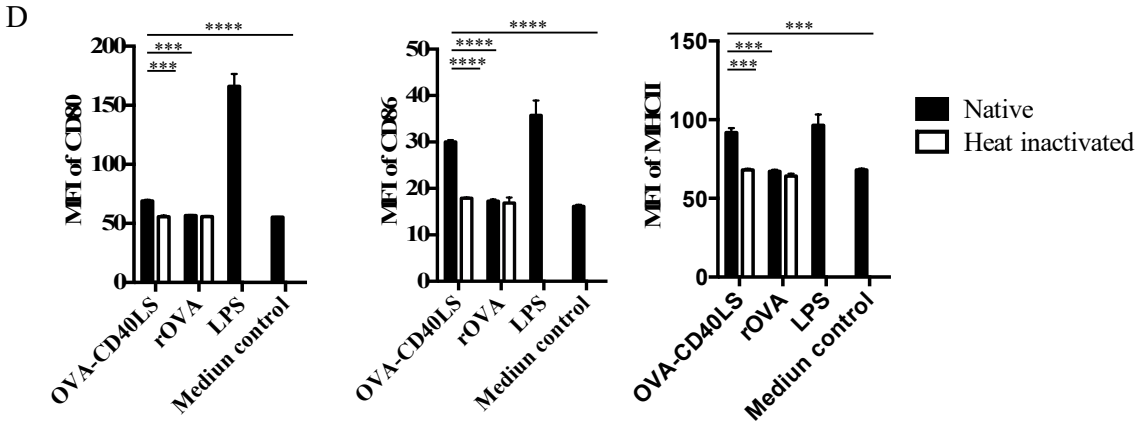
D
MFI of CD80
MFI of CD86
MFI of MHCII
Native
Heat inactivated
OVA-CD40LS
rOVA
LPS
Medium control

Figure 24 Purified OVA-CD40LS stimulated BMDCs maturation

(A) TNF and IL-6 production in mouse BMDCs stimulated with native OVA-CD40LS, heat-inactivated OVA-CD40LS, or rOVA. BMDCs stimulated with LPS and left unstimulated (medium control) served as positive and negative controls, respectively (B) Dot plot showed the expression of CD80, CD86 and MHCII surface markers on BMDCs ($CD11C^+$) stimulated with 0.5 μg/ml of OVA-CD40LS, rOVA, or LPS. (C) The percentage of $CD11C^+CD80^+$, $CD11C^+CD86^+$, or $CD11C^+MHCII^+$ cells. (D) MFI of CD80, CD86 and MHCII expression on BMDCs upon stimulation. Data shown are means ± SD of triplicate stimulations in one experiment. ****P<0.0001, ***P<0.001, **P<0.01. Results shown are representative of two independent experiments.

3.6 OVA-CD40LS induced a strong antigen-specific antibody response via intramucosal injection in the oral cavity

3.6.1 Antibody response induced by OVA-CD40LS by oral intramucosal injection

The ability of OVA-CD40LS to elicit an immune response in mice without adjuvant was tested. Groups of mice (n=5) were injected with of OVA-CD40LS, rOVA, or OVA-CD40LS plus alum, or PBS intramucosally on days 1, 14, and 35. Sera collected after the 3rd immunization was analyzed for anti-OVA IgG. Mice immunized with OVA-CD40LS, rOVA, or OVA-CD40LS plus alum showed serum anti-OVA IgG production. No antibody response was detected with the PBS group. Serum anti-OVA IgG titer from mice immunized with OVA-CD40LS was significantly higher compared to that of the rOVA-immunized mice. A similar anti-OVA IgG titer was observed between the OVA-CD40LS group and OVA-CD40LS plus alum group (Figure 25A).

Sera collected after the 1st (day 13), 2nd (day 24), and 3rd immunization (day 41) were used to analyse the kinetics of the anti-OVA IgG response. The OVA-CD40LS-immunized group produced detectable serum anti-OVA IgG after the first injection. The antibody responses increased after the second injection and maintained at same level after the third injection. The OVA-CD40LS plus alum-immunized mice, the positive control group showed a similar kinetics. In contrast, rOVA-immunized mice did not demonstrate any serum antibody response after the first dose and only a weak response was observed after three injections (Figure 25B).

The serum anti-OVA IgG subtype response was examined (Figure 26). The OVA-CD40L-immunized group showed a higher IgG1 and IgG2a antibody production in mice than that of the rOVA-immunized group. The OVA-CD40LS plus alum-immunized mice showed a similar level of IgG1 and IgG2a response compared to the OVA-CD40LS alone

A

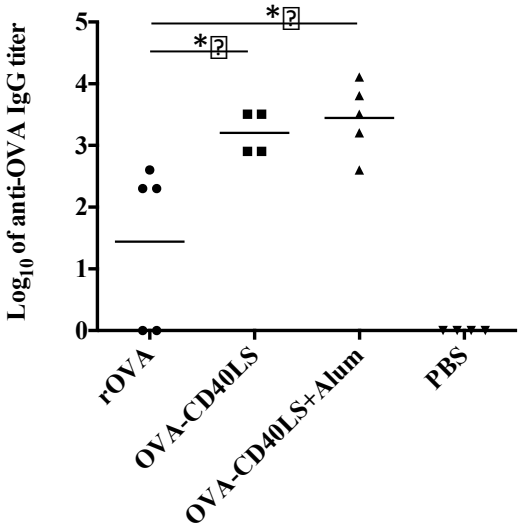

B

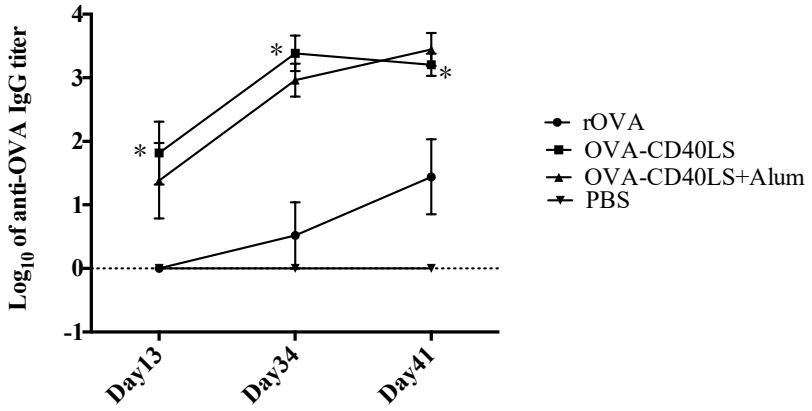

Figure 25 OVA-specific serum IgG titers of mice immunized via oral intramucosal injections

(A) Titers of anti-OVA IgG in sera at euthanasia. Data shown are titer of individual mouse and the mean (horizontal line) of 4-5 mice. (B) Kinetics of serum anti-OVA antibody response. Data shown are means ± SE of 4-5 mice, "*" indicates significant difference between OVA-CD40LS and rOVA immunized groups. *P<0.05.

A

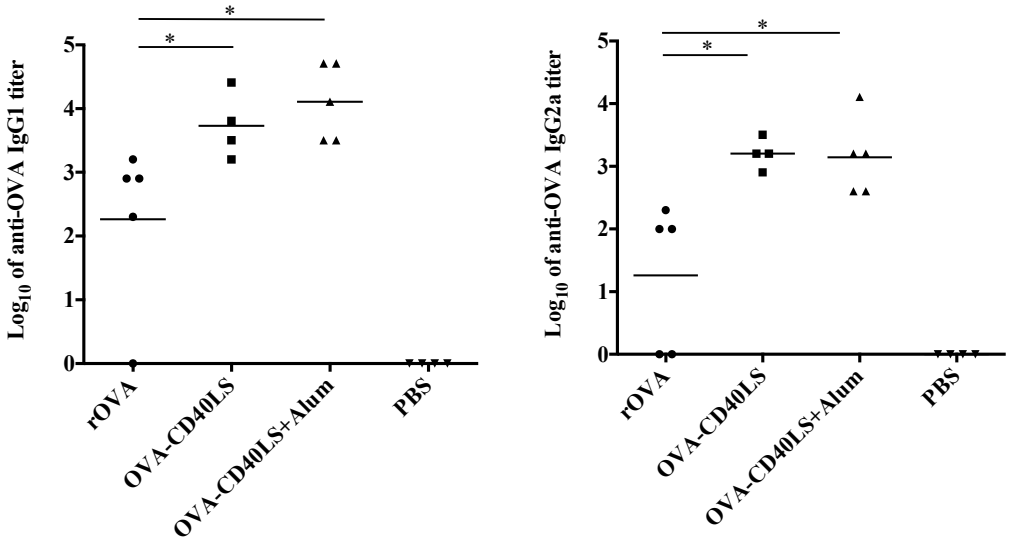

B

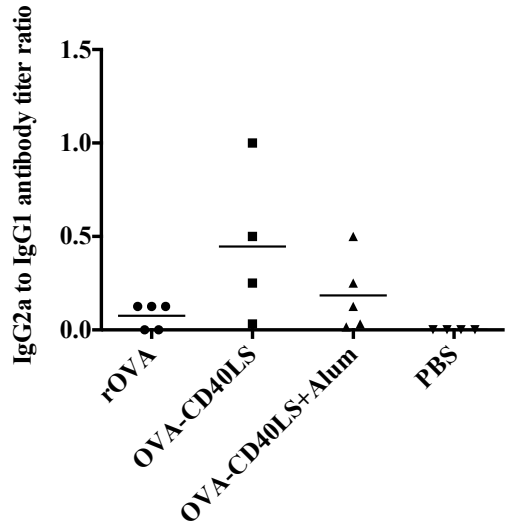

Figure 26 OVA-specific serum IgG1 and IgG2a antibody titers of the mice immunized via oral intramucosal injections

(A) IgG1 and IgG2a titers of sera at euthanasia. (B) IgG2a/IgG1 titer ratios. Data shown are titer of individual mouse and the means (horizontal line) of 4-5 mice. ** P <0.01, * P <0.05.

group (Figure 26A). The anti-OVA IgG2a/IgG1 ratio was compared between groups. Although there was no significant difference between groups, the IgG2a/IgG1 titer ratio was higher in the OVA-CD40LS-immunized mice than the rOVA and OVA-CD40LS plus alum groups (Figure 26B).

To investigate the early immune response, the anti-OVA IgM in sera after the 1st immunization (day13) was evaluated. The anti-OVA IgM levels were similar in all groups including the PBS control group (Figure 27A). The total IgM in each group wasalso evaluated. The results showed that the total serum IgM in the OVA-CD40LS- and rOVA-immunized mice were significantly lower than that of the PBS group. The OVA-CD40LS plus alum-immunized mice showed a similar total IgM level to the PBS group, which represents the base level of the total IgM in mice (Figure 27B).

To investigate the local immune response, saliva samples collected after the 3rd immunization (day 40) were analyzed for anti-OVA IgA. Although it was not statistically significant, the OVA-CD40LS and OVA-CD40LS plus alum-immunized mice showed a trend toward stronger anti-OVA IgA responses compared with rOVA-immunized mice (Figure 28).

3.6.2 T cell response induced by oral mucosal injection of OVA-CD40LS and rOVA

To get some insights into the T cell response induced by the OVA fusion proteins, splenocyte stimulation assay was performed. Splecnocytes were stimulated with purified rOVA (1 μg/ml, 5 μg/ml, and 10 μg/ml), and OT II peptide (200 ng/ml). PMA/Ionnomycine was used as a positive control. After 72 h stimulation, the cell culture supernatants were collected and assayed for IFN-γ and IL-13 production as an indication

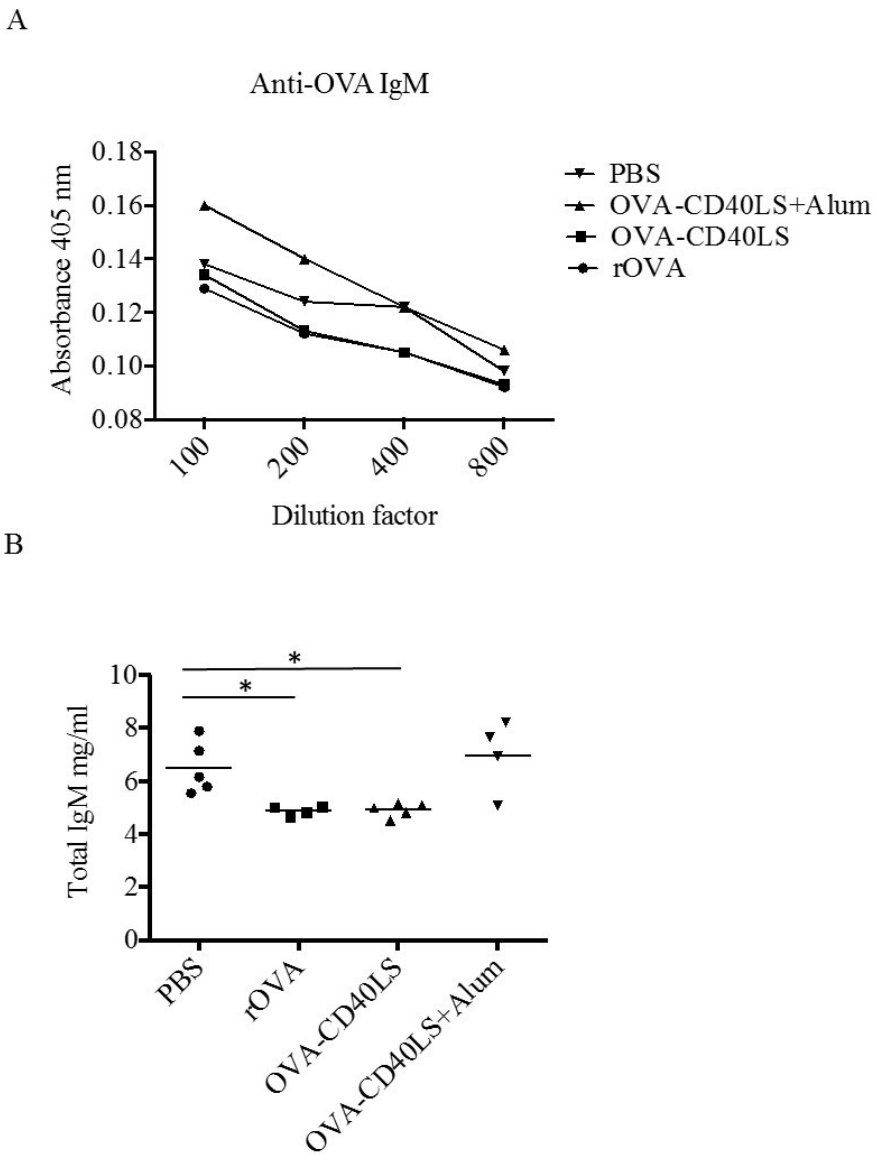

Figure 27 Serum IgM response in mice induced by oral intramusoal injections

(A) Anti-OVA IgM levels after first injection (day 13) in pooled sera. (B) The total serum IgM level in mice at day 13. Data shown are values of individual serum and the means (horizontal line) of 4-5 mice. * P <0.05.

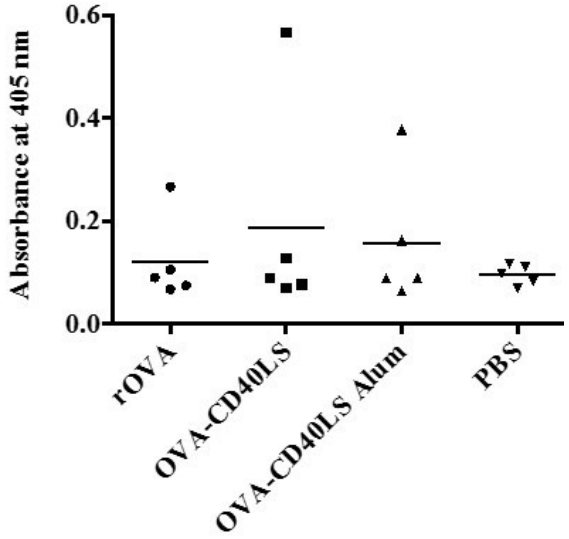

Figure 28 Mucosal OVA-specific IgA response in mice induced by oral intramucosal injections

Saliva samples after 3rd injection (day 40) were tested for anti-OVA IgA levels by ELISA. Saliva samples used in the assay were diluted 1:2. Data shown are value of individual animal and the means (horizontal line) of 4-5 mice.

of Th1 and Th2 responses, respectively. Upon stimulation with rOVA, splenocytes from mice injected with rOVA, OVA-CD40LS, or OVA-CD40LS plus alum produced significantly higher levels of IFN-γ compared to the PBS control group (Figure 29A). The OVA-CD40LS plus alum group produced a higher level of IFN-γ than the rOVA or OVA-CD40LS groups. The IFN-γ level was found similar between the OVA-CD40LS and rOVA group. Upon stimulation with OT II peptide, IFN-γ production was detected only in splenocytes from the OVA-CD40LS plus alum group (Figure 29A).

IL-13 was produced by splenocytes from all groups except PBS after rOVA stimulation (Figure 29B). Stimulation with rOVA induced a higher IL-13 production in the rOVA and OVA-CD40LS plus alum groups compared to the OVA-CD40LS group. The level of IL-13 production observed in the rOVA and OVA-CD40LS plus alum group was similar in response to rOVA stimulation. Both rOVA and OVA-CD40LS plus alum groups showed IL-13 production when stimulated with OT II peptide. The level IL-13 produced by rOVA group was significantly lower than that of OVA-CD40LS plus alum group (Figure 29B). Neither of IFN-γ nor IL-13 production was detected with unstimulated spleen cells (Figure 29). Splenocytes produced high levels of IFN-γ and IL-13 to the positive control PMA/Ionomycine stimulation (data not shown).

3.6.3 Lower lip topical immunization of OVA-CD40LS

With the ultimate goal of using *S. gordonii* to deliver the antigen-targeting fusion protein to the mucosal surface, the ability of OVA-CD40LS to induce an immune response in mice via topical application was tested. To do this, OVA-CD40LS, rOVA, OVA-CD40LS plus alum, or PBS were applied onto the mucosal surface of the lower lip.

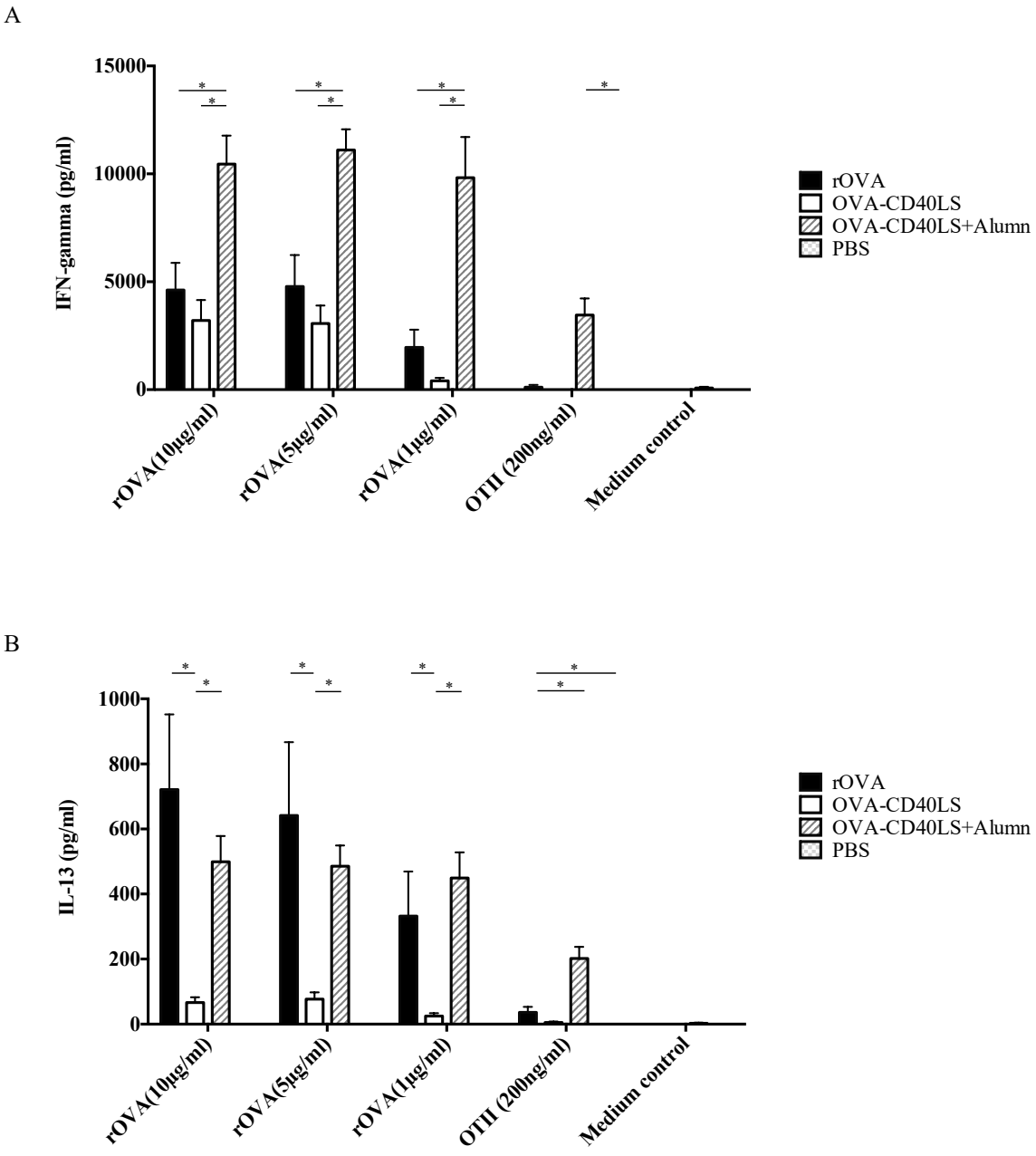

Figure 29 IFN-gamma and IL-13 production by splenocytes from oral intramucosal immunized mice after antigen stimulation

Splenocytes (n=4-5) were stimulated in triplicate with rOVA (10 μg/ml, 5 μg/ml and 1 μg/ml), OTII peptide (200 ng/ml), or left unstimulated (medium control). Data shown are means ± SE. **P*<0.05.

When sera were analyzed, no anti-OVA IgG antibodies were detected in all the groups (data not shown).

The anti-OVA IgM levels in sera after the 1st immunization (day 13) were examined. Although no significant difference of anti-OVA IgM between each immunization groups was detected, the OVA-CD40LS plus alum immunized mice showed slightly higher anti-OVA IgM level then other groups (Figure 30A). The serum total IgM levels were also evaluated. The total IgM level in the OVA-CD40LS plus alum group was significantly higher than that in the other two groups of immunized mice and PBS control group (Figure 30B). No difference of total IgM level in the serum from OVA-CD40LS, rOVA-immunized or PBS control mice was detected (Figure 30B).

To determine whether there was a local immune response induced by the fusion proteins, saliva was collected from the mice after the 3rd immunization (day 40) and assayed by ELISA. In all immunized groups, the anti-OVA IgA level was too low to accurately estimate antibody titer. Therefore, all saliva samples were used in 1:2 dilution. Although there was no significant difference between the groups, the rOVA, OVA-CD40LS and OVA-CD40LS plus alum groups showed a weak salivary IgA antibody response (Figure 31).

3.7 *S. gordonii* expressed a low level of OVA-CD40LS

The above results showed that OVA-CD40LS was able to induce a strong serum anti-OVA IgG response in mice when given by intramucosal injection, suggesting that targeting antigen to CD40 could elicit antigen specific immune response in the murine oral cavity in the protein based immunization setting. The next question I asked was

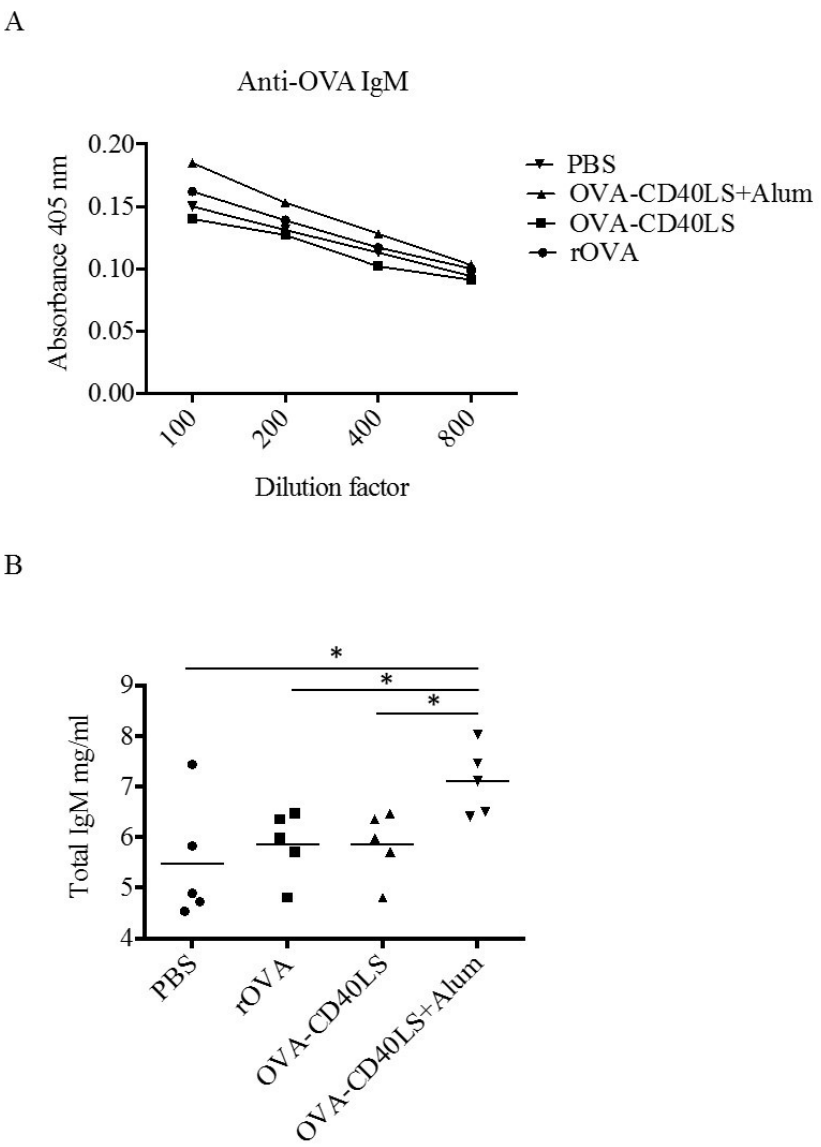

Figure 30 Serum IgM response in mice induced by lower lip topical immunization

(A) Anti-OVA IgM level in pooled sera after first immunization (day 13). (B) Total serum IgM level in sera at day 13 * P <0.05.

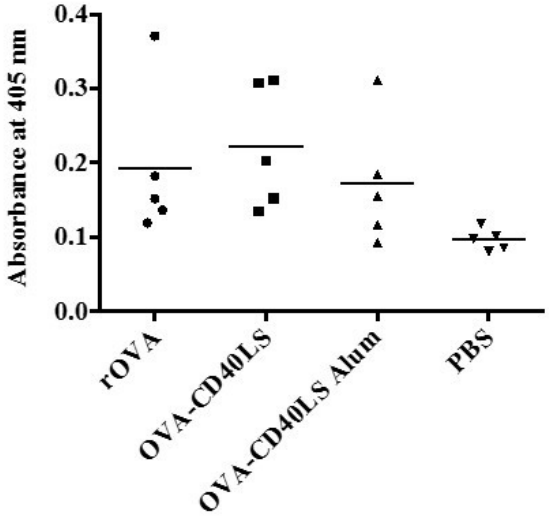

Figure 31 Mucosal OVA-specific IgA response in mice induced by lower lip topical immunization

Saliva samples at day 40 were tested for OVA specific IgA levels by ELISA. Saliva samples used in the assay were diluted 1:2.

whether the OVA-CD40LS could induce an immune response when delivered to the mucosal surface through oral colonization by recombinant *S. gordonii*. To help to work toward answering this question, the *ova-cd40ls* gene was cloned into *S. gordonii* to construct the OVA-CD40LS-expressing recombinant strain.

The *ova-cd40ls* gene was introduced onto the *S. gordonii* chromosome with a gene delivery system using ThyA as a selectable marker (Lee *et al.*, 2016). The genedelivery construct consisted of the *thyA* gene, *ova-cd40ls*, and the gene fragment immediately downstream of *thyA* (5' fragment of *sgo 1142*), were ligated via SfiI restriction sites. The full size delivery gene constructs (3.7 kb) were successfully obtained by PCR using SL841/SL1060 from the ligated DNA (Figure 32A). The PCR product was then transformed into competent *S. gordonii thyA::erm* mutant (Lee *et al.*, 2016). The *thyA* mutant is a thymidine auxotroph and therefore transformants can be selected under thymidine-free condition if the construct has integrated into the chromosome. The genes were integrated into the chromosome by double crossing-over between *thyA* and 5' fragment of *sgo 1142* (Lee *et al.*, 2016). Single colonies were picked and selected by replica plating. The chromosomal DNA was isolated from the erythromycin sensitive, thymidine prototrophic transformants and was screened by PCR. The expected 867 bp of *ova-cd40ls* gene and the 360 bp of r*ova* gene were amplified by PCR with primers SL1048/SL626 and primers SL556/SL655 respectively (Figure 32B). The results showed that OVA-CD40LS gene was successfully introduced into *S. gordonii.* The expression of OVA-CD40LS in recombinant *S. gordonii* was examined. The presence of OVA-CD40LS in the culture supernatant was examined by western blotting. A 35 kDa protein band was detected by the anti-OVA antibody in the culture supernatant of recombinant

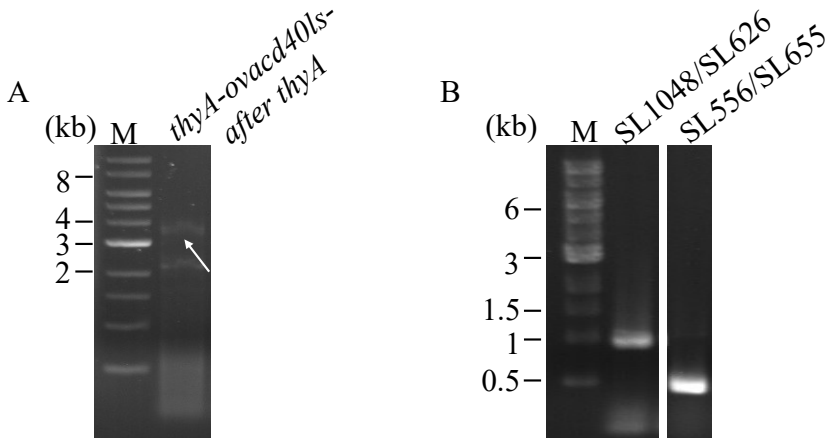

Figure 32 Cloning *ova-cd40ls* gene into *S. gordonii thyA::erm* mutant

(A) PCR amplification of the 3.7 kb delivery gene construct of *thyA-ova-cd40ls-after thyA* (5' fragment of *sgo 1142*) (arrow), which was used to transform *S. gordonii thyA::erm* mutant. (B) PCR amplification of *ova-cd40ls* gene (867 bp) and *cd40ls* (360 bp) from one of the transformants. M: 1 kb DNA ladder.

S. gordonii but not in that of the *thyA* mutant (Figure 33A).

The expression level of OVA-CD40LS in recombinant *S. gordonii* was evaluated. Proteins in the culture supernatants from one litre of tetracycline-induced culture were precipitated by ammonium sulfate. The protein profile was analyzed by SDS-PAGE and the presence of OVA-CD40LS was analyzed by western blotting. No obvious induced 35 kDa band could be identified as the target fusion protein from the complex protein profile showed on the SDS-PAGE gel (Figure 33B). Western blotting showed that the presence of the 35 kDa OVA-CD40LS and smaller size immunoreactive bands in the sample (Figure 33C). The above results suggest that OVA-CD40LS were expressed by *S. gordonii*. The oral colonization of this recombinant *S. gordonii* was not preformed due to the low level of protein expression in this study.

3.8 Attempt in testing antigen-targeting approach using a vaccine antigen

The intramucosal injection of OVA-CD40LS in the murine oral cavity elicited a strong serum antibody response proving that antigen targeting works with the model antigen OVA. However, it is not known if this approach can be applied to other antigens. Previously in our lab, an N-terminus fragment of pertactin was cloned from the *Bordetella pertussis* genome and genetically fused to *cd40ls*. Unlike OVA, pertactin is a virulence factor of *B. pertussis*, which is responsible for pertussis (also known as whooping cough). This protein is one of the components of acellular pertussis vaccine.

Previously, the expression of PRN-CD40LS was tested in *E. coli* with the expression vector pSec, however no protein production was detected. In order to obtain purified PRN-CD40LS, the *prn-cd40ls* gene was subcloned into pComb3X in this study.

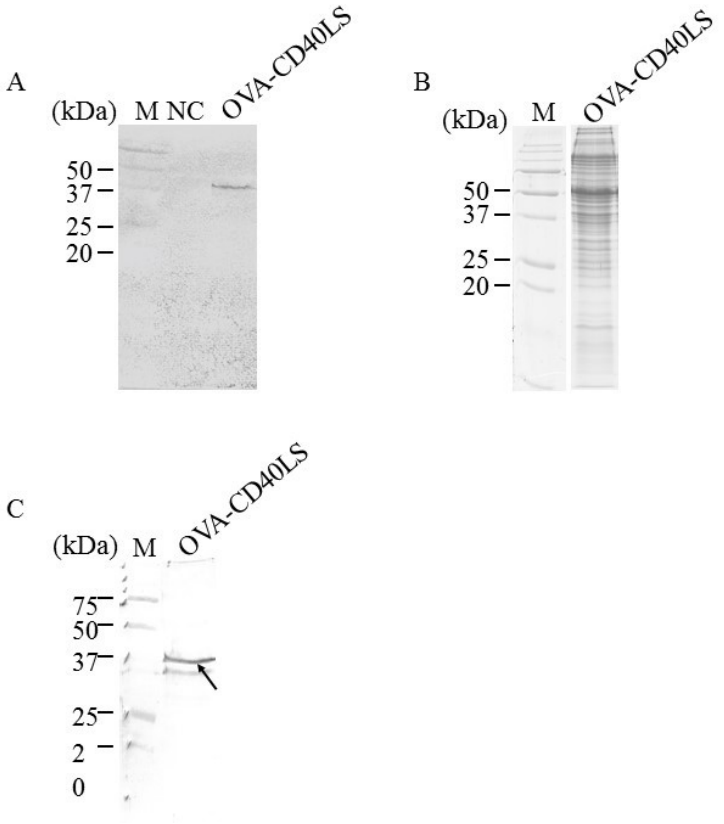

Figure 33 Production of OVA-CD40LS by recombinant *S. gordonii*

(A) Western blotting showing the detection of OVA-CD40LS in the culture supernatant of recombinant *S. gordonii*. NC: *S. gordonii thyA::erm* mutant. (B) SDS-PAGE showing the profile of ammonium sulphate precipitated proteins in the culture supernatant. (C) OVA-CD40LS in the precipitated proteins of *S. gordonii* culture supernatant detected by the anti-OVA antibody (arrow).

Unfortunately, no production of PRN-CD40LS was detected in the *E. coli* cell lysate by western blotting (data not shown). These results suggested that producing PRN-CD40LS in *E. coli* is difficult.

The *prn-cd40ls* gene was previously cloned in *S. gordonii* and the production of the protein was successfully detected (Figure 34A). In the present study, I attempted to purify PRN-CD40LS from *S. gordonii* culture supernatant. The protein production in *S. gordonii* was induced with tetracycline. Due to the low expression level of PRN-CD40LS in the *S. gordonii*, one litre of overnight culture supernatant was prepared and proteins were precipitated by ammonium sulfate. The protein sample was passed through a nickel affinity column. The purification profile was analyzed by SDS-PAGE and western blotting. The SDS-PAGE showed a complex protein profile of the precipitated sample from 1 liter of *S. grodonii* culture supernatant (Figure 34B). A strong protein band at 40 kDa along with a few smaller size bands were detected by the anti-His antibody on western blots (Figure 34C) indicated the presence of 40 kDa PRN-CD40LS and its degradation products. The protein profile was simplified after nickel affinity column chromatography and a 40 kDa and a few smaller size protein bands were present in the eluted fractions (Figure 34B). This 40 kDa protein band and smaller degradation protein bands were also detected in the eluted fractions by western blotting with the anti-His antibody (Figure 34C). Overall, these results suggested that PRN-CD40LS could be at least partially purified from the *S. gordonii* culture supernatant. However, the yield and purity of the PRN-CD40LS was too low to be used for further functionality testing. The expression level of PRN-CD40LS in *S. gorodnii* was also too low for an oral colonization attempt.

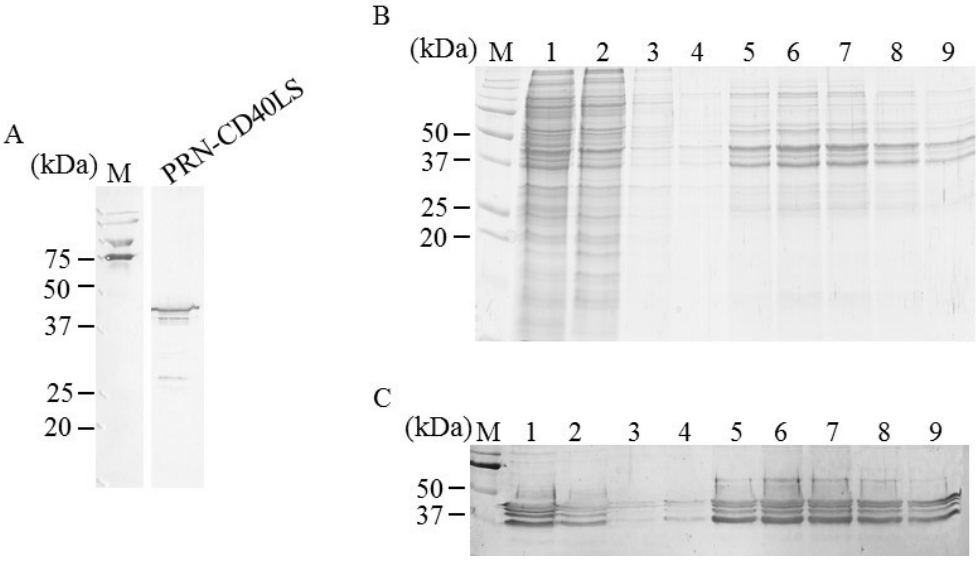

Figure 34 Attempted purification of PRN-CD40LS from *S. gordonii* culture supernatant

(A) Western blot of PRN-CD40LS in *S. gordonii* detected by the anti-His antibody. (B) SDS-PAGE analysis and (C) western blotting of protein purification profile of PRN-CD40L from nickel affinity chromatography. Lane 1: crude proteins, lane 2: flow through, lanes 3-4: wash fractions, lanes 5-9: eluates. M: pre-stained protein markers.

Chapter 4 Discussion

Although the mucosal surface is an ideal immunization site for the induction of both local and systemic immune responses against infections, it is difficult to elicit a robust immune response through direct application of the antigen alone on the mucosal surface (Holmgren & Czerkinsky, 2005). An effective mucosal vaccine has to be able to overcome the physical barriers of the mucosal membrane, targeting to mucosal antigen presenting cells to induce an immune response (Woodrow *et al.*, 2012).

Many studies have used CD40L as an adjuvant or targeting molecule co-delivered with antigens in plasmid DNA or viral vector-based immunization. These studies have shown the successful enhancement of the humoral and cell-mediated immune response in both wild type and CD4-depleted mice (Huang *et al.*, 2004; Li, 2005; Zheng *et al.*, 2005; Kim *et al.*, 2010; Melchers *et al.*, 2011; Auten *et al.*, 2012; Williams *et al.*, 2012; Gupta *et al.*, 2014; Hashem *et al.*, 2014; Rosalia *et al.*, 2015; Gupta *et al.*, 2015). Thus, it is a promising approach for improving the immune response to mucosal immunization. However, it has not been demonstrated that whether the direct immunization of an antigen-targeting fusion protein could lead to an enhancement of the antigen-specific immune response in the oral cavity.

The current study focused on generating a biologically active antigen-targeting fusion protein OVA-CD40LS, and investigating its ability to induce an immune response in the mouse oral cavity.

4.1 Construction and purification of active OVA-CD40LS and rOVA

The antigen-targeting fusion protein OVA-CD40LS and control protein rOVA were constructed and cloned into *E. coli*. The 6 x his tagged OVA-CD40LS and rOVA

were over-expressed by *E. coli* upon IPTG-induction and formed insoluble protein aggregates.

The predicted molecular weight of the OVA-CD40LS is 30.4 kDa, however it was shown as a 35 kDa protein on SDS-PAGE, and was detected with anti-OVA and anti-CD40L antibodies on western blotting (Figure 9, 19 & 22). The discrepancy between the predicted molecular weight and the molecular weight observed during SDS-PAGE/western blotting is not uncommon. The SDS in the protein sample buffer is an anionic detergent that can linearize the proteins (protein denaturation) and impart an even distribution of the negative charges per unit mass of the linearized proteins. This allows the proteins migrate and separate on the polyacrylamide gel based on their molecular weight but not charges. Determination of protein molecular weight using SDS-PAGE in the presence of SDS requires the protein of interest and the molecular markers having the same degree of associations with SDS. However, not all proteins bind to SDS in the same efficiency due to the different amino acid compositions, which causes the proteins appearing to be larger or smaller than the predicted molecular weight on SDS-PAGE/western blotting (Rath *et al.*, 2009). This also explains the migration difference between the OVA-CD40LS and OVA-CD40LS$\Delta_{142\text{-}146}$ observed in figure 11.

Each of the recombinant protein was purified from the denatured (solubilized) *E. coli* cell lysate using nickel affinity column chromatography, and renatured by different refolding approaches. The insoluble proteins in *E. coli* are mainly misfolded protein aggregates formed due to intermolecular interaction of the exposed hydrophobic surfaces of the proteins folding intermediates (Carrió & Villaverde, 2002). To obtain soluble and active recombinant proteins, the insoluble proteins were first denatured with denaturant

and then renatured (refolded) into their native conformation by gradually removing of the denaturant from the system. Many protein-refolding approaches have been developed (Tsumoto *et al.*, 2003; Wang & Geng, 2012). However there is no reliable prediction of which refolding approach would give the desirable results. Therefore, the trial-and-error protein refolding strategy coupled with *in vitro* protein functionality test is still the most common way to obtain an active recombinant protein from the insoluble form (Tsumoto *et al.*, 2003; Vallejo & Rinas, 2004; Wang & Geng, 2012).

In the present study, stepwise dialysis and on-column protein refolding were tested for each recombinant protein. The rOVA remained in solution after refolding by dialysis and showed no activity *in vitro* as expected. However, dialysis refolding of OVA-CD40LS resulted in either protein aggregation (Figure 11) or inactive protein conformation, which could not bind human CD40 (Figure 23) or native CD40 on BMDCs (Figure 24). Biologically active OVA-CD40LS could only obtain by on-column refolding with nickel affinity column chromatography.

4.2 Biologically active OVA-CD40LS purified by "two-rounds" on-column protein refolding with nickel affinity column chromatography

The concept of on-column protein refolding is to immobilize the unfolded protein to a solid support to minimize intermolecular protein interactions during the protein refolding process, which prevents protein aggregation and misfolding (Tsumoto *et al.*, 2003). However, the his-nickel binding between the protein and column resin may become unstable as the protein conformation changes while the urea was gradually removed from the system. The imidazole concentration in the refolding buffer used in this study was reduced to 10 mM in order to minimize protein loss during the refolding

processes. By doing so, the OVA-CD40LS was only partially purified from the crude *E. coli* cell lysate (Figure 12) using a single round of on-column protein refolding (Figure 4B). Interestingly, this partially purified OVA-CD40LS was only a small portion of the total OVA-CD40LS loaded onto the column. The majority of the OVA-CD40LS protein remained strongly bound to the column. This strong interaction between the OVA-CD40LS and the column resin was not due to the his-nickel interaction since the protein remained on the column even after the nickel ions were removed by EDTA wash (data not show). This phenomenon occurs on both agarose based (Figure 12) and non-agarose based nickel affinity columns (Figure 22) suggested that this strong binding was not due to protein-agarose interaction. Moreover, the protein could only be recovered with high concentrations of imidazole under denaturing conditions (Figure 12). To the best of my knowledge, this observation has not been reported in the literature and the reason for the strong binding is not clear.

Nonetheless, this unique property of OVA-CD40LS allowed me to develop a "two-rounds" purification and on-column protein refolding strategy to achieve purification of OVA-CD40LS (Figure 4C). The rationale behind this purification strategy was that the first purification and refolding cycle removed the endotoxin and unwanted proteins from the crude cell lysate and second purification cycle accomplished protein refolding and elution. Because of the strong and stable binding between the OVA-CD40LS and the resin after refolding, the endotoxin and unwanted proteins was able to be removed with extensive washing with TritonX-114 and elution buffers containing 300mM imidazole (Figure 22 A). As the protein profile was significantly simplified by the first purification cycle, the OVA-CD40LS remained on the column was unfolded,

eluted and then used for the second purification cycle on the same column (Figure 22 B). The second purification cycle allowed OVA-CD40LS to be refolded without the extensive washing processes and maximizing the yield of the refolded protein that could be eluted without protein denaturation. The OVA-CD40LS was successfully purified with a good yield. This method may be useful for purification of other recombinant proteins that have similar properties to OVA-CD40LS, especially the CD40LS containing recombinant proteins.

The biologically active OVA-CD40LS was expected to bind to CD40 and induce CD40 cell signaling. In this study, the ability of the OVA-CD40LS bound to human CD40 was confirmed in ELISA binding assay (Figure 23). The purified OVA-CD40LS also stimulated the production of pro-inflammatory cytokines included TNF and IL-6 as well as the up-regulated expression of surface markers included CD80, CD86, and MHC II molecules on mouse BMDCs (Figure 24). These results indicate that the purified protein could specifically interact with CD40 on dendritic cells leads to cell maturation.

It is worth mentioning that although only OVA-CD40LS but not rOVA stimulated the up-regulation of CD80, CD86, and MHC II molecules on mouse BMDCs, the level of increase was marginal. It is possible that 0.5 μg of the OVA-CD40LS was not sufficient to stimulate the full activation of 1 million mouse BMDCs *in vitro*. This can be improved in the future study by using higher amount of purified recombinant fusion protein. It is also possible that the efficiency of the fusion protein to activate the mouse BMDCs via CD40 cell signaling was not optimized. This can be tested in the future study with an additional BMDCs comparison group, which stimulated with recombinant CD40LS. Nonetheless, the results of the current study suggested that the purified OVA-CD40LS is

biologically active *in vitro*.

The rOVA was used as the control protein to OVA-CD40LS. The lack of binding ability of rOVA to human CD40 and stimulation of BMDCs maturation strongly suggests that the biological activities shown by OVA-CD40LS *in vitro* were due to the presence of CD40LS. However, the OVA-CD40LS and rOVA were refolded using different protein-refolding strategies. Therefore, it is possible that the *in vitro* inactive rOVA was due to the dialysis protein-refolding processes. However, this seems to be unlikely.

The possible effects of endotoxin contamination of the protein samples were tested by a heat-inactivated control used in the BMDCs stimulation assay. Endotoxins are heat-stable and can be destroyed when exposed at temperature of 180 ºC for more than 3 hours (Petsch & Anspach, 2000; Magalhães *et al.*, 2007). The heat-inactivation treatment of boiling for 5 min can inactivate proteins but not endotoxins. Thus, the heat-inactivated OVA-CD40LS was not able to induce BMDCs maturation (Figure 24), suggesting that there was no endotoxin contamination of the protein preparation.

4.3 Attempted to purify OVA-CD40LSΔ$_{142\text{-}146}$ in its native conformation

Human and mouse CD40/CD40L share a high degree of homology and were able to cross react with each other (van Kooten & Banchereau, 2000). The two amino acids K143 and Y145 located on the extracellular domain of human CD40L were demonstrated to be critical for its function (Bajorath *et al.*, 1995). These two amino acids were also found in the same locations on the mouse CD40 ligand. There is a good probability that these two amino acids are also critical for the function of mouse CD40L.

In this study, OVA-CD40LSΔ$_{142\text{-}146}$ was constructed by deleting the amino acids

from K142 toY146 on mouse CD40L. The DNA construct of OVA-CD40LSΔ$_{142\text{-}146}$ was cloned into *E. coli* and the protein was found in the insoluble fraction of *E. coli* cell lysate. The partially purified OVA-CD40LSΔ$_{142\text{-}146}$ could still bind to human CD40 and stimulate BMDCs maturation (Figure 14). The possibility of a false positive result in the BMDCs stimulation assay, because of endotoxin contamination, could be excluded by the result of the heat-inactivated control. However, the OVA-CD40LSΔ$_{142\text{-}146}$ purified via on-column refolding on the hydrophobic affinity column could no longer stimulate BMDCs (Figure 21). These results suggested that the refolding of OVA-CD40LSΔ$_{142\text{-}146}$ on nickel affinity column and phenyl-sepharose column resulting in different protein conformations. This different protein conformation was probably due to the different interactions between the unfolded OVA-CD40LSΔ$_{142\text{-}146}$ and the column resins.

In addition to the improper protein refolding, the different amino acid mutation approaches can affect protein structure, which can lead to changes in protein properties such as stability, catalytic activity or the ability to interact with other proteins (Studer *et al.*, 2013). The non-functional human CD40L mutant constructed by Bajorath *et al.*, (1995) was an amino acid substitution mutant, whereas the mouse CD40LS mutant constructed in the present study was a deletion mutant. In general, amino acid substitution mutation only changes the side chains and does not alter the total amino acid number (Chen *et al.*, 2009), which causing relatively small and localized changes in protein structures (Schaefer & Rost, 2012). On the other hand, the amino acid deletion mutation tends to cause more dramatic structural and functional changes to the proteins (Chen *et al.*, 2009; Zhang *et al.*, 2010). Therefore, the deletion mutant of mouse CD40LSΔ$_{142\text{-}146}$ might not be a non-functional mutant as predicted (Bajorath *et al.*, 1995).

It is possible that the OVA-CD40LS$\Delta_{142\text{-}146}$ refolded on nickel affinity column retained its native conformation. It is also possible that the OVA-CD40LS$\Delta_{142\text{-}146}$ was a dysfunctional mutant and refolding on phenyl-sepharose column yielded the correct protein conformation. The combination of deletion mutation and the protein refolding on nickel affinity column led to the *in vitro* functional OVA-CD40LS$\Delta_{142\text{-}146}$.

In the present study, it was difficult to conclude which protein-refolding approaches resulted the native conformation of OVA-CD40LS$\Delta_{142\text{-}146}$. Therefore, the protein was not carried into further investigation in this study and only rOVA was used as the control protein.

4.4 OVA-CD40LS induced a strong serum IgG immune response in the oral cavity via buccal intramucosal injection

The purified OVA-CD40LS was found to be able to induce BMDCs maturation (Figure 23 & 24). The next question was whether OVA-CD40LS could induce a stronger immune response than rOVA in the mouse oral cavity. To answer this question, the *in vivo* function of the OVA-CD40LS was tested in oral mucosal immunization.

The ideal oral mucosal immunization is to directly apply antigens onto the mucosal surface. However, the protective nature of the oral mucosa represents a major challenge. In addition, the mucosal fluids dilute the antigen and limit its deposition onto the epithelium. The antigen can also be trapped in the mucus and being degraded by proteases (Kweon, 2011). To avoid the effects of these factors, mice were immunized with OVA-CD40LS via intramucosal injections.

It has been reported that the migration of buccal derived iDCs, LCs and newly recruited iDCs to the draining cervical LNs was observed following application of

fluorescein isothiocyanate and the hapten dibutyl phthalate (Chalermsarp & Azuma, 2009). Several studies have demonstrated that the administration of plasmid DNA, protein antigens and hapten with appropriate adjuvant could induce a buccal DC activated antigen-specific humoral and cell mediated immune response (Sin *et al.*, 2001; Chalermsarp & Azuma, 2009; Aramaki *et al.*, 2011; Hashem *et al.*, 2014).

Upon immunization, it was expected that the immune response against OVA would be amplified when targeting to CD40 via CD40LS. The OVA-CD40LS induced a strong systemic antibody response when injected into the buccal mucosal layer. The anti-OVA IgG response was significantly higher than that from the rOVA-immunized mice (Figure 25 A) suggesting that OVA-CD40LS was functional *in vivo* to deliver OVA to CD40 expressed on antigen presenting cell surface leading to an enhanced antibody response.

For the first time, this study demonstrated that targeting protein antigen to CD40 via CD40LS through buccal intramucosal injection could induce a strong antibody response in mice.

The kinetic analysis showed that an immune response was induced after only one OVA-CD40LS injection but not rOVA. In addition, only a weak antibody response was detected after repeated rOVA injections (Figure 25 B). It was worth noting that mice received almost two times more molecules of rOVA than OVA-CD40LS per μg of the protein because of their different molecular weight, and OVA-CD40LS induced a more robust antibody response. These results strongly indicate that targeting antigen to CD40 via CD40L induced a stronger immune response in a more efficient manner than antigen alone.

The purpose of including an OVA-CD40LS plus alum group in the experiment was to show immune response against the fusion protein could be induced and serve as a "positive" control. Alum is an adjuvant commonly used for generating mainly a humoral immunity, particularly an IgG1 antibody response by activating $CD4^+$ Th2 cells (Gupta, 1998). The anti-OVA IgG titer induced by OVA-CD40LS was comparable to those induced by OVA-CD40LS plus alum (Figure 25B) suggesting that targeting antigen to CD40 via CD40L was sufficient to induce strong antibody response without additional adjuvant.

4.5 Weak IgA response induced by OVA-CD40LS in oral cavity via buccal intramucosal injection

Typically, mucosal immunization can induce both a systemic and local immune response. Many studies have investigated the buccal mucosa as a vaccination site (Etchart *et al.*, 1997; Desvignes *et al.*, 1998; Etchart *et al.*, 2001; Nudel *et al.*, 2011). A few studies demonstrated that local antigen-specific IgA production was induced by protein antigens and live bacteria with adjuvants via buccal intramucosal injection (Ma *et al.*, 2014; Polak *et al.*, 2014). On the other hand, studies using plasmid DNA immunization via buccal intramucosal injections showed only an antigen specific IgG but not salivary IgA response (Nudel *et al.*, 2011). In the present study, targeting antigen to CD40 via CD40L induced a strong systemic anti-OVA IgG response, but only weak salivary IgA response (Figure 28). This suggests that although the buccal mucosal surface is a good immunization site, injection of antigen into the mucosal layer might not be a good way to induce a mucosal immune response. The mechanisms behind the preferential expression of IgA instead of IgG are not clear. It is thought that activation of dendritic cells and local

expression of cytokines, such as transforming growth factor-β (TGF- β) (Coffman *et al.*, 1989), are important for the B cell class switch towards IgA expression. It is possible that the dendritic cells activated via the CD40-CD40LS interaction cannot efficiently prime T cells for inducing IgA expression by B cells.

In the literature, most studies focus on the systemic antibody response and cell-mediated immune response induced by DNA vaccination on the buccal mucosa. Little information is available about the amount of protein antigen required for induction of a salivary IgA response via buccal intramucosal injection. The use of 30-50 μg/mouse of protein antigen with adjuvant was common in the literatures (Wu *et al.*, 2014; Yang *et al.*, 2016), which is much higher than the amount of OVA-CD40LS or rOVA used in the present study. Therefore, it was possible that 1 μg/mouse of OVA-CD40LS or rOVA was not sufficient to induce antigen specific IgA response in mouse oral cavity.

4.6 T cell response induced by OVA-CD40LS in oral cavity.

In general, Ig class switching of the antigen-activated B cells requires the interaction with $CD4^+$ T helper cells, which provide the CD40 activation signal and the cytokines produced by the activated T cells. The signal generated by the CD40-CD40L interaction promotes the proliferation of activated B cells, the differentiation and survival of germinal center B cells, memory cell formation, Ig secretion, and Ig isotype switching (van Kooten & Banchereau, 2000). In mice, IFN-γ secreted by Th1 cells promotes IgG2a production by B cells, but inhibits IgG1 and IgE production. IL-4 secreted by Th2 cells promotes the production of IgG1 and IgE and suppresses the production of IgG2a (Kindt *et al.*, 2007). In the present study, both antigen specific IgG1 and IgG2a antibodies were

induced in mice injected with OVA-CD40LS, rOVA or OVA-CD40LS plus alum (Figure 26A). Although the difference in the IgG2a/IgG1 titer ratio between immunization groups was not statistically significant, OVA-CD40LS induced a higher IgG2a/IgG1 ratio antibody response compared with that induced by rOVA (Figure 26B). The results suggest that targeting rOVA to CD40 via CD40L shifted the isotype ratio of OVA specific antibody towards a Th1-skewed phenotype. Alum is a vaccine adjuvant that induces Th2-biased immune response (Gupta, 1998). Comparing to the OVA-CD40LS plus alum-immunized group, the OVA-CD40LS alone induced a higher IgG2a/IgG1 titer ratio, which supported that targeting rOVA to CD40 via CD40L induced a Th1-skewed immune response. The above data are in agreement with the ability of CD40 activated dendritic cells to induce a Th1-type immune response reported in the literature (Cella *et al.*, 1996; Koch *et al.*, 1996).

The T cell response was further investigated by splenocyte stimulation with rOVA and OT II peptide ($OVA_{323-339}$). Splenocytes from the PBS-group did not show any IFN-γ or IL-13 production in response to rOVA suggesting that the T cell response seen with OVA-CD40LS, rOVA and OVA-CD40LS plus alum groups are antigen specific. Spleen cells from OVA-CD40LS-immunized mice produced IFN-γ but not IL-13 in response to rOVA stimulation (Figure 29) supporting a Th1-skewed response. Comparing to the OVA-CD40LS-immunized mice, a significantly higher level of IL-13 production was observed with the spleen cells from rOVA-immunized mice (Figure 29) indicating a Th2-skewed response induced by rOVA without targeting to CD40. In addition, splenocytes from the OVA-CD40LS plus alum-immunized mice showed significantly higher level of OVA-specific IFN-γ and IL-13 response compared to the OVA-CD40LS-

immunized mice (Figure 29). It also appears that the presence of alum leaded to a greater increase of IL-13 response than that of the IFN-γ response (Figure 29), which consistent with the ability of alum to induce Th2-skewed response. This result further supported that OVA-CD40LS alone induces Th1-skewed response in mice.

Taken together, the results suggest that targeting antigen to CD40 via CD40L shifted the T cell response towards a Th1 phenotype.

As mentioned before, the mice received significantly more molecules of rOVA than OVA-CD40LS per μg of the protein due to different molecular weight of the two proteins. The possible effect of the uneven amount of protein antigens used during immunization on the phenotype of the induced immune response was not determined in this study.

Interestingly, the magnitude of the T cell response observed in the OVA-CD40LS-immunized and rOVA-immunized mice is at odds with the antibody response induced in the two immunized groups. Despite a similar IFN-γ and a higher IL-13 response observed in the rOVA group compared to the OVA-CD40LS group (Figure 29), the anti-OVA total IgG, IgG1, and IgG2a was significantly lower in the rOVA group (Figure 25&26). The OVA-CD40LS plus alum induced a significantly higher Th1 and Th2 response compared to OVA-CD40LS alone (Figure 29), but did not correspond to the anti-OVA total IgG, IgG1 and IgG2a titer induced in the two groups (Figure 25 & 26). Moreover, only spleen cells from OVA-CD40LS plus alum-immunized mice showed IFN-γ and IL-13 production in response to OT II peptide stimulation (Figure 29).

In the present study, only IFN-γ and IL-13 production were evaluated in splenocyte stimulation. Ideally, other cytokines could be examined in future studies. IL-4

is a typical cytokine mainly produced by activated $CD4^+$ T cells (Paul, 1987), which stimulates B cell to preferentially secrete IgG1 and IgE (Kindt *et al.*, 2007). Other cytokines such as IL-5 and IL-10 are also associated with B cell IgG class switch and antibody production (Saraiva & Anne O'Garra, 2010). TGF-β is another cytokine produced by activated T cells that can induce the production of IgG2a and IgA by antigen-activated B cells. A more complete cytokine profile would be beneficial to investigate T cell response in future studies. In addition, a T cell proliferation assay and co-culture of antigen-loaded dendritic cells with the spleen cells can be used in future studies.

Furthermore, only the T cell response in spleen was investigated in this study. Buccal topical or injection of protein antigen was found to induce a strong serum antigen-specific IgG1 and IgG2a 10 days after immunization with local B cell and T cell priming in the cervical LNs that directly drain to the buccal mucosa but not in the spleen or lung (Etchart *et al.*, 2001). Therefore, evaluation of the T cell response only in the spleen might lead to a biased result in this study. It is necessary to investigate the B cell and T cell response in cervical LN at early time point after buccal immunization.

Another possible reason for the inconsistent T cell and antibody response observed in this study is that the antibody response might be partially due to T cell independent B cell activation events. Hashem and colleagues have demonstrated that targeting an influenza virus antigen to CD40 via CD40L triggered a Th1-polarized antibody response in mice immunized with adenoviral vectors in both wild type and CD4-delpleted mice (Hashem *et al.*, 2014). Other research groups have also shown that using CD40L in the form of a DNA vaccine as a targeting molecule or vaccine adjuvant

were able to induce an antigen-specific IgG response even when $CD4^+$ T cells were absent (Kikuchi *et al.*, 2000; Zheng *et al.*, 2005; Auten *et al.*, 2012; Hashem *et al.*, 2014). In the LNs and spleen, B cells in the follicle are activated through direct transportation of antigen by diffusion or cell-mediated transport by macrophages, migrating DCs, follicular dendritic cells, or antigen activated B cells (Batista & Harwood, 2009; Jason, 2010; Baumjohann *et al.*, 2013). Once injected into the buccal mucosal layer, OVA-CD40LS can not only target dendritic cells, but also other CD40 expressing cells such as macrophages, and newly recruited monocytes, which can potentially promote efficient antigen transporting and directly induced B cell activation via a CD40-CD40L interaction in the cervical LNs or spleen.

It is known that CD40-activated DCs prime cells for effective cross-presentation of antigen for cytotoxic T cell activation (O'Sullivan & Thomas, 2003), CD40LS used as either a targeting molecule or an adjuvant in DNA immunization induced a $CD8^+$ T cell response against various antigens in wild type and CD4-depleted mice (Zheng *et al.*, 2001; Zheng *et al.*, 2005; Hashem *et al.*, 2014). In addition, studies have demonstrated that the buccal mucosa is an excellent site for inducing an antigen specific $CD8^+$ T cell respons. In some cases, the buccal mucosa was considered as an inductive site for priming $CD8^+$ T cell response rather than the effective site (Desvignes *et al.*, 1998). Therefore, it is important to investigate the $CD8^+$ T cells response induced by OVA-CD40LS in the oral cavity, especially via buccal mucosal immunization in the future studies.

Taken together, targeting antigen to CD40 via CD40L through buccal intramucosal injections elicits a Th1-skewed systemic antibody response. However, the

magnitude of the T cell response in the spleen did not correspond to the magnitude of the antibody response. There are many possible explanations for the inconsistent T cell and antibody response detected in this study, but no clear conclusion can be drawn without a thoroughly investigation of the T cell response induced by rOVA and OVA-CD40LS in mice.

4.7 Weak antibody response induced by OVA-CD40LS via oral mucosal surface immunization

In this study, OVA-CD40LS induced a strong antigen-specific IgG response indicating that the fusion protein is functional *in vivo*. The ability of OVA-CD40LS to induce an immune response was tested via oral topical immunization. No serum anti-OVA IgG production was detected in either of the OVA-CD40LS, rOVA nor OVA-CD40LS plus alum group (data not shown). Only a weak salivary anti-OVA IgA response was detected. Although the difference between the anti-OVA IgA level of each group was not statistically significant, there was a trend that OVA-CD40LS, rOVA and OVA-CD40LS plus alum induced higher salivary IgA response than the PBS-control group. OVA-CD40LS seemed to induce a slightly higher level of IgA than rOVA and OVA-CD40LS plus alum-immunized group (Figure 28). Overall, surface immunization with an antigen-targeting fusion protein failed to induce a strong antigen-specific antibody response.

Topical immunization is different than intramucosal injection. Unlike intramucosal injection that delivers the protein antigen directly under the mucosal membrane, protein antigens delivered by topical immunization have to be able to penetrate the top layer of the oral mucosa, which contains mucosal fluids such as saliva

and mucus, as well as proteases. Moreover, the protein antigens are also diluted by the mucosal fluid or swallowed by the animal, which may have significant impact on the immunization outcomes. In this study, 1.5% carboxymethyl cellulose (CMC) was added to the protein samples to decrease the fluidity of the vaccine sample. CMC is a cellulose derivative with carboxymethyl groups (-CH2-COOH) bound to some of the hydroxyl groups of the glucopyranose monomers that make up the cellulose backbone. CMC is used in food and non-food products as a viscosity modifier or thickener (Yang & Zhu, 2007). The thick and less fluid nature of the protein sample is easy to apply and dry on the mucosal surface. The use of CMC as a non-adjuvant additive in intranasal DNA and protein vaccination has been previously reported (Hamajima *et al.*, 1998; Gonzalez *et al.*, 2003; Du *et al.*, 2011). However, CMC has not been used in protein vaccination on the buccal mucosal surface. Whether the use of CMC in the protein sample formulation has any negative effect on buccal topical immunization is unknown. It is possible that the protein antigens were trapped within the CMC matrix on the mucosal surface, which prevented absorption of the protein antigens by the mucosal epithelium layer. The purpose of using a layer of liquid bandage was to prevent protein loss. Ideally, the liquid bandage would form a thin layer on top of the immunization site and seal the protein antigens onto the mucosal surface, which prevent the protein antigens been washed off and swallowed due to mouse drinking and eating behaviors. However, to the best of my knowledge, the use of liquid bandage in topical mucosal immunization has not been reported. Therefore, the effects of the liquid bandage on the delivery or the function of the fusion protein are unknown.

The optimal amount of vaccine antigen required for mucosal immunization varies

depending on the type of antigen, adjuvant, and the site of immunization (Neutra & Kozlowski, 2006). For example, several recent studies have demonstrated that intranasal immunization with10 μg of antigen plus adjuvant was able to induce both antigen-specific serum IgG and mucosal IgA responses in mice (Goff *et al.*, 2013; Gao *et al.*, 2015; Habibi *et al.*, 2015; Zhang *et al.*, 2016). On the other hand, 30 μg of measles virus nucleoprotein was used to elicit an antigen-specific IgG response via buccal topical immunization (Etchart *et al.*, 2001). It was possible that 1 μg of the OVA-CD40LS or rOVA was not sufficient to induce an immune response when administrated on the buccal mucosal surface. In addition, the actual amount of the protein absorbed by the mucosal layers is unknown due to the inevitable protein loss during topical immunization.

The maximum amount of the fusion protein that could be used for each dose of topical immunization was limited by the concentration of the purified proteins prior to freeze-dring and the maximum volume that the mouse lower lip area was able to hold. The highest concentration of purified OVA-CD40LS obtained in this study was 44 μg/ml, which gave the maximum of 100 μg/ml of protein after concentrating via freeze-drying. Concentrating the protein over 100 μg/ml could affect the protein solubility and cause potential negative effects on protein activity due to the over-saturated salt content in the concentrated protein samples. Increasing the yield of the purified protein was also found to be difficult. Although the "two-rounds" purification approach significantly increased the protein concentration in the eluate, the majority of the OVA-CD40LS still remained on the column after second-round purification and could only be eluted after unfolding. As well, mouse lower lip can only hold a maximum of 10 μl of protein sample. Due the above limiting factors, using larger dose of OVA-CD40LS such as 10 μg/mouse for

topical immunization was not possible in this study.

4.8 OVA-CD40LS did not induce an enhanced IgM production in mice by either intramucosal injection or mucosal surface application.

B-1 cells represent the major B cell population in the peritoneal cavity and are also found as marginal zone B cells in the splenic marginal zone. They are also present in the subcapsular area of LNs, the dome region of Peyer's patches, newly formed mucosa-associated lymphoid tissue and the sub-epithelial area of tonsils (Frasca *et al.*, 2005). This B cell population generates most of the "natural" IgM antibodies, which presence in the host from birth without even stimulation. As the critical immunomodulatory and protective factor in inflammatory and autoimmune disease (Grönwall *et al.*, 2012), large amount of "natural" IgM antibodies were secreted by B-1 cells upon activation (Boes, 2000; Baumgarth, 2010).

To get some clues about whether OVA-CD40LS targeted directly to the B-1 cell population after immunization, the levels of antigen-specific IgM and the total IgM in sera collected after the first injection or topical application were evaluated. There was no significant induction of the anti-OVA IgM in sera of any of the immunized groups (Figure 27A & 30A). These results are not surprising as the antigen-specific IgM is mostly produced by conventional B (B-2) cells after antigen stimulation (Baumgarth *et al.*, 1999). At 12 days post immunization, antigen-specific IgG was detected in the OVA-CD40LS and OVA-CD40L plus alum-immunized mice. Therefore, it is possible that anti-OVA IgM expressing B cells have undergone class switch and the level of total IgM antibody response in the serum returned to the level of steady state.

Intramucosal injection of OVA-CD40LS did not induce an increased total serum

IgM level (Figure 27B) compare to the PBS-control group. On the other hand, it appears that the natural IgM expression was lower in the OVA-CD40LS and rOVA-immunized group than the PBS control and OVA-CD40LS plus alum group. However, the reason behind this observation is not clear. Furthermore, buccal topical application of OVA-CD40LS and rOVA induced similar level of serum total IgM compared to the PBS-control group (Figure 30B). These data suggested that targeting antigen to CD40 via CD40L at the buccal mucosa did not lead to B-1 cell activation.

It is worth noting that intramucosal injection and mucosal surface application of the OVA-CD40L plus alum seems to show a higher total IgM expression compared with OVA-CD40LS (Figure 27B & 30B). Alum is a potent adjuvant that induces a rapid recruitment of eosinophils, neutrophils, monocytes, NK cells, NKT cells, and DCs to the site of vaccination and leads to the production of proinflammatory cytokines and chemokines (Mckee *et al.*, 2009). It is possible that B-1 cells were activated and accumulated in the regional LNs and secreted an increased amount of natural IgM in response to the innate signals (Choi & Baumgarth, 2008; Baumgarth, 2010) induced by alum. It is unknown whether OVA-CD40LS plays a role in the induction of natural IgM expression in B cells with the help of alum, due to the lack of a rOVA plus alum control group.

4.9 Attempt to test antigen-targeting approach in *S. gordonii* based oral mucosal vaccine model

The intramucosal injection of OVA-CD40LS was able to induce a strong anti-OVA IgG response. The next question was whether this antigen targeting fusion protein would function similarly when delivered to the mucosal surface by a recombinant *S.*

gordonii vector.

S. gordonii is a Gram-positive commensal bacterium and one of the pioneer organisms colonizing the human oral mucosa and tooth surface (Pozzi & Wells, 1997). This bacterium colonizes early in life and remains throughout life, making it an excellent candidate for a live oral mucosal vaccine (Carlsson *et al.*, 1970). Moreover, this bacterium is naturally genetically competent, which allows easy transformation of heterologous antigen DNA under laboratory conditions (Pozzi & Wells, 1997). The expression of a variety of heterologous protein antigens in *S. gordonii* has been reported (Lee *et al.*, 1999; Giomarelli *et al.*, 2004; Lee *et al.*, 2004; Lee & Faubert, 2006).

In this study, the OVA-CD40LS DNA was introduced into the chromosome of *S. gordonii.* The expression of OVA-CD40LS by *S. gordonii* was confirmed. However, the level of expression was very low (Figure 33). Despite the possible effects of the immunization regimen on the performance of the protein, the earlier results suggested one μg of the OVA-CD40LS did not elicit a good immune response when given directly onto the mucosal surface. Therefore, it was unlikely that oral colonization of the recombinant *S. gordonii* with a low expression of OVA-CD40LS would be able to induce any detectable antibody response. Nevertheless, the recombinant *S. gordonii* strain expressing OVA-CD40LS was successfully constructed in this study. This is an important first step in achieving the goal of applying the antigen-targeting approach to a *S. gordonii*-based live oral vaccine.

The low expression level of heterologous proteins observed in this study is not uncommon for *S. gordonii*. In fact, the inability of this bacterium to produce high levels of heterologous proteins is one of the major limitations of developing *S. gordonii* to be a

successful live vaccine vector. There are many factors that are thought to affect the heterologous protein expression in *S. gordonii* including codon-usage bias, inefficient translocation and folding of proteins, and protein degradation by cell-wall-associated and extracellular proteases (Tjalsma *et al.*, 2004; Lee *et al.*, 2009; Davis *et al.*, 2011). Future efforts are required to improve the expression of OVA-CD40LS in *S. gordonii* in order to test antigen targeting in a live oral vaccine model.

4.10 Conclusion

The current study showed that a relatively small amount of functional OVA-CD40LS in the absence of an adjuvant was capable of eliciting a strong systemic antibody response comparable to that with alum, but a weak mucosal IgA antibody response. Moreover, CD40LS as a targeting molecule appears to promote a Th1-skewed antibody response. On the other hand, oral mucosal surface application of OVA-CD40LS only induced a weak IgA response and no IgG response. The exact reason of this suboptimal immune response is not clear.

In conclusion, antigen targeting to CD40 via CD40L could induce a strong systemic antibody response in the murine oral cavity when the protein antigen was delivered into the mucosal layer. This proved that the hypothesis that targeting antigen to antigen-presenting cells in oral mucosa via CD40-CD40L can elicit an enhanced immune response is correct. In addition, this study showed that buccal mucosa is an excellent immunization site for induction of a strong antibody response using protein antigens.

4.11 Future direction

The major finding of this study was that buccal intramucoal injection of small amount of OVA-CD40LS (1 μg) was able to induce a robust systemic antibody response, suggesting that antigen targeting to CD40 via CD40LS is a promising approach to enhance immune response in oral cavity. At the same time, many subsequent questions were generated by the present study and required further investigation.

Firstly, it is important to investigate whether the systemic antibody response observed in the present study can be optimized by using larger amount of antigen targeting fusion protein such as 10 μg /mouse or even 30 μg /mouse via buccal intramucosal injection. Although the current paradigm in vaccination is that parenteral injection normally does not induce an IgA response, there is evidence suggesting that the injection of antigen can induce mucosal local immune response (Clements & Freytag, 2016). Therefore, it would be interesting to test if a local IgA response can be initiated with larger amounts of antigen. Therefore, improving the yield during protein purification of OVA-CD40LS is one of the immediate goals for future studies.

Secondly, the present study focused on the investigation of antigen specific IgG and IgA production induced by OVA-CD40LS in the mouse oral cavity. Because CD40L is a potent stimulator of a variety type of cells including dendritic cells, B cells, macrophages, and monocytes (van Kooten & Banchereau, 2000), the mechanisms behind the induction of the immune response by OVA-CD40LS in the oral cavity can be complex. Therefore, to obtain a better picture of the immune response induced by OVA-CD40LS, both antigen-specific and non-specific antibody production should be examined at different time points after immunization. Furthermore, whether the antibody response

observed in the present study was mediated via a T-dependent or T-independent pathway is unknown due to the limited investigation into the T cell response. Thus, future studies should investigate the T cell response induced in both cervical LNs and the spleen at different time points and the production of signature cytokines for different T cell subsets such as IL-4, IL-5, IL-10, IL-2, and TGF-β. In addition, whether a cell-mediated T cell response can be induced by OVA-CD40LS is an important direction for future investigation. It is worth noting that the BALB/c mice strain used in this study do not express MHC I molecule haplotype H-2Kb. As a result, the antigen-presenting cells does not present the MHC I H-2Kb-restricted OT I peptide upon immunization, which limits the investigation of $CD8^+$ T cell response induced by OVA-CD40LS and rOVA. In future immunization experiments, the use of C57BL/6 mice strain should be considered.

Finally, another direction that can be further pursued from the present study is the investigation of the potential of antigen targeting via CD40LS applied to a *S. grodonii* based live oral mucosal vaccine. The results from this study failed to show the ability of OVA-CD40LS to induce an immune response applied to the buccal mucosal surface. Improving the topical mucosal immunization method to eliminate the factors that may diminish the performance of the protein such as the use of CMC and a liquid bandage is required for future study. In addition, higher amounts of the protein antigens should be used, which again requires the improvement of the protein purification processes. At the same time, efforts are required to improve the protein expression by recombinant *S. gordonii,* which is essential for future oral colonization experiments.

References

Ahmad, S. I., Kirk, S. H., & Eisenstark, A. (1998). Thymine metabolism and thymineless death in prokaryotes and eukaryotes. *Annual Review of Microbiology,* **52**: 591-625.

Amorij, J., Kersten, G. F. A., Saluja, V., Tonnis, W. F., Hinrichs, W. L. J., Slütter, B., . . . Jiskoot, W. (2012). Towards tailored vaccine delivery: Needs, challenges and perspectives. *Journal of Controlled Release,* **161**: 363-376.

Ansel, K. M., Harris, R. B. S., & Cyster, J. G. (2002). CXCL13 is required for B1 cell homing, natural antibody production, and body cavity immunity. *Immunity,* **16**: 67-76.

Aramaki, O., Chalermsarp, N., Otsuki, M., Tagami, J., & Azuma, M. (2011). Differential expression of co-signal molecules and migratory properties in four distinct subsets of migratory dendritic cells from the oral mucosa. *Biochemical and Biophysical Research Communications,* **413**: 407-413.

Arizon, M., Nudel, I., Segev, H., Mizraji, G., Elnekave, M., Furmanov, K., . . . Hovav, A. (2012). Langerhans cells down-regulate inflammation-driven alveolar bone loss. *Proceedings of the National Academy of Sciences of the United States of America,* **109**: 7043-7048.

Auten, M. W., Huang, W., Dai, G., & Ramsay, A. J. (2012). CD40 ligand enhances immunogenicity of vector-based vaccines in immunocompetent and $CD4^+$ T cell deficient individuals. *Vaccine,* **30**: 2768-2777.

Bajorath, J., Chalupny, N. J., Marken, J. S., Siadak, A. W., Skonier, J., Gordon, M., . . . Aruffo, A. (1995). Identification of residues on CD40 and its ligand which are critical for the receptor-ligand interaction. *Biochemistry,* **34**: 1833-1844.

Barbas, C. F. I., Burton, D. R., Scott, J. K., & Silverman, G. J. (2001). ***Phage display: A laboratory manual***. Cold Spring Harbor, NY: Cold Spring Harbor Laboratory Press.

Batista, F. D., & Harwood, N. E. (2009). The who, how and where of antigen presentation to B cells. *Nature Reviews Immunology,* **9**: 15-27.

Baumgarth, N. (2010). The double life of a B-1 cell: Self-reactivity selects for protective effector functions. *Nature Reviews Immunology,* **11**: 34-46.

Baumgarth, N., Herman, O., Jager, G., & Brown, L. (1999). Innate and acquired humoral immunities to influenza virus are mediated by distinct arms of the immune system. *Proceedings of the National Academy of Sciences of the United States of America,* **96**: 2250-2255.

Baumjohann, D., Preite, S., Reboldi, A., Ronchi, F., Ansel, K., Lanzavecchia, A., & Sallusto, F. (2013). Persistent antigen and germinal center B cells sustain T follicular helper cell responses and phenotype. *Immunity,* **38**: 596-605.

Belz, G. T., Smith, C. M., Kleinert, L., Reading, P., Brooks, A., Shortman, K., . . . Heath, W. R. (2004). Distinct migrating and nonmigrating dendritic cell populations are involved in MHC class I- restricted antigen presentation after lung infection with virus. *Proceedings of the National Academy of Sciences of the United States of America,* **101**: 8670-8675.

Birkholz, K., Schwenkert, M., Kellner, C., Gross, S., Fey, G., Schuler-Thurner, B., . . . Dörrie, J. (2010). Targeting of DEC-205 on human dendritic cells results in efficient MHC class II- restricted antigen presentation. *Blood,* **116**: 2277-2285.

Bishop, G. A., & Hostager, B. S. (2003). The CD40-CD154 interaction in B cell-T cell liaisons. *Cytokine and Growth Factor Reviews,* **14**: 297-309.

Bishop, G. A., Moore, C. R., Xie, P., Stunz, L. L., & Kraus, Z. J. (2007). TRAF proteins in CD40 signaling. *Advances in Experimental Medicine and Biology,* **597**: 131-151.

Boes, M. (2000). Role of natural and immune IgM antibodies in immune responses. *Molecular Immunology,* **37**: 1141-1149.

Bonifaz, L., Bonnyay, D., Mahnke, K., Rivera, M., Nussenzweig, M. C., & Steinman, R. M. (2002). Efficient targeting of protein antigen to the dendritic cell receptor DEC-205 in the steady state leads to antigen presentation on major histocompatibility complex class I products and peripheral $CD8^+$ T cell tolerance. *The Journal of Experimental Medicine,* **196**: 1627-1638.

Bonifaz, L. C., Bonnyay, D. P., Charalambous, A., Darguste, D. I., Fujii, S., Soares, H., . . . Steinman, R. M. (2004). In vivo targeting of antigens to maturing dendritic cells via the DEC-205 receptor improves T cell vaccination. *The Journal of Experimental Medicine,* **199**: 815-824.

Boscardin, S. B., Hafalla, J. C. R., Masilamani, R. F., Kamphorst, A. O., Zebroski, H. A., Rai, U., . . . Nussenzweig, M. C. (2006). Antigen targeting to dendritic cells elicits long-lived T cell help for antibody responses. *The Journal of Experimental Medicine,* **203**: 599-606.

Brandtzaeg, P. (2009). Mucosal immunity: Induction, dissemination, and effector functions. *Scandinavian Journal of Immunology,* **70**: 505-515.

Brandtzaeg, P., Kiyono, H., Pabst, R., & Russell, M. W. (2008). Terminology: Nomenclature of mucosa-associated lymphoid tissue. *Mucosal Immunology,* **1**: 31-37.

Brandtzaeg, P., & Johansen, F. (2005). Mucosal B cells: Phenotypic characteristics, transcriptional regulation, and homing properties. *Immunological Reviews,* **206**: 32-63.

Brimnes, J., Kildsgaard, J., Jacobi, H., & Lund, K. (2007). Sublingual immunotherapy reduces allergic symptoms in a mouse model of rhinitis. *Clinical & Experimental Allergy,* **37**: 488-497.

Bursch, L. S., Wang, L., Igyarto, B., Kissenpfennig, A., Malissen, B., Kaplan, D. H., & Hogquist, K. A. (2007). Identification of a novel population of langerin^{+} dendritic cells. *The Journal of Experimental Medicine,* **204**: 3147-3156.

Caminschi, I., Proietto, A. I., Ahmet, F., Kitsoulis, S., Shin Teh, J., Lo, J. C. Y., . . . Lahoud, M. H. (2008). The dendritic cell subtype-restricted C-type lectin Clec9A is a target for vaccine enhancement. *Blood,* **112**: 3264-3273.

Caminschi, I., & Shortman, K. (2011). Boosting antibody responses by targeting antigens to dendritic cells. *Trends in Immunology,* **33**: 71-77.

Carlsson, J., Grahnén, H., Jonsson, G., & Wikner, S. (1970). Early establishment of streptococcus salivarius in the mouth of infants. *Journal of Dental Research,* **49**: 415-418.

Carrió, M. M., & Villaverde, A. (2002). Construction and deconstruction of bacterial inclusion bodies. *Journal of Biotechnology,* **96**: 3-12.

Cella, M., Scheidegger, D., Palmer-Lehmann, K., Lane, P., Lanzavecchia, A., & Alber, G. (1996). Ligation of CD40 on dendritic cells triggers production of high levels of interleukin-12 and enhances T cell stimulatory capacity: T-T help via APC activation. *The Journal of Experimental Medicine,* **184**: 747-752.

Cerutti, A. (2008). The regulation of IgA class switching. *Nature Reviews Immunology,* **8**: 421-434.

Chalermsarp, N., & Azuma, M. (2009). Identification of three distinct subsets of migrating dendritic cells from oral mucosa within the regional lymph nodes. *Immunology,* **127**: 558-566.

Chamcha, V., Jones, A., Quigley, B. R., Scott, J. R., & Amara, R. R. (2015). Oral immunization with a recombinant *lactococcus lactis*-expressing HIV-1 antigen on group A *streptococcus pilus* induces strong mucosal immunity in the gut. *Journal of Immunology,* **195**: 5025-5034.

Chen, J., Wu, Y., Yang, H., Bergelson, J., Kreitman, M., & Tian, D. (2009). Variation in the ratio of nucleotide substitution and indel rates across genomes in mammals and bacteria. *Molecular Biology and Evolution,* **26**: 1523-1531.

Cho, H., Kim, J., Lee, Y., Kim, J. M., Kim, Y. B., Chun, T., & Oh, Y. (2010). Enhanced humoral and cellular immune responses after sublingual immunization against human papillomavirus 16 L1 protein with adjuvants. *Vaccine,* **28**: 2598-2606.

Clements, J. D., & Freytag, L. C. (2016). Parenteral vaccination can be an effective means of inducing protective mucosal responses. *Clinical and Vaccine Immunology : CVI,* **23**: 438-441.

Coffman, R. L., Lebman, D. A., & Shrader, B. (1989). Transforming growth factor beta specifically enhances IgA production by lipopolysaccharide-stimulated murine B lymphocytes. *The Journal of Experimental Medicine,* **170**: 1039-1044.

Cohn, L., Chatterjee, B., Esselborn, F., Smed-Sörensen, A., Nakamura, N., Chalouni, C., . . . Delamarre, L. (2013). Antigen delivery to early endosomes eliminates the superiority of human blood BDCA3$^+$ dendritic cells at cross presentation. *The Journal of Experimental Medicine,* **210**: 1049-1063.

Coombes, J. L., Siddiqui, K. R. R., Arancibia-Cárcamo, C. V., Hall, J., Sun, C., Belkaid, Y., & Powrie, F. (2007). A functionally specialized population of mucosal CD103$^+$ DCs induces Foxp3$^+$ regulatory T cells via a TGF-β– and retinoic acid– dependent mechanism. *The Journal of Experimental Medicine,* **204**: 1757-1764.

Cui, Z., & Mumper, R. (2002). Bilayer films for mucosal (genetic) immunization via the buccal route in rabbits. *Pharmaceutical Research,* **19**: 947-953.

Da Silva, A. J., Zangirolami, T. C., Novo-Mansur, M., Giordano, R. d. C., & Martins, E. A. L. (2014). Live bacterial vaccine vectors: An overview. *Brazilian Journal of Microbiology,* **45**: 1117-1129.

Davis, E., Kennedy, D., Halperin, S. A., & Lee, S. F. (2011). Role of the cell wall microenvironment in expression of a heterologous SpaP-S1 fusion protein by *streptococcus gordonii*. *Applied and Environmental Microbiology,* **77**: 1660-1666.

Del Rio, M., Bernhardt, G., Rodriguez- barbosa, J., & Förster, R. (2010). Development and functional specialization of CD103$^+$ dendritic cells. *Immunological Reviews,* **234**: 268-281.

Desvignes, Estèves, Etchart, Bella, Czerkinsky, & Kaiserlian. (1998). The murine buccal mucosa is an inductive site for priming class i- restricted CD8$^+$ effector T cells in vivo. *Clinical & Experimental Immunology,* **113**: 386-393.

Di Fabio, S., Medaglini, D., Rush, C. M., Corrias, F., Panzini, G. L., Pace, M., . . . Titti, F. (1998). Vaginal immunization of cynomolgus monkeys with *streptococcus gordonii* expressing HIV-1 and HPV 16 antigens. *Vaccine,* **16**: 485-492.

Diehl, L., Annemieke Th, D. B., Schoenberger, S. P., Ellen IH Van, D. V., Ton N.M. Schumacher, Cornelis J.M. Melief, . . . Rene, E. M. T. (1999). CD40 activation in vivo overcomes peptide-induced peripheral cytotoxic T-lymphocyte tolerance and augments anti-tumor vaccine efficacy. *Nature Medicine,* **5**: 774-779.

Disanto, J. P., Bonnefoy, J. Y., Gauchatt, J. F., Fischer, A., & De Saint Basile, G. (1993). CD40 ligand mutations in X- linked immunodeficiency with hyper-IgM. *Nature,* **361**: 541-543.

Du, Y., Hashizume, T., Kurita-Ochiai, T., Yuzawa, S., Abiko, Y., & Yamamoto, M. (2011). Nasal immunization with a fusion protein consisting of the hemagglutinin A antigenic region and the maltose- binding protein elicits $CD11c^{+}$ $CD8^{+}$ dendritic cells for induced long-term protective immunity. *Infection and Immunity,* **79**: 895-904.

Dwivedy, A., & Aich, P. (2011). Importance of innate mucosal immunity and the promises it holds. *International Journal of General Medicine,* **4**: 299-311.

Etchart, N., Buckland, R., Liu, M. A., Wild, T. F., & Kaiserlian, D. (1997). Class I-restricted CTL induction by mucosal immunization with naked DNA encoding measles virus haemagglutinin. *The Journal of General Virology,* **78 (Pt 7)**: 1577-1580.

Etchart, N., Desmoulins, P. O., Chemin, K., Maliszewski, C., Dubois, B., Wild, F., & Kaiserlian, D. (2001). Dendritic cells recruitment and in vivo priming of $CD8^{+}$ CTL induced by a single topical or transepithelial immunization via the buccal mucosa with measles virus nucleoprotein. *Journal of Immunology,* **167**: 384-391.

Fanslow, W. C., Srinivasan, S., Paxton, R., Gibson, M. G., Spriggs, M. K., & Armitage, R. J. (1994). Structural characteristics of CD40 ligand that determine biological function. *Seminars in Immunology,* **6**: 267-278.

Flamar, A., Xue, Y., Zurawski, S. M., Montes, M., King, B., Sloan, L., . . . Zurawski, G. (2013). Targeting concatenated HIV antigens to human CD40 expands a broad repertoire of multifunctional $CD4^{+}$ and $CD8^{+}$ T cells. *Aids,* **27**: 2041-2051.

Frasca, D., Riley, R. L., & Blomberg, B. B. (2005). Humoral immune response and B-cell functions including immunoglobulin class switch are downregulated in aged mice and humans. *Seminars in Immunology,* **17**: 378-384.

Fujkuyama, Y., Tokuhara, D., Kataoka, K., Gilbert, R. S., Mcghee, J. R., Yuki, Y., . . . Fujihashi, K. (2012). Novel vaccine development strategies for inducing mucosal immunity. *Expert Review of Vaccines,* **11**: 367-379.

Gao, Y., Su, Q., Yi, Y., Jia, Z., Wang, H., Lu, X., . . . Bi, S. (2015). Enhanced mucosal immune responses induced by a combined candidate mucosal vaccine based on hepatitis A virus and hepatitis E virus structural proteins linked to tuftsin. *PLoS ONE,* **10**. doi: 10.1371/journal.pone.0123400.

Giomarelli, B., Maggi, T., Younson, J., Kelly, C., & Pozzi, G. (2004). Expression of a functional single-chain fv antibody on the surface of *streptococcus gordonii*. *Molecular Biotechnology,* **28**: 105-112.

Goff, P., Eggink, D., Seibert, C., Hai, R., Martínez-Gil, L., Krammer, F., & Palese, P. (2013). Adjuvants and immunization strategies to induce influenza virus hemagglutinin stalk antibodies. *PLoS One,* **8**. doi: 10.1371/journal.pone.0079194.

Gonzalez, D., Tzianabos, A. O., Genco, C. A., & Gibson III, F.,C. (2003). Immunization with *porphyromonas gingivalis* capsular polysaccharide prevents *P. gingivalis*-elicited oral bone loss in a murine model. *Infection and Immunity,* **71**: 2283-2287.

Graf, D., Muller, S., Korthauer, U., van Kooten, C., Weise, C., & Kroczek, R. A. (1995). A soluble form of TRAP (CD40 ligand) is rapidly released after T cell activation. *European Journal of Immunology,* **25**: 1749-1754.

Gräslund, S., Nordlund, P., Weigelt, J., Hallberg, B. M., Bray, J., Gileadi, O., . . . Gunsalus, K. C. (2008). Protein production and purification. *Nature Methods,* **5**: 135.

Griffith, J. W., Sokol, C. L., & Luster, A. D. (2014). Chemokines and chemokine receptors: Positioning cells for host defense and immunity. *Annual Review of Immunology,* **32**: 659-702.

Grönwall, C., Vas, J., & Silverman, G. J. (2012). Protective roles of natural IgM antibodies. *Frontiers in Immunology,* **3**: 66-75.

Gupta, R. K. (1998). Aluminum compounds as vaccine adjuvants. *Advanced Drug Delivery Reviews,* **32**: 155-172.

Gupta, S., Termini, J. M., Raffa, F. N., Williams, C. A., Kornbluth, R. S., & Stone, G. W. (2014). Vaccination with a fusion protein that introduces HIV-1 gag antigen into a multitrimer CD40L construct results in enhanced $CD8^+$ T cell responses and protection from viral challenge by vaccinia-gag. *Journal of Virology,* **88**: 1492-1501.

Gupta, S., Termini, J. M., Rivas, Y., Otero, M., Raffa, F. N., Bhat, V., . . . Stone, G. W. (2015). A multi-trimeric fusion of CD40L and gp100 tumor antigen activates dendritic cells and enhances survival in a B16-F10 melanoma DNA vaccine model. *Vaccine,* **33**: 4798-4806.

Ha, S., Tsuji, M., Suzuki, K., Meek, B., Yasuda, N., Kaisho, T., & Fagarasan, S. (2006). Regulation of B1 cell migration by signals through toll-like receptors. *The Journal of Experimental Medicine,* **203**: 2541-2550.

Habibi, M., Asadi Karam, M. R., Shokrgozar, M. A., Oloomi, M., Jafari, A., & Bouzari, S. (2015). Intranasal immunization with fusion protein MrpH·FimH and MPL adjuvant confers protection against urinary tract infections caused by uropathogenic *escherichia coli* and *proteus mirabilis*. *Molecular Immunology,* **64**: 285-294.

Hamajima, K., Sasaki, S., Fukushima, J., Kaneko, T., Xin, K., Kudoh, I., & Okuda, K. (1998). Intranasal administration of HIV-DNA vaccine formulated with a polymer, carboxymethylcellulose, augments mucosal antibody production and cell- mediated immune response. *Clinical Immunology and Immunopathology,* **88**: 205-210.

Hashem, A. M., Gravel, C., Chen, Z., Yi, Y., Tocchi, M., Jaentschke, B., . . . Li, X. (2014). CD40 ligand preferentially modulates immune response and enhances protection against influenza virus. *Journal of Immunology,* **193**: 722-734.

Hatzifoti, C., & Heath, A. W. (2007). CD40-mediated enhancement of immune responses against three forms of influenza vaccine. *Immunology,* **122**: 98-106.

Hawiger, D., Inaba, K., Dorsett, Y., Guo, M., Mahnke, K., Rivera, M., . . . Nussenzweig, M. C. (2001). Dendritic cells induce peripheral T cell unresponsiveness under steady state conditions in vivo. *The Journal of Experimental Medicine,* **194**: 769-780.

Hayakawa, K., Hardy, R. R., Herzenberg, L. A., & Herzenberg, L. A. (1985). Progenitors for ly-1 B cells are distinct from progenitors for other B cells. *The Journal of Experimental Medicine,* **161**: 1554-1568.

Hervouet, C., Luci, C., Bekri, S., Juhel, T., Bihl, F., V, M. B., . . . F, A. (2013). Antigen-bearing dendritic cells from the sublingual mucosa recirculate to distant systemic lymphoid organs to prime mucosal CD8 T cells. *Mucosal Immunology,* **7**: 280-291.

Herzenberg, L. A., Stall, A. M., Lalor, P. A., Sidman, C., Moore, W. A., & Parks, D. R. (1986). The ly-1 B cell lineage. *Immunological Reviews,* **93**: 81-102.

Holmgren, J., & Czerkinsky, C. (2005). Mucosal immunity and vaccines. *Nature Medicine,* **11**: 45-53.

Hovav, A. H. (2013). Dendritic cells of the oral mucosa. *Mucosal Immunology,* **7**: 27-37.

Huang, C., Wang, C., Wu, T., Wu, K., Lee, C., & Peng, H. (2008). Neonatal sublingual vaccination with salmonella proteins and adjuvant cholera toxin or CpG oligodeoxynucleotides induces mucosal and systemic immunity in mice. *Journal of Pediatric Gastroenterology and Nutrition,* **46**: 262-271.

Huang, H. I., Wu, P. Y., Teo, C. Y., Chen, M. N., Chen, Y. C., Silin, D., & Tao, M. H. (2004). Improved immunogenicity of a self tumor antigen by covalent linkage to CD40 ligand. *International Journal of Cancer,* **108**: 696-703.

Hutchings, A. B., Helander, A., Silvey, K. J., Chandran, K., Lucas, W. T., Nibert, M. L., & Neutra, M. R. (2004). Secretory immunoglobulin A antibodies against the sigma 1 outer capsid protein of reovirus type 1 lang prevent infection of mouse peyer's patches. *The Journal of Virology,* **78**: 947-957.

Huub, F. J. S., Ferro, V. A., Strioga, M. M., & Virgil, E. J. C. S. (2015). Choice and design of adjuvants for parenteral and mucosal vaccines. *Vaccines,* **3**: 148-171.

Iwasaki, A. (2016). Exploiting mucosal immunity for antiviral vaccines. *Annual Review of Immunology,* **34**: 575-608.

Iwasaki, A., & Kelsall, B. L. (1999). Freshly isolated peyer's patch, but not spleen, dendritic cells produce interleukin 10 and induce the differentiation of T helper type 2 cells. *The Journal of Experimental Medicine,* **190**: 229-240.

Jason, G. C. (2010). B cell follicles and antigen encounters of the third kind. *Nature Immunology,* **11**: 989-996.

Joffre, O. P., Sancho, D., Zelenay, S., Keller, A. M., & Reis, E. S. (2010). Efficient and versatile manipulation of the peripheral $CD4^+$ T- cell compartment by antigen targeting to DNGR- 1/ CLEC9A. *European Journal of Immunology,* **40**: 1255-1265.

Karpusas, M., Hsu, Y. M., Wang, J. H., Thompson, J., Lederman, S., Chess, L., & Thomas, D. (1995). 2 A crystal structure of an extracellular fragment of human CD40 ligand. *Structure (London, England : 1993),* **3**: 1031-1039.

Kastenmüller, W., Kastenmüller, K., Kurts, C., & Seder, R. A. (2014). Dendritic cell-targeted vaccines - hope or hype? *Nature Reviews Immunology,* **14**: 705-711.

Keselman, A., Li, E., Maloney, J., & Singer, S. M. (2016). The microbiota contributes to $CD8^+$ T cell activation and nutrient malabsorption following intestinal infection with giardia duodenalis. *Infection and Immunity,* **84**: 2853-2860.

Kikuchi, T., Worgall, S., Singh, R., Malcolm A.S. Moore, & Ronald, G. C. (2000). Dendritic cells genetically modified to express CD40 ligand and pulsed with antigen can initiate antigen-specific humoral immunity independent of $CD4^+$ T cells. *Nature Medicine,* **6**: 1154-1159.

Kildsgaard, J., Brimnes, J., Jacobi, H., & Lund, K. (2007). Sublingual immunotherapy in sensitized mice. *Annals of Allergy, Asthma & Immunology,* **98**: 366-372.

Kim, S., Joo, D., Lee, J., Shim, B., Cheon, I. S., Jang, J., . . . Chang, J. (2012). Dual role of respiratory syncytial virus glycoprotein fragment as a mucosal immunogen and chemotactic adjuvant. *PLoS ONE,* **7**. doi: 10.1371/journal.pone.0032226.

Kim, Y., Kim, Y., Lee, J., Han, S., Ko, H., Park, H., . . . Kang, C. (2010). CD40-targeted recombinant adenovirus significantly enhances the efficacy of antitumor vaccines based on dendritic cells and B cells. *Human Gene Therapy,* **21**: 1697-1706.

Kindt, T. J., Goldsby, R. A., & Osborne, B. A. (Eds.). (2007). *Kuby immunology* (6th ed.). New York, NY: W.H. Freeman.

Knight, J. B., Halperin, S. A., West, K. A., & Lee, S. F. (2008). Expression of a functional single-chain variable-fragment antibody against complement receptor 1 in *streptococcus gordonii*. *Clinical and Vaccine Immunology,* **15**: 925-931.

Koch, F., Stanzl, U., Jennewein, P., Janke, K., Heufler, C., Kampgen, E., . . . Schuler, G. (1996). High level IL-12 production by murine dendritic cells: Upregulation via MHC class II and CD40 molecules and downregulation by IL-4 and IL-10. *The Journal of Experimental Medicine,* **184**: 741-746.

Kooten, C. v., & Banchereau, J. (1997). Functions of CD40 on B cells, dendritic cells and other cells. *Current Opinion in Immunology,* **9**: 330-337.

Kraan, H., Vrieling, H., Czerkinsky, C., Jiskoot, W., Kersten, G., & Amorij, J. (2014). Buccal and sublingual vaccine delivery. *Journal of Controlled Release,* **190**: 580-592.

Krummel, M. F., Bartumeus, F., & Audrey Gérard. (2016). T cell migration, search strategies and mechanisms. *Nature Reviews Immunology,* **16**: 193-201.

Kwa, S., Lai, L., Gangadhara, S., Siddiqui, M., Pillai, V. B., Labranche, C., . . . Amara, R. R. (2014). CD40L-adjuvanted DNA/ modified vaccinia virus ankara simian immunodeficiency virus SIV239 vaccine enhances SIV-specific humoral and cellular immunity and improves protection against a heterologous SIVE660 mucosal challenge. *Journal of Virology,* **88**: 9579-9589.

Kweon, M. (2011). Sublingual mucosa: A new vaccination route for systemic and mucosal immunity. *Cytokine,* **54**: 1-5.

Laemmli, U. K. (1970). Cleavage of structural proteins during the assembly of the head of bacteriophage T4. *Nature,* **227**: 680-685.

Larsson, O., & Olgart, L. (1989). The enhancement of carbachol- induced salivary secretion by VIP and CGRP in rat parotid gland is mimicked by forskolin. *Acta Physiologica Scandinavica,* **137**: 231-236.

Le Borgne, M., Etchart, N., Goubier, A., Lira, S. A., Sirard, J. C., van Rooijen, N., . . . Dubois, B. (2006). Dendritic cells rapidly recruited into epithelial tissues via CCR6/ CCL20 are responsible for $CD8^+$ T cell crosspriming in vivo. *Immunity,* **24**: 191-201.

Lee, C. W., Lee, S. F., & Halperin, S. A. (2004). Expression and immunogenicity of a recombinant diphtheria toxin fragment A in streptococcus gordonii. *Applied and Environmental Microbiology,* **70**: 4569-4574.

Lee, P., & Faubert, G. M. (2006). Oral immunization of BALB/c mice by intragastric delivery of *streptococcus gordonii*- expressing giardia cyst wall protein 2 decreases cyst shedding in challenged mice. *FEMS Microbiology Letters,* **265**: 225-236.

Lee, S. F., Halperin, S. A., Wang, H., & Macarthur, A. (2002a). Oral colonization and immune responses to *streptococcus gordonii* expressing a pertussis toxin S1 fragment in mice. *FEMS Microbiology Letters,* **208**: 175-178.

Lee, S. F. (2003). Oral colonization and immune responses to *streptococcus gordoni*i: Potential use as a vector to induce antibodies against respiratory pathogens. *Current Opinion in Infectious Diseases,* **16**: 231-235.

Lee, S. F., Halperin, S. A., Knight, J. B., & Tait, A. (2002b). Purification and immunogenicity of a recombinant *bordetella pertussis* S1S3FHA fusion protein expressed by *streptococcus gordonii*. *Applied and Environmental Microbiology,* **68**: 4253-4258.

Lee, S. F., Hulbah, M., & Halperin, S. A. (2016). Development of a gene delivery system in *streptococcus gordonii* using thymidylate synthase as a selection marker. *Journal of Microbiological Methods,* **125**: 43-48.

Lee, S. F., Li, Y., & Halperin, S. A. (2009). Overcoming codon-usage bias in heterologous protein expression in *streptococcus gordonii*. *Microbiology,* **155**: 3581-3588.

Lee, S. F., March, R. J., Halperin, S. A., Faulkner, G., & Gao, L. (1999). Surface expression of a protective recombinant pertussis toxin S1 subunit fragment in *streptococcus gordonii*. *Infection and Immunity,* **67**: 1511-1516.

Lehmann, C., Heger, L., Heidkamp, G., Baranska, A., Lühr, J., Hoffmann, A., & Dudziak, D. (2016). Direct delivery of antigens to dendritic cells via antibodies specific for endocytic receptors as a promising strategy for future therapies. *Vaccines,* **4**: 8-39.

Li, J., Ahmet, F., Sullivan, L. C., Brooks, A. G., Kent, S. J., Rose, R., . . . Caminschi, I. (2015). Antibodies targeting Clec9A promote strong humoral immunity without adjuvant in mice and non- human primates. *European Journal of Immunology,* **45**: 854-864.

Li, J., Liu, Y., Wang, F., Ma, G., & Su, Z. (2004). Hydrophobic interaction chromatography correctly refolding proteins assisted by glycerol and urea gradients. *Journal of Chromatography A,* **1061**: 193-199.

Li, W. (2005). Synergistic antibody induction by antigen–CD40 ligand fusion protein as improved immunogen. *Immunology,* **115**: 215-222.

Lundholm, P., Asakura, Y., Hinkula, J., Lucht, E., & Wahren, B. (1999). Induction of mucosal IgA by a novel jet delivery technique for HIV-1 DNA. *Vaccine,* **17**: 2036-2042.

Lutz, M. B., Kukutsch, N., Ogilvie, A. L. J., Rößner, S., Koch, F., Romani, N., & Schuler, G. (1999). An advanced culture method for generating large quantities of highly pure dendritic cells from mouse bone marrow. *Journal of Immunological Methods,* **223**: 77-92.

Lycke, N. (2012). Recent progress in mucosal vaccine development: Potential and limitations. *Nature Reviews Immunology,* **12**: 592-605.

Ma, D. Y., & Clark, E. A. (2009). The role of CD40 and CD154/CD40L in dendritic cells. *Seminars in Immunology,* **21**: 265-272.

Ma, Y., Tao, W., Krebs, S., Sutton, W., Haigwood, N., & Gill, H. (2014). Vaccine delivery to the oral cavity using coated microneedles induces systemic and mucosal immunity. *Pharmaceutical Research,* **31**: 2393-2403.

Macri, C., Dumont, C., Johnston, A. P., & Justine, D. M. (2016). Targeting dendritic cells: A promising strategy to improve vaccine effectiveness. *Clinical & Translational Immunology,* **5**: e66. doi: 10.1038/cti.2016.6.

Magalhães, P.,O., Lopes, A. M., Mazzola, P. G., Rangel-Yagui, C., Penna, T. C. V., & Pessoa, A. (2007). Methods of endotoxin removal from biological preparations: A review. *Journal of Pharmacy & Pharmaceutical Sciences,* **10**: 388-404.

Maggi, T., Oggioni, M. R., Medaglini, D., Bianchi Bandinelli, M. L., Soldateschi, D., Wiesmuller, K. H., . . . Pozzi, G. (2000). Expression of measles virus antigens in *streptococcus gordonii*. *The New Microbiologica,* **23**: 119-128.

Maggi, T., Spinosa, M., Ricci, S., Medaglini, D., Pozzi, G., & Oggioni, M. R. (2002). Genetic engineering of *streptococcus gordonii* for the simultaneous display of two heterologous proteins at the bacterial surface. *FEMS Microbiology Letters,* **210**: 135-141.

Mahnke, K., Qian, Y., Fondel, S., Brueck, J., Becker, C., & Enk, A. H. (2005). Targeting of antigens to activated dendritic cells in vivo cures metastatic melanoma in mice. *Cancer Research,* **65**: 7007-7012.

Mantegazza, A. R., Savina, A., Vermeulen, M., Pérez, L., Geffner, J., Hermine, O., . . . Amigorena, S. (2008). NADPH oxidase controls phagosomal pH and antigen cross-presentation in human dendritic cells. *Blood,* **112**: 4712-4722.

Mascarell, L., Lombardi, V., Louise, A., Saint-Lu, N., Chabre, H., Moussu, H., . . . Moingeon, P. (2008). Oral dendritic cells mediate antigen-specific tolerance by stimulating T H1 and regulatory $CD4^+$ T cells. *The Journal of Allergy and Clinical Immunology,* **122**: 603-609.

Matteoli, G., Mazzini, E., Iliev, I. D., Mileti, E., Fallarino, F., Puccetti, P., . . . Rescigno, M. (2010). Gut CD103 dendritic cells express indoleamine 2,3- dioxygenase which influences T regulatory/ T effector cell balance and oral tolerance induction. *Gut,* **59**: 595-604.

Mayer, L. (2003). Mucosal immunity. *Pediatrics,* **111**: 1595-600.

Mazzei, G. J., Edgerton, M. D., Losberger, C., Lecoanet-Henchoz, S., Graber, P., Durandy, A., . . . Bonnefoy, J. Y. (1995). Recombinant soluble trimeric CD40 ligand is biologically active. *The Journal of Biological Chemistry,* **270**: 7025-7028.

McGhee, J. R., Mestecky, J., Dertzbaugh, M. T., Eldridge, J. H., Hirasawa, M., & Kiyono, H. (1992). The mucosal immune system: From fundamental concepts to vaccine development. *Vaccine,* **10**: 75-88.

Mckee, A. S., Munks, M. W., Macleod, M. K. L., Fleenor, C. J., Van Rooijen, N., Kappler, J. W., & Marrack, P. (2009). Alum induces innate immune responses through macrophage and mast cell sensors, but these sensors are not required for alum to act as an adjuvant for specific immunity. *Journal of Immunology,* **183**: 4403-4414.

Medaglini, D., Pozzi, G., King, T., & Fischetti, V. (1995). Mucosal and systemic immune responses to a recombinant protein expressed on the surface of the oral commensal bacterium streptococcus gordonii after oral colonization. *Proceedings of the National Academy of Sciences of the United States of America,* **92**: 6868-6872.

Medaglini, D., Ciabattini, A., Spinosa, M. R., Maggi, T., Marcotte, H., Oggioni, M. R., & Pozzi, G. (2001). Immunization with recombinant *streptococcus gordonii* expressing tetanus toxin fragment C confers protection from lethal challenge in mice. *Vaccine,* **19**: 1931-1939.

Medaglini, D., Rush, C. M., Sestini, P., & Pozzi, G. (1997). Commensal bacteria as vectors for mucosal vaccines against sexually transmitted diseases: Vaginal colonization with recombinant streptococci induces local and systemic antibodies in mice. *Vaccine,* **15**: 1330-1337.

Medina, E., & Guzmán, C. A. (2001). Use of live bacterial vaccine vectors for antigen delivery: Potential and limitations. *Vaccine,* **19**: 1573-1580.

Melchers, M., Matthews, K., de Vries, R.,P., Eggink, D., van Montfort, T., Bontjer, I., . . . Sanders, R. W. (2011). A stabilized HIV-1 envelope glycoprotein trimer fused to CD40 ligand targets and activates dendritic cells. *Retrovirology,* **8**: 48-62.

Mestecky, J. (1987). The common mucosal immune system and current strategies for induction of immune responses in external secretions. *Journal of Clinical Immunology,* **7**: 265-276.

Meyer, M., Garron, T., Lubaki, N. M., Mire, C. E., Fenton, K. A., Klages, C., . . . Bukreyev, A. (2015). Aerosolized ebola vaccine protects primates and elicits lung-resident T cell responses. *The Journal of Clinical Investigation,* **125**: 3241-3255.

Moingeon, P., & Mascarell, L. (2012). Induction of tolerance via the sublingual route: Mechanisms and applications. *Clinical and Developmental Immunology,* **2012**: 1740-2522.

Murakami, M., Tsubata, T., Shinkura, R., Nisitani, S., Okamoto, M., Yoshioka, H., . . . Honjo, T. (1994). Oral administration of lipopolysaccharides activates B-1 cells in the peritoneal cavity and lamina propria of the gut and induces autoimmune symptoms in an autoantibody transgenic mouse. *The Journal of Experimental Medicine,* **180**: 111-121.

Murugappan, S., Patil, H., Frijlink, H., Huckriede, A., & Hinrichs, W. (2014). Simplifying influenza vaccination during pandemics: Sublingual priming and intramuscular boosting of immune responses with heterologous whole inactivated influenza vaccine. *The AAPS Journal,* **16**: 342-349.

Nagai, Y., Shiraishi, D., Tanaka, Y., Nagasawa, Y., Ohwada, S., Shimauchi, H., . . . Sugawara, S. (2015). Transportation of sublingual antigens across sublingual ductal epithelial cells to the ductal antigen- presenting cells in mice. *Clinical & Experimental Allergy,* **45**: 677-686.

Nagao, K., Ginhoux, F., Leitner, W. W., Motegi, S., Bennett, C. L., Clausen, B. E., . . . Udey, M. C. (2009). Murine epidermal langerhans cells and langerin-expressing dermal dendritic cells are unrelated and exhibit distinct functions. *Proceedings of the National Academy of Sciences of the United States of America,* **106**: 3312-3317.

Neubert, K., Lehmann, C. H. K., Heger, L., Baranska, A., Staedtler, A. M., Buchholz, V. R., . . . Dudziak, D. (2014). Antigen delivery to $CD11c^{+}CD8^{-}$ dendritic cells induces protective immune responses against experimental melanoma in mice in vivo. *Journal of Immunology,* **192**: 5830-5838.

Neutra, M. R., & Kozlowski, P. A. (2006). Mucosal vaccines: The promise and the challenge. *Nature Reviews Immunology,* **6**: 148-158.

Neutra, M. R., Mantis, N. J., & Jean-Pierre Kraehenbuhl. (2001). Collaboration of epithelial cells with organized mucosal lymphoid tissues. *Nature Immunology,* **2**: 1004-1009.

Ninomiya, A., Ogasawara, K., Kajino, K., Takada, A., & Kida, H. (2002). Intranasal administration of a synthetic peptide vaccine encapsulated in liposome together with an anti-CD40 antibody induces protective immunity against influenza A virus in mice. *Vaccine,* **20**: 3123-3129.

Novak, N., Haberstok, J., Bieber, T., & Allam, J. (2008). The immune privilege of the oral mucosa. *Trends in Molecular Medicine,* **14**: 191-198.

Nudel, I., Elnekave, M., Furmanov, K., Arizon, M., Clausen, B. E., Wilensky, A., & Hovav, A. (2011). Dendritic cells in distinct oral mucosal tissues engage different mechanisms to prime $CD8^+$ T cells. *Journal of Immunology,* **186**: 891-900.

Oggioni, M. R., Medaglini, D., Romano, L., Peruzzi, F., Maggi, T., Lozzi, L., . . . Pozzi, G. (1999). Antigenicity and immunogenicity of the V3 domain of HIV type 1 glycoprotein 120 expressed on the surface of *streptococcus gordonii*. *AIDS Research and Human Retroviruses,* **15**: 451-459.

Oggioni, M. R., Manganelli, R., Contorni, M., Tommasino, M., & Pozzi, G. (1995). Immunization of mice by oral colonization with live recombinant commensal streptococci. *Vaccine,* **13**: 775-779.

O'Sullivan, B., & Thomas, R. (2003). Recent advances on the role of CD40 and dendritic cells in immunity and tolerance. *Current Opinion in Hematology,* **10**: 272-278.

Pabst, O., & Mowat, A. M. (2012). Oral tolerance to food protein. *Mucosal Immunology,* **5**: 232.

Park, H., Ferko, B., Byun, Y., Song, J., Han, G., Roethl, E., . . . Nguyen, H. H. (2012). Sublingual immunization with a live attenuated influenza A virus lacking the nonstructural protein 1 induces broad protective immunity in mice. *PLoS ONE,* **7**: e39921. doi: 10.1371/journal.pone.0039921.

Paul, W. E. (1987). Interleukin 4/ B cell stimulatory factor 1: One lymphokine, many functions. *The FASEB Journal,* **1**: 456-461.

Pedersen, G. K., Ebensen, T., Gjeraker, I. H., Svindland, S., Bredholt, G., Guzmán, C. A., & Cox, R. J. (2011). Evaluation of the sublingual route for administration of influenza H5N1 virosomes in combination with the bacterial second messenger c-di-GMP. *PloS One,* **6**: e26973. doi: 10.1371/journal.pone.0026973.

Pennington, S. H., Thompson, A. L., Wright, A. K. A., Ferreira, D. M., Jambo, K. C., Wright, A. D., . . . Gordon, M. A. (2016). Oral typhoid vaccination with live-attenuated typhi strain Ty21a generates Ty21a-responsive and heterologous influenza virus-responsive CD4 and CD8 T cells at the human intestinal mucosa. *The Journal of Infectious Diseases,* **213**: 1809-1819.

Perez-Lopez, A., Behnsen, J., Sean-Paul, N., & Raffatellu, M. (2016). Mucosal immunity to pathogenic intestinal bacteria. *Nature Reviews Immunology,* **16**: 135-148.

Perry, D., & Kuramitsu, H. K. (1981). Genetic transformation of streptococcus mutans. *Infection and Immunity,* **32**: 1295-1297.

Petsch, D., & Anspach, F. B. (2000). Endotoxin removal from protein solutions. *Journal of Biotechnology,* **76**: 97-119.

Polak, D., Benzki-Namdar, E., Houri-Haddad, Y., & Shapira, L. (2014). Mucosal vaccination shapes the expression of salivary antibodies and establishment of $CD8^{+}$ T- cells. *Journal of Periodontology,* **85**: 991-997.

Pozzi, G., & Wells, J. M. (Eds.). (1997). *Gram-positive bacteria: Vaccine vehicles for mucosal immunization: Vaccine vehicles for mucosal immunization*. New York, NY: Springer Berlin Heidelberg.

Pullen, S. S., Labadia, M. E., Ingraham, R. H., Mcwhirter, S. M., Everdeen, D. S., Alber, T., . . . Kehry, M. R. (1999). High-affinity interactions of tumor necrosis factor receptor-associated factors (TRAFs) and CD40 require TRAF trimerization and CD40 multimerization. *Biochemistry,* **38**: 10168-10177.

Quezada, S. A., Jarvinen, L. Z., Lind, E. F., & Noelle, R. J. (2004). CD40/CD154 interactions at the interface of tolerance and immunity. *Annual Review of Immunology,* **22**: 307-328.

Rakoff-Nahoum, S., Paglino, J., Eslami-Varzaneh, F., Edberg, S., & Medzhitov, R. (2004). Recognition of commensal microflora by toll-like receptors is required for intestinal homeostasis. *Cell,* **118**: 229-241.

Rath, A., Glibowicka, M., Nadeau, V. G., Chen, G., & Deber, C. M. (2009). Detergent binding explains anomalous SDS-PAGE migration of membrane proteins. *Proceedings of the National Academy of Sciences of the United States of America; Detergent Binding Explains Anomalous SDS-PAGE Migration of Membrane Proteins,* **106**: 1760-1765.

Rhee, J. H., Lee, S. E., & Kim, S. Y. (2012). Mucosal vaccine adjuvants update. *Clinical and Experimental Vaccine Research,* **1**: 50-63.

Romani, N., Clausen, B. E., & Stoitzner, P. (2010). Langerhans cells and more: Langerin- expressing dendritic cell subsets in the skin. *Immunological Reviews,* **234**: 120-141.

Rosalia, R. A., Cruz, L. J., van Duikeren, S., Tromp, A. T., Silva, A. L., Jiskoot, W., . . . Ossendorp, F. (2015). CD40-targeted dendritic cell delivery of PLGA-nanoparticle vaccines induce potent anti- tumor responses. *Biomaterials,* **40**: 88-97.

Round, J. L., & Mazmanian, S. K. (2010). Inducible Foxp3+ regulatory T- cell development by a commensal bacterium of the intestinal microbiota. *Proceedings of the National Academy of Sciences of the United States of America,* **107**: 12204-12209.

Rui-Qing Wu, Dun-Fang Zhang, Tu, E., Qian-Ming Chen, & Chen, W. (2014). The mucosal immune system in the oral cavity-an orchestra of T cell diversity. *International Journal of Oral Science,* **6**: 125-132.

Sambrook, J., Fritsch, E. F., & Maniatis, T. (1989). *Molecular cloning: A laboratory manual.* (2ed ed.). New York, NY: Cold Spring Harbor Laboratory Press.

Saraiva, M., & Anne O'Garra. (2010). The regulation of IL-10 production by immune cells. *Nature Reviews Immunology,* **10**: 170-181.

Schaefer, C., & Rost, B. (2012). Predict impact of single amino acid change upon protein structure. *BMC Genomics,* **13**: s4. doi: 10.1186/1471-2164-13-S4-S4.

Sheridan, B., Pham, Q., Lee, Y., Cauley, L., Puddington, L., & Lefrançois, L. (2014). Oral infection drives a distinct population of intestinal resident memory CD8+ T cells with enhanced protective function. *Immunity,* **40**: 747-757.

Shim, B., Choi, Y., Cheon, I. S., & Song, M. K. (2013). Sublingual delivery of vaccines for the induction of mucosal immunity. *Immune Network,* **13**: 81-85.

Sin, J. I., Kim, J. J., Zhang, D., & Weiner, D. B. (2001). Modulation of cellular responses by plasmid CD40L: CD40L plasmid vectors enhance antigen- specific helper T cell type 1 $CD4^+$ T cell-mediated protective immunity against herpes simplex virus type 2 in vivo. *Human Gene Therapy,* **12**: 1091-1102.

Singh, S., Schluns, K., Yang, G., Anthony, S., Barry, M., & Sastry, K. (2016). Intranasal vaccination affords localization and persistence of antigen- specific $CD8^+$ T lymphocytes in the female reproductive tract. *Vaccines,* **4**: 7-17.

Snider, D. P., & Segal, D. M. (1987). Targeted antigen presentation using crosslinked antibody heteroaggregates. *Journal of Immunology,* **139**: 1609-1616.

Song, J., Kim, J., Kwon, H., Shim, D., Parajuli, N., Cuburu, N., . . . Kweon, M. (2009). CCR7-CCL19/ CCL21-regulated dendritic cells are responsible for effectiveness of sublingual vaccination. *Journal of Immunology,* **182**: 6851-6860.

Song, J., Nguyen, H. H., Cuburu, N., Horimoto, T., Ko, S., Park, S., . . . Kweon, M. (2008). Sublingual vaccination with influenza virus protects mice against lethal viral infection. *Proceedings of the National Academy of Sciences of the United States of America,* **105**: 1644-1649.

Studer, R. A., Dessailly, B. H., & Orengo, C. A. (2013). Residue mutations and their impact on protein structure and function: Detecting beneficial and pathogenic changes. *The Biochemical Journal,* **449**: 581-594.

Sudhakar, Y., Kuotsu, K., & Bandyopadhyay, A. K. (2006). Buccal bioadhesive drug delivery-A promising option for orally less efficient drugs. *Journal of Controlled Release,* **114**: 15-40.

Sun, C., Hall, J. A., Blank, R. B., Bouladoux, N., Oukka, M., Mora, J. R., & Belkaid, Y. (2007). Small intestine lamina propria dendritic cells promote de novo generation of Foxp3 T reg cells via retinoic acid. *The Journal of Experimental Medicine,* **204**: 1775-1785.

Sung, S. J., Fu, S. M., Rose, C. E., Gaskin, F., Ju, S., & Beaty, S. R. (2006). A major lung CD103 (alphaE)-beta7 integrin-positive epithelial dendritic cell population expressing langerin and tight junction proteins. *Journal of Immunology,* **176**: 2161-2172.

Tanaka, Y., Nagashima, H., Bando, K., Lu, L., Ozaki, A., Morita, Y., . . . Sugawara, S. (2016). Oral $CD103^{-}CD11b^{+}$ classical dendritic cells present sublingual antigen and induce $Foxp3^{+}$ regulatory T cells in draining lymph nodes. *Mucosal Immunology.* Advance online publication. doi: 10.1038/mi.2016.46 [doi]

Thurnheer, M. C., Zuercher, A. W., Cebra, J. J., & Bos, N. A. (2003). B1 cells contribute to serum IgM, but not to intestinal IgA, production in gnotobiotic ig allotype chimeric mice. *Journal of Immunology,* **170**: 4564-4571.

Tjalsma, H., Antelmann, H., Jongbloed, J. D. H., Braun, P. G., Darmon, E., Dorenbos, R., . . . van Dijl, J. M. (2004). Proteomics of protein secretion by bacillus subtilis: Separating the "secrets" of the secretome. *Microbiology and Molecular Biology Reviews,* **68**: 207-233.

Troy, E. D. (1984). Human mucosal langerhans cells: Postmortem identification of regional variations in oral mucosa. *Journal of Investigative Dermatology,* **82**: 21-24.

Tsuji, T., Matsuzaki, J., Kelly, M. P., Ramakrishna, V., Vitale, L., He, L., . . . Gnjatic, S. (2011). Antibody- targeted NY- ESO-1 to mannose receptor or DEC-205 in vitro elicits dual human $CD8^+$ and $CD4^+$ T cell responses with broad antigen specificity. *Journal of Immunology,* **186**: 1218-1227.

Tsumoto, K., Ejima, D., Kumagai, I., & Arakawa, T. (2003). Practical considerations in refolding proteins from inclusion bodies. *Protein Expression and Purification,* **28**: 1-8.

Upadhyay, J., Upadhyay, R., Agrawal, P., Jaitley, S., & Shekhar, R. (2013). Langerhans cells and their role in oral mucosal diseases. *North American Journal of Medical Sciences,* **5**: 505-514.

Vallejo, L. F., & Rinas, U. (2004). Strategies for the recovery of active proteins through refolding of bacterial inclusion body proteins. *Microbial Cell Factories,* **3**: 11-22.

van Egmond, M., Damen, C. A., van Spriel, A.,B., Vidarsson, G., van Garderen, E., & van, d. W. (2001). IgA and the IgA fc receptor. *Trends in Immunology,* **22**: 205-211.

van Kooten, C., & Banchereau, J. (2000). CD40-CD40 ligand. *Journal of Leukocyte Biology,* **67**: 2.

Viswanathan, R. K., & Busse, W. W. (2012). Allergen immunotherapy in allergic respiratory diseases: From mechanisms to meta-analyses: From mechanisms to meta-analyses. *Chest,* **141**: 1303-1314.

Wang, C., & Geng, X. (2012). Refolding and purification of recombinant human granulocyte colony-stimulating factor using hydrophobic interaction chromatography at a large scale. *Process Biochemistry,* **47**: 2262-2266.

Wang, L., Liu, W., Yang, M., Peng, D., & Chen, L. (2013). Development of a *streptococcus gordonii* vaccine strain expressing *schistosoma japonicum* sj- F1 and evaluation of using this strain for intranasal immunization in mice. *Parasitology Research,* **112**: 1701-1708.

Welty, N. E., Staley, C., Ghilardi, N., Sadowsky, M. J., Igyártó, B.,Z., & Kaplan, D. H. (2013). Intestinal lamina propria dendritic cells maintain T cell homeostasis but do not affect commensalism. *The Journal of Experimental Medicine,* **210**: 2011-2024.

Williams, B. J., Bhatia, S., Adams, L. K., Boling, S., Carroll, J. L., Li, X. L., . . . Mathis, J. M. (2012). Dendritic cell based PSMA immunotherapy for prostate cancer using a CD40-targeted adenovirus vector. *PloS One,* **7**: e46981. doi: 10.1371/journal.pone.0046981 [doi].

Woodrow, K. A., Bennett, K. M., & Lo, D. D. (2012). Mucosal vaccine design and delivery. *Annual Review of Biomedical Engineering,* **14**: 17-46.

Wu, C., Yang, L., Yang, H., Knoff, J., Peng, S., Lin, Y., . . . Wu, T. (2014). Enhanced cancer radiotherapy through immunosuppressive stromal cell destruction in tumors. *Clinical Cancer Research,* **20**: 644-657.

Yang, M., Yang, A., Qiu, J., Yang, B., He, L., Tsai, Y., . . . Hung, C. (2016). Buccal injection of synthetic HPV long peptide vaccine induces local and systemic antigen-specific $CD8^+$ T- cell immune responses and antitumor effects without adjuvant. *Cell & Bioscience,* **6**: 17-26.

Yang, X., & Zhu, W. (2007). Viscosity properties of sodium carboxymethylcellulose solutions. *Cellulose,* **14**: 409-417.

Yin, W., Gorvel, L., Zurawski, S., Li, D., Ni, L., Duluc, D., . . . Oh, S. (2016). Functional specialty of CD40 and dendritic cell surface lectins for exogenous antigen presentation to CD8(+) and CD4(+) T cells. *EBioMedicine,* **5**: 46-58.

Zhang, C., Ohno, T., Kang, S., Takai, T., & Azuma, M. (2014). Repeated antigen painting and sublingual immunotherapy in mice convert sublingual dendritic cell subsets. *Vaccine,* **32**: 5669-5676.

Zhang, X., Yang, T., Cao, J., Sun, J., Dai, W., & Zhang, L. (2016). Mucosal immunization with purified OmpA elicited protective immunity against infections caused by multidrug-resistant acinetobacter baumannii. *Microbial Pathogenesis,* **96**: 20-25.

Zhang, Z., Wang, Y., Wang, L., Gao, P., & Kolokotronis, S. (2010). The combined effects of amino acid substitutions and indels on the evolution of structure within protein families. *PLoS ONE,* **5**: e14316. doi: 10.1371/journal.pone.0014316.

Zheng, M., Shellito, J. E., Marrero, L., Zhong, Q., Julian, S., Ye, P., . . . Kolls, J. K. (2001). $CD4^+$ T cell-independent vaccination against *pneumocystis carinii* in mice. *The Journal of Clinical Investigation,* **108**: 1469-1474.

Zheng, M., Ramsay, A. J., Robichaux, M. B., Kliment, C., Crowe, C., Rapaka, R. R., . . . Kolls, J. K. (2005). $CD4^+$ T cell- independent DNA vaccination against opportunistic infections. *The Journal of Clinical Investigation,* **115**: 3536-3544.